Stony Brook University

LOW INTENSITY PULSED ULTRASOUND: COUNTERMEASURE FOR MICROGRAVITY-INDUCED BONE LOSS

Low intensity Ultrasound will countermeasure catabolic effects of microgravity

08/09/2011

A Dissertation Presented
by

Sardar Muhammad Zia Uddin

to

The Graduate School

In partial fulfillment of the

Requirements

For the Degree of

Doctor of Philosophy

In

Biomedical Engineering

Stony Brook University

Stony Brook University

The Graduate School

Sardar Muhammad Zia Uddin

We, the dissertation committee for the above candidate for the
Doctor of Philosophy degree,
Hereby recommend acceptance of this dissertation.

Yi-Xian Qin PhD, Dissertation Advisor
Professor, Department of Biomedical Engineering
Stony Brook University

Michael Hadjiargyrou PhD, Chairperson of Defense,
Associate Professor, Department of Biomedical Engineering
Stony Brook University

Stefan Judex, PhD
Professor, Department of Biomedical Engineering
Stony Brook University

Robert Majeska, PhD
Adjunct Professor, Department of Biomedical Engineering
City College of New York

This dissertation is accepted by the Graduate School

Charles Taber
Interim Dean of the Graduate School

Abstract of the Dissertation

Low Intensity Pulse Ultrasound – Countermeasure to Microgravity induced Bone Loss

by

Sardar Muhammad Zia Uddin

Doctor of Philosophy

in

Department of Biomedical Engineering

Stony Brook University

2012

Microgravity (MG) during space flight is known to have adverse effect on bone quality and quantity. Data collected from studies conducted on astronauts show a loss of 1-1.6% bone mineral density (BMD) per month of space-flight. This decreased BMD has been recorded in the load-bearing region of the legs and spine. The reduction in bone quality can be due to decreased osteoblast and/or increased osteoclast activity when exposed to microgravity. During space-flights, rigorous exercise has been used to reduce to bone loss due to microgravity, but thus far it has proven inadequate to produce significant results. Some studies have considered using drugs and various growth factors to maintain bone mass in a MG environment, but it can become too expensive to maintain over longer periods of time besides the systemic effects of such treatments. The effects of MG are partially attributed to the lack of mechanical force on bone tissue, which alters osteogenic gene expression, reduces rate of cell growth, proliferation, differentiation, cytoskeleton polymerization and cellular morphology. Thus, to reverse these adverse effects on bone physiology, it is important to provide cells with mechanical stimuli that can provide essential signals for cells to counter the adverse effects of microgravity.

Low intensity pulsed ultrasound (LIPUS) can be readily applied *in vivo;* human studies have shown anabolic effects on osteopenic bone tissue. Furthermore, LIPUS has the potential to be an inexpensive and non-invasive targeted therapy for disuse induced bone loss. The objective

of this study was to examine effects of ultrasound on a disuse bone model and osteoblast cell cultures in simulated microgravity. This will help us understand the effects of ultrasound on microgravity induced osteoporosis and provide a non-invasive and more targeted approach to reduce bone loss during space-flight. Ultrasound may provide an option towards future human space explorations. It is hypothesized that LIPUS stimulation will reverse the detrimental effects of microgravity on bone strength. The overall hypothesis will be tested by studying the effects of LIPUS on osteoblasts and MSCs in simulated microgravity in hind limb suspended mice models. The hypothesis was tested with *in vivo* and *in vitro* disuse models.

Three-month old C57BL/6 mice were randomized to age match (AM), non-suspended sham (NS), non-suspended –LIPUS (NU), suspended sham (SS), and suspended-LIPUS (SU) groups. The results from the *in vivo* after four weeks of suspension, micro CT analyses showed significant decreases in trabecular bone volume/tissue volume (BV/TV) (36%, $P<0.005$),bone mineral density (BMD) (3%, $P<0.05$), Trabecular thickness (Tb.Th) (12.5%, $p<0.005$), and increased in bone surface/bone volume (BS/BV) (16%,$p<0.005$) relative to age match (AM). Application of LIPUS for 20 min/day for 5 days/week, significantly increased, BMD (3%, $p<0.05$), Tb.Th (6%, $p<0.05$), and increased BS/BV (10%, $p<0.005$) relative to AM mice.

Histomorphometric analyses showed increased bone formation at metaphysis endosteal and trabecular surfaces (0.104 ± 0.07 vs. 0.031 ± 0.30 $\mu m^3/(\mu m^2)/d$) in SU mice relative to SS. Four-point bending tests of SS femurs showed reduced elastic modulus (53%, $p<0.05$), yield (33%, $P<0.05$), and ultimate strength (45%,$p <0.05$) at the femoral diaphysis relative to AM samples. LIPUS stimulation mitigated the adverse effects of disuse on bone elastic modulus (42%, $p<0.05$), yield strength (29%, $p<0.05$), and ultimate strength (39%, $p<0.05$) relative to SS

femurs. Analyses of contralateral control limbs from SU or NU showed that LIPUS had no systemic effects, supporting the hypothesis that LIPUS provided targeted stimulation.

The *in vitro* studies were conducted with MSCs and Osteoblast cells in Simulated Microgravity (SMG) conditions. MSCs were cultured in a 1D clinostat to simulate microgravity (SMG) and treated with LIPUS at 30mW/cm^2 for 20 min/day. The results showed significant increases in ALP, OST, RANKL, RUNX2, and decreases in OPG in LIPUS treated SMG cultures compared to non-treated cultures. SMG significantly reduced ALP positive cells by 70%, $p<0.01$and ALP activity by 22%, $p<0.05$), while LIPUS treatment restored ALP positive cell number and activity to equivalence with normal gravity controls. Extracellular matrix (ECM) collagen and mineralization was assessed by Sirius Red and Alizarin Red staining, respectively. SMG cultures showed little or no collagen or mineralization, but LIPUS treatment restored collagen content to 50 %,($p<0.05$) and mineralization by 45% ($p<0.05$) in SMG cultures relative to SMG samples.

The data from the osteoblast study showed that osteoblast exposure to SMG results in significant decreases in proliferation (38% and 44% at day 4 and 6, respectively, $p<0.01$), collagen content (22%, $p<0.05$) and mineralization (37%, $p < 0.05$) and actin stress fibers. In contrast, LIPUS stimulation under SMG condition significantly increases the rate of proliferation (24% by day 6, $p<0.05$), collagen content (52%, $p < 0.05$) and matrix mineralization (25%, $p<0.001$) along with restoring formation of actin stress fibers in the SMG-exposed osteoblasts. The gene expression analysis showed significant increase in expression of RUNX2 and OST and reduced RANKL expression after LIPUS exposure.

Collectively, the data suggest LIPUS has the potential to provide essential mechanotransductive anabolic stimulus to counter measure disuse-induced bone loss while showing no adverse effect on healthy bone. It also showed increased structural and mechanical integrity in LIPUS treated disuse bones. Furthermore, LIPUS increased MSCs osteogenic differentiation and osteoblastic activity in SMG. The gene expression data indicates that LIPUS has anabolic and anti-resorptive effects on osteoblast cells.

Table of Contents

List of Figures

List of Tables

List of Abbreviations

Growth Factors and Proteins

Matrix extracellular phosphoglycoprotein (MEPE)
Microphthalmia-associated transcription factor (MITF)
Mitogen Activated Protein Kinases (MPAK)
Bone Morphogenic Protein (BMP)
Parathyroid Hormone (PTH)
parathyroid hormone receptor 1 (PTHr1)
Procollagen peptide (PICP)
Epidermal Growth Factor Receptor (EFGr)
Proteoglycan Growth Factor Receptor (PDGFβ receptor)
Insulin Growth Factor-1 (IGF1)
Extracellular signal-regulated Kinases (ERK)
Jun N-terminal Kinases (JNK)
Stress activated Protein Kinases (SAPK)
Activator Protein-1 (AP-1)
Vascular Endothelial Growth Factor (VEGF)
Platelet Derived Growth Factor (PDGF)
Fibroblast Growth Factor (FGF)
Transforming Growth Factor (TGF)
Receptor activator Kappa –B Ligand (RANKL)
Runt-related transcription factor 2 (RUNX2)
Collagen type 1A (COL1A1)
Cyclooxygenase (COX)
Osterix (OSX)
Alkaline Phosphatase (ALP)

Cells

Mesenchymal Stem Cells (MSCs)
Hematopoietic Stem Cells (HSCs)

Microcomputed Tomography (MicroCT)

Bone Mineral Density (BMD)
Bone Volume / Bone Tissue (BV/TV)
Bone Surface / Bone Volume (BS/BV)
Trabecular Thickness (Tb.Th)
Trabecular Number (Tb.N)
Cortical Thickness (Cort.Th)
Bone Area (BA)
Endosteal Surface (Endo.S)/
Periosteal Surface (Peri.S)

Histomorphometry

Mineral Deposition rate (Mar)
Double Labels (dL)
Single label Surface (dLS)
Bone Formation Rate (BFR)

Mechanical Testing

Moment of Interia (I)
Young's Elastic Modulus (E)
Stress (σ)
Strain (ε)
Stiffness (S)
Applied Force (F)
Distance between Supports (L)

Experimental Groups

In Vivo Study
Age Match (AM)|
Non-Suspended Sham (NS)
Non-Suspended + LIPUS (NU)
Suspended Sham (SS)
Suspended Sham + LIPUS (SU)

In Vitro
Gravity (G)
Gravity + LIPUS (GU)
Microgravity (M)
Microgravity + LIPUS (MU)

Others

Extracellular Matrix (ECM)
Basic Multicellular Units (BMU)
Bone Mineral Density (BMD)
Hindlimb Suspension (HLS)
Random Position Machine (RPM)
Rotating Wall Vessel (RWV)
Poly-methyl methacrylate resin (PMMA)
Microgravity (MG)
Simulated Microgravity (SMG)
Low Intensity Pulsed Ultrasound (LIPUS)

Acknowledgements

As a Biomedical Engineer, I know there is not much place for God in the corridors of labs but as a person of faith and a devout Muslim, Allah has always been in my heart. I know many will consider this not relevant but to me, my faith has always provided the strength to carry on and to get educated. In my darkest of hours I sought refuge with Allah and looked for peace in mostly unlikely place being a biomedical engineer. Today when I am about achieve a milestone in my life, I Thank Him for all the blessings and seek His guidance for the journey ahead.

The journey to Ph.D. completion is a long one that goes through many ups and downs. Once I was told that Ph.D. is not about just being intelligent, it is more about being persistent and determined. In my experience throughout the Ph.D. I have encountered many obstacles both in academics and personal life. They have taught me that one needs proper guidance and hard-work to achieve milestones in life. To get to this point in my life I have been blessed with many mentors, friends and family who have helped through hard times and without them I wouldn't have made it this far.

I am greatly thankful to Dr. Yi-Xian Qin for giving me the opportunity to work in his lab. He always encouraged me to be creative in my experimental approach and provided his feedback whenever required. He was a supportive and patient mentor, who always appreciated quality of data and hard-work. Without his commitment and support I wouldn't have been able to complete my PhD dissertation.

I am thankful to my Dissertation Committee, Dr. Michael Hadjigyrou, Dr. Stefan Judex and Dr. Robert Majeska, as they provided me with constructive feedback in my doctoral research and enabled me to critically analyze that research. Dr. Michael Hadjiargyrou, who I have known for more than a decade now, has been an outstanding mentor, advisor and friend to me. There are few people in your life who leave a long lasting impact on you and I have no hesitation in saying that Michael is such a person, in my life. He has guided me through my academic career, as well as helped me in personal life. He always challenged me to do better and supported me in difficult times. His advice and mentorship was not limited to research; it even extended to helping me grow in my personal life. Without him I wouldn't be where I am today.

There is a long list of colleagues and friends who helped me in my PhD research. I am thankful to members of Qin, Judex, Rubin and Hadjiargyrou labs for their support .I would like to particularly mention Dr. David Komatsu for teaching me different techniques in my undergraduate years and recently in editing my dissertation; Frederick Serra-Hsu, Jiqi Cheng for helping me in initial ultrasound setup; Gunes Uzer, Gabriel Pagnotti and Xia Zhao for innumerable discussions about our research; and last but not least, Alyssa Tuthill, as she provided invaluable technical and moral support during my doctoral dissertation.

I am thankful to the Department of Biomedical Engineering (BME) faculty and staff as over the years they have been really helpful and supportive. I have been associated with BME

since my years as an Undergraduate research student; since then I have moved on to complete my Masters and now, here I stand before you, coming full circle by completing my doctoral dissertation. I would like to take a moment to will specially thank Dr. Partap Singh Khalsa as he introduced me to BME and gave me my first research project. It wouldn't be just not to pay my thanks to Anne Marie and Nubia Andrade for providing their support in departmental matters. Lastly I would like to thank Dr. Rubin Clinton and BME faculty for maintaining the high standard of BME over the years.

I come from Pakistan, where higher education is rare and people still find it hard to meet day to day needs. I come from a family which is not known for their education but my parents did everything to make sure that I get the best education possible and there is no way possible: that I can repay them for that whatever I become I will owe it to my parents. I lost my mother early on during my undergraduate years, but her courage always stayed with me; my father struggled to get me educated and it is his persistence that inspired me to achieve my goals. My siblings always gave me the hope to carry on and cheered me up even during hardest of times. I got married couple of years back but I have known my wife for a long time and she always has been there in my darkest hours to remind me that everything will be alright. I only hope I can fulfill their dreams.

The journey to Ph.D. completion is one which requires effort of one but inspiration and support of many. There are many whom I haven't mentioned that helped me along and I thank all of them as I recognize that it is impossible to get to this point without their help.

Regards to everyone!!!

Chapter 1

Background and Significance

1.1 Bone Anatomy – Tissue to Cell

Bone is a mineralized tissue made up of bone cells and calcified extra cellular matrix (ECM). It functions to provide mechanical support, a niche for hematopoietic and mesenchymal stem cells, serves as calcium reservoir and provides attachment sites for tendons and ligaments. The calcified matrix allows it to be hard enough to protect internal organs and flexible enough to absorb energy subsequent to impacts.

The bone matrix is composed of organic and inorganic components. The organic component contains 90% collagen type I and 10% of non-collagenous protein such as fibronectin, osteopontin, osteocalcin, bone sialoprotein, and other proteoglycans, growth factors, and enzymes. Collagen is a fibrous protein which provides the bone matrix with its tensile strength and facilitates matrix mineralization. Calcium phosphate hydroxyapatite $[Ca_{10}(PO4)_6(OH)_2]$forms the inorganic part of the bone matrix and provides bone with its necessary rigidity and hardness. The bone matrix also retains 99% of the body's calcium and 85% of its phosphorous. Without proper calcification bone loses its rigidity and becomes too flexible, while a lack of proper collagen can make it brittle [2].

The shape and structure of bone is maintained by processes known as modeling and remodeling. Modeling regulates bone growth in response to physiological and biomechanical conditions at specific anatomic sites. During modeling bone formation and resorption are not coupled and bone tissue can be added or removed independently, based up physiological demand. It is mostly restricted to skeletal growth. In contrast, bone remodeling is the process by which adult bone structure is maintained as it goes through day to day wear and tear. Daily activities and physiological processes can induce microfractures in bone tissue which are then

resorbed and replaced by newly formed bone. These resorptive and formative activities are highly coordinated and are referred to as coupled remodeling. Decoupling of resorption and formation can lead to osteopenia and in severe cases osteoporosis. The remodeling cycle takes about 6 months and approximately 10% of bone tissue is remodeled each year[3].

The modeling and remodeling processes are controlled by three main types of cells; osteoclasts, osteoblasts, and osteocytes. Osteoclasts are large multinucleated cells responsible for bone resorption that arise from hematopoietic stem cells. Osteoclast differentiation and maturation is strongly regulated by receptor activation of nuclear factor kappa-B ligand (*RANKL*) ,which is excreted by cells of mesenchymal origin. Mature osteoclasts adhere to damaged bone and secrete hydrogen ions to create localized acidic compartment that breaks down the calcified matrix. Osteoblasts are bone forming cells derived from mesenchymal stem cells (MSC). Mature osteoblasts secrete type 1 collagen, osteocalcin, osteopontin, and other matrix proteins. Calcium binding lipids secreted from osteoblasts accumulate calcium within lipid vesicles and interact with phosphate ions to make hydroxyapatite crystals along the length of collagen type 1 fibers. As osteoblasts mature, many become trapped within the calcified matrix and further differentiate into osteocytes. These cells form long cytoplasmic processes to communicate with other cells in the matrix. Osteocytes are the most abundant cells in bone and are located in lacunae and interconnected through cytoplasmic extensions forming canaliculi. Osteocytes are known as the mechanosensory cells of bone as they mediate mechanical signals in the ECM and regulate the activity of osteoblasts and osteoclasts [3].

On the tissue level bone is divided into cortical and trabecular bone. Cortical (compact or dense) bone is compressed bone and accounts for 80% of total bone mass. Trabecular bone is highly porous bone comprising 50-90% of bone volume. Trabecular bone forms a network of

interconnected struts forming a sponge like structure. Trabecular struts form a network which is connected to the cortical bone at its endosteal surface. Both cortical and trabecular bone are composed of osteons (the basic unit of bone), interconnected osteocytes (residing in lacunae) embedded within calcified matrix (lamellae), forming a circular unit with a central canal to facilitate blood and nutrient supply. Trabecular bone osteons are saucer shaped while cortical bone has a network of circular osteons with a central canal to facilitate blood and nutrient supply, cortical bone osteon network is commonly known as the Haversian system [3]. Trabecular struts forms a network which is connected with cortical at endosteal surface of cortical bone.

1.2 **Bone Remodeling**:

Bone is a dynamic tissue capable of adapting to mechanical stimuli and repairing localized damage. The metabolic activity of bone is regulated by the synergistic activity of osteoblasts and osteoclasts. These cells regulate bone formation and resorption within bones, at sites such as the periosteum, endosteum, trabecular, and Haversian regions. Together these cells from the basic multicellular units (BMU) that execute bone remodeling and this activity is orchestrated by the osteocytes.

Bone remodeling is initiated by the presence of localized damage or mechanical demand on the bone. It induces changes in bone lining, which induces activation of osteoclasts to resorb bone, which is, in turn, followed by a reversal phase (characterized by osteoclast apoptosis), and finally new bone formation by osteoblasts. This coupling of osteoclast resorption followed by osteoblast formation (BMU) is mainly responsible for the removal of old and/or damaged bone as well as bone adaptation to altered mechanical demands[4]. Disruption of this BMU coupling can lead to pathological conditions such as osteopenia, where bone resorption outpaces bone formation, leading to net bone loss. Healthy bone goes through constant remodeling by

formation of BMUs and the number of BMUs in a specified volume of tissue can be used to determine rate of remodeling in bone.

Osteoblasts are derived from mesenchymal stem cells (MSCs) that reside in the marrow. Differentiation of MSCs to osteoblasts is influenced by a variety of biochemical and biomechanical factors. Commitment of MSCs to the osteoblast lineage is controlled by expression of the transcription factors Runx2 [5, 6] , Dlx5,[7] and Msx2[8-10]. Following osteoblast commitment, increases are seen in the expression of type 1 collagen, osteocalcin, bone-sialoprotein (BSP) [11], osterix (OSX) [12], alkaline phosphatase (ALP) [13] and Wnt signaling proteins [14, 15] as the osteoblasts matures from pre-osteoblasts to mature osteoblasts. As osteoblasts deposit matrix some become incorporated into the matrix causing them to differentiate into osteocytes and form long extensions/processes to connect to other developing osteocytes. Differentiation into osteocytes is associated with elevated expression of E11 [16], dentin matrix protein-1(DMP-1) [17], matrix extracellular phosphoglyco protein (MEPE) [18, 19] and Sclerostin (SOST) [20, 21]. Osteocytes are terminally differentiated cells and most abundant in bone tissue.

Osteoclasts are derived from hematopoietic stem cells (HSC's). As HSC differentiate into mononucleated clear cells and accumulate at sites of resorption they fuse to form multinucleated immature osteoclasts (i.e., polykaryon). Formation of immature osteoclasts requires expression of macrophage colony stimulating factor (M-CSF) [22, 23] and receptor activation of nuclear factor κB ligand (RANKL). Further maturation of osteoclast is dependent on increased expression of AP-1, c-fos [24, 25], microphthalmia -associated transcription factor (MITF) [26, 27] and nuclear factor of activated T cells, calcineurin dependent 1 (NFAT-c1) [27]. Most

importantly, RANKL expression is important for differentiation, maturation and ultimate survival of osteoclast cells.

RANKL is a soluble and membrane bound ligand expressed by pre-osteoblasts and stromal cells [28, 29]. RANKL has two receptors RANK [30, 31] and osteoprotegerin (OPG)[32, 33]; RANK receptors are membrane bound receptors present on osteoclasts and their precursors while OPG is a soluble receptor produced by pre-osteoblasts and stromal cells. RANKL interacts with RANK to activate osteoclastogenesis by inducing expression of TNF receptor-associated family members, nuclear factor-κB, c-fos, JNK, c-src and serine/ threonine kinases [30, 31] OPG is secreted by pre-osteoblasts and stromal cells to function as an inhibitor of osteoclastogenesis by binding to RANKL thereby preventing RANKL-RANK interactions[28, 32]. As such the ratio of RANKL to OPG determines the rate of osteoclastogenesis and BMU activity.

Different anabolic and catabolic agents affect bone homeostasis by altering the RANKL/OPG ratio. Resorptive factors such as Parathyroid hormone (continuous) (PTH)[34], prostaglandins [35], interleukins [36], vitamin D3 [37], glucocorticoids [38] and corticosteroids [39] are known to induce pre-osteoblasts and stromal cells to increase RANKL expression leading to bone loss. In contrast, anabolic agents such as high frequency low amplitude vibration [40] and ultrasound [41, 42] induce OPG expression thereby decreasing the RANKL/OPG ratio and thus favoring in bone formation. Figure 1 illustrates dynamic interactions of different bone cells in the process of bone remodeling through different pathways.

1.3 Stem Cells

Stem cells are non-committed, highly proliferative cells with the potential to differentiate into a multitude of different cell types. Stem cells are sub-divided into three types; totipotent, pluripotent, and multipotent stem cells. Totipotent cells are capable of differentiating into all cell types with the potential to create complete organisms. These cells are obtained by extracting them from blastocysts. Pluripotent stem cells are extracted later in development from the inner mass of the blastomere and have capability to differentiate in to all cell types except for the germal layers. Recent advancements in stem cell biology have led to the discovery of methods that can be used to reverse differentiate somatic cells into pluripotent stem cells. These cells are known as induced pluripotent stem cells (iPSC) [43]. Multipotent stem cells can be isolated postnataly and are capable of differentiating into the cell types found in their tissue of origin. Embryonic stem (ES) cells have huge potential in tissue engineering but their use is hampered by immunogenicity and ethical issues. The advent of iPSC avoids these problems and therefore offers tremendous potential. However, understanding of these cells is still in the early stages and recent studies have shown immunogenicity and tumorigenesis can arise in iPSC treated mice [44, 45]. Adult multipotent stem cells are readily available and also have outstanding potential for tissue engineering.

Mesenchymal stem cells (MSC) are type multipotent stem cells that can be extracted from fat, bone marrow, amniotic fluid, and umbilical cord matrix [46, 47]. Adipose and bone are the most commonly used sources of MSCs due to their ease of extraction. MSCs were first isolated by Friedenstein et al. and characterized as colony forming fibroblast like adherent cells [48, 49]. Currently there is no single marker unique to MSCs, thus different subsets of markers are used. The most common markers are CD105+, CD73+, CD90+, CD14-, CD34-, and CD45-

[49]. Depending on the biochemical and biomechanical environment, MSCs can differentiate into adipocytes [47], osteoblast [50], chondrocytes [51], myocytes[52] , and cardiomyocytes [53], with some studies suggesting they also have neuronal potential [54]

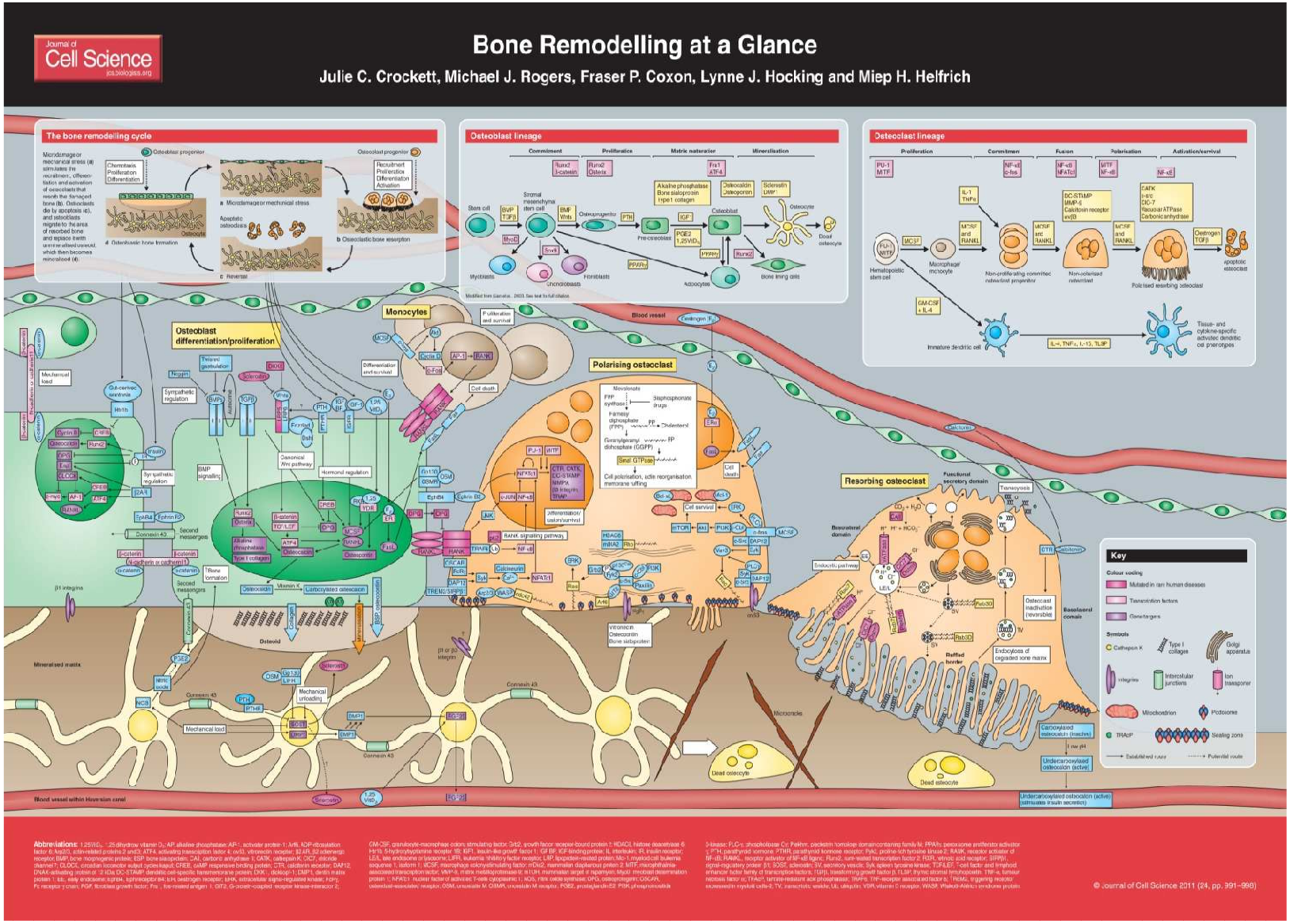

Figure 1. Bone remodeling is an complex process depending on interplay of Osteoblast, Osteocytes,Osteoclast and there progenitor stem cells, mesenchymal stem cells and hematopoietic stem cells[1] (courtesy of Journal of Cell Sciences)

Bone serves as a supporting organ for the skeletal system and experiences different kinds of mechanical stimuli including tension, compression, fluid shear stress, and hypostatic pressure. These external mechanical forces provide mechanical stimuli to bone cells by inducing transient structural deformation in the extracellular matrix. These deformations can activate mechanosensitive cellular structures including integrins, cytoskeletal proteins, stretch receptors, ion channels, G protein coupled receptors and nuclei. These changes result in activation of downstream signaling pathways such as calcium signaling, focal adhesion kinases, mitogen activated protein kinases (MPAK), G proteins, nitric acid, RhoA, and Rock, along with other mechanotransductive pathways [55]. Different mechanosensitive receptors and pathways can be activated with different stimuli. The level of activation with respect to different stimuli and pathways is still not clear.

Different mechanical stimuli direct MSCs into different lineages, with studies showing that compressive forces induce chondrogenesis while tensile forces induce osteogenesis. For examples, application of hydrostatic pressure [51] and uniaxial confined compression [56] on MSCs has been shown to increase the expression of chondrogenic genes such as aggrecan, Type II collagen, Sox9, and bone morphogenic protein (BMP) 6[51, 56]; in comparison, tension [57] , cyclic tensile strain,[58] and stretch [59] have been shown to induce osteogenic genes such as ALP, beta-catenin, RUNX2 and Wnt 8. Furthermore, cyclic tensile strain has been shown to result in rearrangement of the cellular cytoskeleton and inhibition of adipogenesis [57-59]. Studies done by Ruz and Chen [60] and McBeth el al.[61] have shown the importance of changes in cytoskeletal tensions, cell shape, and size in the differentiation of MSCs towards osteogenic or adipogenic lineages by regulating RHoA and GTPase in F-actin stress fibers [60, 61]. These studies also reported enhanced adipogenic differentiation in low stress areas of MSCs

matrix [60, 61]. A study by Feng et al. confirmed that cytoskeletal disassembly and deactivation of F-actin enhanced adipogenesis in stem cells [62].

Mechanical stimulation has been shown to increase chondrogenesis and osteogenesis, depending on the mechanical signal, while inhibiting adipogenesis. However, the effects of mechanical stimulation on MSC proliferation are not clear yet. Kereny et al. reported that 2.5% tensile strain decreased MSC proliferation while increasing the expression of RUNX2, BMP-2, collagen type I, and osteocalcin through the activation of the ERK –p38 pathway [50]. In contrast, Riddle et al. has shown that fluid shear stress enhances MSC proliferation through activation of calcium signaling and MAPK signaling [63]. It is likely that rates of proliferation and differentiation are dependent on the relative activation of different mechanotransductive pathways and more detail studies are required to identify fully elucidate the details of these pathways.

1.4 Biomechanical Loading and Bone Remodeling

Mechanical loading within the physiological range also impacts bone growth and structure. Bone adapts to mechanical stress by forming more bone in high stress regions until the stresses return to the physiological range. This is illustrated in the classic study by Wolff that showed formation of trabecular struts aligning with the direction of maximum stresses in the proximal femur [64]. The same patterns have also been observed in vertebral bodies, proximal tibiae, and calcanei. The direction of trabeculae increases bone strength and stiffness in the direction of trabecular alignment [64]. Cortical bone mostly experiences tensile and compressive stresses, and regions which experience higher tensile stresses have their collagen fibers aligned longitudinally whereas regions of high compression have collagen fibers that are aligned

transversely [65] . These characteristics demonstrate how local mechanical stresses affect directionality during one remodeling.

Bone remodeling is highly influenced by its mechanical environment. Lack of mechanical loading, referred to as disuse, induces bone loss by altering the balance between bone formation and resorption. Overuse can induce tissue damage (micro-factures) which activate osteoclast activity and lead to bone remodeling. If the rate of bone damage is higher than the rate of remodeling, accumulation of microfractures will result in the formation of stress fractures. Both disuse and overuse increase the number of bone remodeling sites leading to increased apoptosis in osteocytes [66].

Bone disuse lowers the stresses on bones, which in turn reduces bone formation and increases bone resorption on periosteal, endosteal, and trabecular surfaces. Long term disuse can lead to structural changes in long bones, with cross-sectional geometry showing rounder shaped long bones rather than the typical triangular shape, which reduce their moments of inertia and strength [67]. The growing and mature skeleton respond differently to disuse with bone loss concentrated in different areas of bone surfaces [68-70]. For example, studies performed on growing dogs showed higher bone loss on periosteal surfaces, due to reductions in appositional bone formation, that resulted in smaller bones with reduced second moments of inertia [68]. In contrast, mature dogs showed increased bone loss on endosteal surfaces causing expansion of the marrow cavities, as well as increased cortical porosity [68]. Distal bones of the forelimbs showed the highest bone loss in young and adult dogs, suggesting higher sensitivity to lack of mechanical stresses at this location [68].

The distal-most regions of bones show the highest catabolic activity under conditions of disuse along with the highest anabolic response to mechanical stimulation. The high sensitivity of distal bone regions may be due to their proximity to the ground thus experiencing greater gravity and/or being farther from the heart which causes lower interstitial pressure [71]. Long-term bed rest patients experience the highest bone loss in bones farthest from heart while bone increases in skull due to increased interstitial pressure [72]. Progressive bone loss due to disuse can lead to osteopenia (T score between -1 to -2.5) and in severe cases osteoporosis (T score below -2.5).

Normal daily activities provide essential mechanical stimulation for bone to maintain its strength and structure. Repetitive loading induces bone remodeling as new bone replaces old and damaged bone. The amount of micro-damage is highest in trabecular bone and increases with age as the ability to replace damaged bone decreases. Excessive mechanical loading can increase the level of micro- damage leading to the formation of stress fractures, increasing trabecular break down, and inducing micro cracks in cortical bone [73, 74]. Micro damage induces increased osteoclast activation and results in increased number of BMUs [73]. Excessive damage leads to progressive loss of bone stiffness and strength and total tissue failure due to fracture.

1.5 Disuse Models

Osteoporosis is characterized by decreased bone mineral density and break down of bone microstructure leading to compromised bone structure and strength [75]. Osteoporosis can arise due to aging, with post-menopausal woman most commonly affected, or long-term disuse resulting from extended bed rest or space travel. Regardless of the cause, bone loss is more severe in trabecular bone then in cortical bone. Moreover, these losses are site specific and

concentrated in weight bearing bones such as the femur, tibia, and vertebra. Post-menopausal bone loss is induced by reduced estrogen and is therefore most often studied by ovaricectomy (OVX) animal models [76]. The most common species used are rat [76], mouse [77], dog [78, 79], monkey [80, 81], sheep [82], goat [83, 84], and minipig [85]. Microgravity or long-term bed rest induced bone lost has been studied by using immobilized (IM) [86] rat [87], mouse [88], and dog [68] models. The IM can be induced in limbs by nerve [89], spinal cord [89], and tendon resection[90], limb casting[70], limb bandaging,[91] or hind-limb suspensions[92]. Different methods have different advantages and disadvantages; Table 1 is a comparison between some of the most commonly used models.

The degree of bone loss in IM models is site specific with weight bearing bones experiencing the highest amount of bone loss. IM increases the rate of bone resorption and decrease formation in trabecular and endocortical bone resulting in increased bone marrow area [91, 93]. Cortical bone loss requires long term immobilization [94]. Long-term studies in dogs have shown increased rates of resorption in endosteal surfaces and suppressed rates of bone formation on periosteal surfaces, leading to cortical bone loss[95]. Early trabecular bone loss eventually plateaus, despite continued immobilization, and a similar plateau is expected for cortical bone loss, but has not yet been demonstrated [96]. The earliest detectable trabecular bone loss is found in the proximal and distal tibial metaphysis after 14 days of IM. This is followed by the caudal vertebral bodies at 21 days [97]. The earliest effects on cortical bone can be seen in the femoral shaft at around 21 days via a detectable decrease in bone mineral density [98]. These effects are similar to mechanical disuse in weight-bearing bones[99].

Table 1: Disuse models and physiological effects

Attributes	**Suspension[92]**	**Limb taping[93]**	**Nerve resection[90, 103]**	**Tenotomy[104-106]**	**Limb casting[69, 103]**
Site	Hindlimbs	One hindlimb	One hindlimb	Lower hindlimb	One limb
Surgery	No	No	Yes (Sciatic or femoral nerve)	Yes (knee calcaneal)	No
Hardware	Specialized cages tail harness	No (tape)	No	No	No
Time frame	Short term <5w	Long term	Long term	Short term	Long term
Responses					
Blood Flow affected	Yes	Potential problem	Potential	?	↓ (?)
Cellular fluid shift	Yes	No	No	No	No
Muscle function	Yes	Restricted	No	Mildly affected	No
Nerve function	Yes	Yes	No	No	Yes
Cancellous bone loss	No	↓(50)	↓(50)(72)	↓(50)	↓(60) (68)
Tb Formation	↓(66)	↓(35)	↓(50)	↓(45)	↓
Tb Resorption	No	↑(50)	↑(150)	↑(125)	↑
Cortical bone loss	No	↓(10)	↓(4)	-	↓(50) (14)
Formation (Ps)	↓(85)	↓(90)	↓(40)	-	↓
Resorption (Ec)	No	↑(19)	↑(100)	-	↑
Muscle weight	↓(48)	↓(55)	↓(70)	-	↓
Convenience	Daily care	Daily care	Minor care	Excellent	Weekly care
Recovery Possible	Yes	Yes	No	Possible	Yes

Ps- Periosteal; Ec- endocortical; Tb – trabecular
↑ % increase ↓ % decrease; - no data? - unknown

Table 1. Describing different disuse models and experimental conditions along with physiological responses. Table compares hind limb suspension, limb taping, nerve resection, tentomy and limb casting as different disuse models.

IM models present valuable tools to study the effects of mechanical disuse on bone due to long- term bed rest or long term microgravity but these models also have some limitations when compared to the physiology of human bone. Rodents (rats and mice) are the most common IM model for studying disuse induced bone loss. Rats are inexpensive, easy to maintain, and have a relatively short lifespan with rapid growth [100]. The small size of rats makes them easy to maintain but also reduces the amount of bone and serum samples that can be collected for analyses [100]. Furthermore, rats go through an elongated bone modeling phase (up to 12 months) and undergo little to no intracortical remodeling [101]. Studies have shown that the bone modeling phase significantly slows down as the skeleton matures and is limited to a region 1mm below the growth plate. However, trabecular bone 1mm below the growth plate undergoes remodeling and can be analyzed to study the effects of immobilization on bone remodeling [102]. Bone loss due to aging is concentrated at perimedullary or pre-endocortical bone with minimal effects seen in intracortical bone [70, 87]. The rat model has its limitations, but with proper experimental design these limitations can be accounted for. The mouse model has the same limitations but the broad availability of transgenic mouse models provides for better understating of the role of genetics in bone remodeling [100].

Larger animal models utilizing both primates and non-primates have also been used in IM studies but they are significantly more expensive and harder to maintain due to the longer life spans and slow skeletal growth [100]. Despite these limitations, dogs have been used to study Haversian remodeling [107] and monkeys have been used to study age related osteopenia [108].

1.6 The Effects of Microgravity

Changes in bone strength and loss of total body calcium during space flight have been reported in different studies [109-112]. Astronauts' bones show significant losses following their time in space. Detailed analyses have revealed that bone loss is predominant in weight bearing bones, [113] with large losses in trabecular bone [109] and no significant changes in bone shape and radii [114]. Furthermore, five-year follow up studies have shown that bones continue to lose density over a period of six months after astronauts' return to Earth, and that it takes more than five years for bones to recover from the effects of spaceflight [112].

The effects of microgravity on bone architecture are due to a combination of compromised systemic endocrine-metabolism and regional uncoupling of osteoblast/osteoclast functioning. Studies conducted in Euro Mir 95 showed significant decrease in levels of parathyroid hormone (PTH), bone alkaline phosphatase (ALP), intact osteocalcin, and type 1 pro-collagen peptide (PICP) [115]. These changes affect the cellular activity of bone cells and lead to uncoupling of osteoblast/osteoclast activity. The dynamics of bone remodeling are further affected by reduced numbers and activity of osteoblasts, as in space [116-118] they show lower proliferation, maturation, and impaired bone mineralization. Reduced osteoblast activity along with increased osteoclast activity will lead to the loss of BMD as well as reduced rates of trabecular bone formation and maturation of cortical bone [119]. Space flight data from animals shows that there is no significant effects on osteoclast activity in a space environment [118, 120], but contrary to these data, *in vitro* studies conducted in space show that microgravity impairs osteoclastogenesis and bone resorption [121].

Space studies conducted on astronauts and rats have provided valuable data regarding the effects of microgravity on bone. However, the high cost of space flight has necessitated the development of ground based models of unloading to further analyze the effects of microgravity on a cellular and organ level both *in vivo* and *in vitro*. Previous studies have used hind limb suspension (also known as tail suspension), nerve resection, and total body or leg immobilization models to study the effects of microgravity. The hind limb suspension (HLS) model is generally considered better than the other models as it only affects hind limbs and the forelimbs remain under normal gravity conditions. Thus, HLS enables the study of regional changes in the hind limbs due to loss of gravity/mechanical stress and fluid shifting in hind limbs, while also reducing the systemic effects of microgravity [122, 123]. Furthermore HLS causes the least stress and variation in circadian rhythms and the condition is reversible [124].

Skeletal unloading by HLS simulates the effects of microgravity on bone architecture and osteoblast/osteoclast coupling in many important ways, such as, HLS induces reductions in bone formation, mineralization, and maturation [122, 125-129]; trabecular and periosteal bone showed higher sensitivity to HLS [130]; osteoblast numbers, maturation, and differentiation are significantly reduced in HLS animals, as are anabolic markers [129, 131, 132] . Further, *ex vivo* studies have shown reduced proliferation of osteoprogenitor cells and impaired osteoblastic differentiation [128, 133].

HLS appears to affect the local regulation of bone remodeling but not the systemic factors such as PTH and corticosterone showing little change [134]. Instead, under HLS, local factors such as bone morphogenetic proteins (BMPs), transforming growth factor-β (TGF-β), basic and acidic fibroblast growth factors (bFGF, aFGF), and insulin like growth factors (IGF-1, IGF-II) appear to play a major role in stimulation and proliferation of bone cells, collagen production and

proteoglycans syntheses [135, 136]. Under HLS, bone biomechanical integrity is also compromised with the ones being more prone to fractures [137-139]. All of these changes in bone quality make HLS a good model to study microgravity induced bone loss.

To understand the biological processes underlying bone loss, *in vitro* studies have been conducted on space station using a variety of different bone cells. Osteoblasts and Osteoclasts cultured in space show significantly reduced glucose utilization, and rates of proliferation and mineralization [140-143]. The expression of osteogenic markers is also reduced, with mRNA and protein levels of ALP, COX-2, osteocalcin, and collagen 1 decreased relative to ground-cultured controls [144, 145].In addition, cytoskeletal and nuclear morphology are significantly disorganized, causing cell arrest and hindering cell division and proliferation [142, 146, 147]. Reduction in the expression of mechanosensitive receptors such as epidermal growth factor receptor (EGFr), proteoglycan growth factor beta receptor (PDGFβ receptor), and signaling molecules such as c-fos and shc [148, 149] along with changes in cell physiology adversely affect anabolic activity of osteoblasts.

Conducting *in vitro* studies on the International Space Station is expensive and technically challenging; therefore in order to perform detailed studies of the cellular and molecular mechanism underlying migrogravity induced bone loss, different ground-based simulated microgravity models have been used. The two most common simulated microgravity models are the Random Position Machine (RPM) and the Rotating Wall Vessel (RWV). RWV simulates MG by simulating continuous free fall [150, 151] and RPM exposes cells to different orientations and positions resulting in the gravity vector to being zero, ”gravity-vector averaging” [152]. Studies conducted using these simulated modeled microgravity (MMG) models show down regulation of ALP, Runx2,PTH receptor 1 (PTHr1), BMP4, procollagen, and

osteoglycin, along with other regulatory genes in osteoblasts [135]. Furthermore, matrix mineralization studies show a significant reduction in formation of calcium nodules and collagen matrix formation [144, 153]**.**Taken together, these studies reveal that osteoblasts grown in MMG have the same alterations in cell morphology, cytoskeletal organization, apoptosis rates, and gene expression as cells cultured in space flight.

Experiments conducted in space show that microgravity significantly reduces osteoblast numbers by 60% [143]. This is due to either a higher rate of apoptosis, lower level of differentiation or reduced rate of proliferation. In order to study this in more detail, microgravity experiments have been conducted on MSCs while in space flight and were found to significantly reduce their rate of differentiation into osteoblasts. Basso et al. showed that MSCs extracted from 14 day HLS rats had a 66% reduction in the formation of ALP positive colony forming units and a 76% reduction in osteoblast forming units that was associated with a 50% loss in bone volume, 35% loss in osteoblast number and 46% reduction in bone formation [154]. SMG studies using MSCs has shown down regulation of osteogenic markers, BMP6, COL1A1, osteocalcin, RUNX2 and osteoprotegerin along specific genes and transcription factors required for osteogenesis [155]. MG down-regulates different signaling pathways, altering MSCs' ability to differentiate into osteoblasts but it is not clearly understood which specific pathways are affected.

The effects of MG on osteoblasts and MSCs have been well-studied, but the mechanism behind these changes is still not clear. Recent studies have evaluated different, possibly affected pathways. Zhenget al. suggested that the role of ERK1/2 is to reduce expression of RUNX2 through increasing phosphorylation of p38MAPK in MG [156]. In addition, microgravity reduces activation of IGF-1 activity in cells through deactivation of the IGF-1 receptor, affecting the downstream Ras and Akt pathways which are responsible for proliferation and apoptosis

respectively [135, 157]. Furthermore, other studies have implicated the focal adhesion complex and downstream pathways [141, 143] in mediating the effects of MG on MSCs.

1.7 Countermeasures:

Microgravity affects bone at different levels leading to overall bone loss and increased fracture risk. To make human space exploration possible, it is important to engineer countermeasures to mitigate the catabolic effects of microgravity. Astronauts spend ~2.5 hours per day exercising but this is still not sufficient to prevent bone loss. Furthermore, excessive exercise can have adverse effects on bone quality. Some studies have shown anabolic effects using drugs and growth factors but these pharmacological agents are hampered by systemic adverse effects, reduced efficacy in space, and are expensive to utilize for long time periods[158].

In past decades, researchers have explored the anabolic effects of different mechanical stimuli on bone because the process of bone remodeling is sensitive to mechanical signals and stimuli. Studies have shown that MSCs, osteoblasts, and osteocytes are particularly responsive to mechanical stimulation. Mechanical stimulation induces activation of different enzymes such as MAPKs, Cox-2, iNOS,and alters cell morphology resulting in activation of Ras-ERk1/2, p38-MAPK, β-Catenin, Sclerostin, NF-κB, SMADs, and Akt pathways in a threshold dependent manner [159]. Many different signaling pathways have been identified that respond to mechanical signals by altering levels of growth factors, transcription factors, inducing enzymatic activity, and changing cellular morphology. Mechanostimulation enhances the release of growth factors, including insulin growth factor (IGF),vascular endothelial growth factor (VEGF), platelet-derived growth factor (PDGF), basic fibroblast growth factors (bFGF), transforming growth factor β(TGFβ), and bone morphogenic protein (BMP), that are necessary for regulating

localized osteogenesis [135, 160].The activation of intracellular pathways in combination with elevated growth factors activates transcription factors RUNX2, Osterix, β-catenin, and ATF4 leading to osteogenic differentiation of progenitor cells and osteoblast maturation[159].

The MAPKs pathways have been of particular interest to researchers studying mechano-transduction [161, 162]. There are three distinct MAPKs pathways: extracellular signal-regulated kinases (ERK1/2), junN-terminal kinase/stress activated protein kinases (JNK/SAPK)), and p-38 MAPKs pathway (anti-apoptotic pathway). ERK1/2 and JNK pathways are initiated by Rho GTPase, namely Rac (regulates actin stress fibers) and Rho (formation of membrane ruffles), and Cdc42 (formation of peripheral filopodia) [162]. The collective function of these proteins is to regulate cell membrane morphology and activity of membrane bound receptors, which are important for mechanotransduction [162].

Recent studies have evaluated the effects of microgravity on mechanotransductive pathways. Bikel et al. reported a significant reduction of different integrin subunits in HLS rats after 7 days of suspension along with inactivation of the IGF pathway. The IGF receptor is associated with the Ras –ERK1/2 pathway, regulating proliferation and the RUNX2 transcription factor, and the Akt –anti-apoptosis pathway. The inactivation of IGF can lead to reduced rates of proliferation and increased rates of apoptosis in MG conditions [135]. Zhang et al. observed significant decreases in phosphorylation of ERK1/2 and increased activation of p38-MAPKs in MSCs in MG. Furthermore, MSCs showed increased adipogenic markers in MG environments, suggesting that p38-MAPK activation induces expression of adipogenic transcription factors and such as PPAR γ2 and inactivation of ERK1/2 causes a reduction of RUNX2 levels [156]. The function of the p38-MPAK pathway seems to be cell dependent, as in osteoblasts it activates the osteoblastic transcriptional factor activator protein-1 (AP-1) [159], whereas in MSCs, it seems to

activate adipogenic transcription factors like PPAR γ2 [156]. MG studies performed with fibroblasts showed no significant changes in activity of JNK and p-38 MAPKs but a reduction in ERK1/2 activity [162].

Different models of mechanotransduction have been used to understand the effects of mechanotransduction, namely: cyclic strain [163-166], vibration [167-169], and low intensity pulsed ultrasound [170-174]. Cyclic strain has shown encouraging results *in vitro* but its *in vivo* applications are limited. Mechanical vibration has shown good results in both *in vitro* and *in vivo* studies, but there are issues involved about the systemic effects of vibrations in whole body vibrations. Ultrasound acoustic vibrations can be readily applied *in vivo* and human studies and have shown it to have anabolic effects on osteopenic tissue and bone fractures. Ultrasound provides a non-invasive and targeted treatment to regions of interest and can be calibrated easily. Moreover, as the FDA has already approved use of low intensity pulsed ultrasound for non-union fractures, the path toward regulatory approval as a countermeasure for disuse induced bone loss is easier than for a novel methodology.

1.8 Low intensity Pulsed Ultrasound:

An ultrasound wave provides pressure waves which induce biochemical events in bone cells [175-177]. The effects of LIPUS have been well-studied and show that cells treated with LIPUS have altered intercellular activity, cytokine release [178], gene expression [179], calcium mineralization [180], Akt pathway activation [181], potassium influx [182], angiogenesis [183], adenyl cyclase activity, and TGF-b synthesis [184]. These studies and many others suggest an increase in rate of bone formation in the presence of LIPUS.

The exact mechanism through which LIPUS activates osteoblasts to increase the rate of bone formation remains unknown. LIPUS is known to induce acoustic streaming in interstitial fluid as well as localized mechanical vibrations in the extracellular matrix [185] that result in local deformation of osteoblast cell membranes and shear stresses and strains [163, 164, 186-189]. These mechanical deformations activate receptors on cell membrane such as integrins, mechanosensitive-calcium channels, G-proteins, IGF, TGF-β/BMP, and gap junctions, activating different downstream pathways [181, 188, 190-193].

Studies have also examined the effects of LIPUS on different mechanotransductive pathways. Tang et al. reported activation of the Akt pathway and p-13 kinases, through aggregation of integrin expression, resulting in induction of nitric oxide, hypoxia inducible factor-1, and increased activity of cox-2 [191, 192]. Ultrasound treated osteoblasts also show higher nuclear localization of β-catenin and activation of Wnt signaling pathway[194]. A microarray study done on ultrasound treated osteoblasts showed enhanced gene expression of integrins, TGF-β family, IGF family, MAPKs pathway, ATP-related, guanine nucleotide binding protein family, lysyl gene, and apoptosis-associated gene families compared to non-treated osteoblasts [195-198].

These cellular studies indicate that ultrasound treatment can activate mechanotransductive pathways and significantly increase osteogenic differentiation in progenitor cells and osteogenic maturity in osteoblasts. Catabolic effects of microgravity are due to a lack of mechanical stress in zero gravity that leads to inactivation of mechanotransductive pathways. Ultrasound exposure has mechanotransductive properties that allow it to induce mechanical stress in bone cells and activate osteogenic pathways leading to bone formation. Therefore, the anabolic effects of ultrasound may be able to be used as a countermeasure to prevent the

catabolic effects of microgravity. *The objective of these experiments is to study the ability of ultrasound to function as a countermeasure to the catabolic effects of MG on osteoblasts and mesenchymal stem cells in an in vitro simulated microgravity system and on bone quality and architecture in a HLS mouse model*. These studies will test the overall hypothesis that ultrasound prevents the catabolic effects of microgravity in simulated microgravity *in vitro* and *in vivo* .

Chapter 2

Hypotheses and Specific Aims

2.0 Hypotheses and Specific Aims

Given the degree to which microgravity induces bone loss, the future of human space flight requires the development of a non-invasive and targeted mechanotransductive therapy to maintain bone integrity. These experiments were designed to study the therapeutic potential of LIPUS in the *in vivo* and *in vitro* disuse models. The experiments were designed to quantify bone formation, MSCs differentiation, and osteoblast activity under disuse conditions and determine if LIPUS treatment could mitigate these detrimental effects. The study was divided into three Specific Aims: Specific Aim 1 examined the effects of LIPUS treatment in mice subjected to a hind limb suspension (HLS) disuse model for 4 weeks; Specific Aim 2 was designed to study the effects of LIPUS on the differentiation of MSCs into osteoblasts under simulated a microgravity (SMG) environment; and Specific Aim 3 was designed to study the effects of LIPUS on osteoblast activity in an SMG environment.

Specific Aims

2.1 *Specific Aim 1:* Determine if LIPUS can prevent bone loss in hind limb suspended mice *in vivo*.

Hypothesis 1A: LIPUS treatment will reduce the loss of bone quality/quantity in hind limb suspended mice.

Hypothesis 1B: LIPUS treatment will enhance bone mechanical properties in hind limb suspended mice.

2.2 *Specific Aim 2:* Determine the effects of LIPUS on human mesenchymal stem cell differentiation in microgravity *in vitro*.

Hypothesis 2: LIPUS exposure will enhance osteogenic differentiation in MSCs under microgravity conditions relative to non-treated cultures

2.3 *Specific Aim 3A:* Evaluate the effects of LIPUS on osteoblast activity during simulated microgravity *in vitro*

Hypothesis 3A: Ultrasound will increase osteoblastic activity in microgravity conditions.

Specific Aim 3B: Evaluate the effects of LIPUS on osteoblast gene expression during simulated microgravity *in vitro*

Hypothesis 3B: Ultrasound will enhance expression of osteogenic genes.

Chapter 3:

Anabolic Effects of low intensity pulsed ultrasound partially retain bone microstructure and mechanical properties in a murine disuse model

Specific Aim 1: *Determine if LIPUS can prevent bone loss in hind limb suspended mice in vivo.*

3.1 Abstract:

Long-term bed rest, brain/spinal cord injury, and space travel induces bone loss due to decreased mechanical stress. Different anabolic and anti-resorptive agents have been used to limit or mitigate bone loss under such conditions. However, the results for these treatments have been mixed, in part due to the localized nature of disuse induced bone loss which is concentrated on loading bearing bones. This study was based on the hypothesis that low intensity pulsed ultrasound (LIPUS) generated acoustic wave can provide non-invasive, anabolic and targeted stimulus that can reduce bone loss under disuse conditions. Three-month old C57BL/6 mice were randomized to five groups, age match (AM), non-suspended sham (NS), non-suspended –LIPUS (NU), suspended sham (SS), and suspended-LIPUS (SU) groups. After four weeks of suspension, micro CT analyses showed significant decreases in trabecular bone volume/ tissue volume (BV/TV) (36%, $p<0.005$),bone mineral density (BMD) (3%, $p<0.05$), trabecular thickness (Tb.Th) (12.5%, $p<0.005$), and increase in bone surface/bone volume (BS/BV) (16%,$p<0.005$) relative to age match (AM). Application of LIPUS for 20 min/day for 5 days/week, significantly increased BMD (3%, $p<0.05$), Tb.Th (6%, $p<0.05$), and decreased BS/BV (10%, $p<0.005$) relative to SS mice.

Histomorphometric analyses showed a breakdown of bone microstructure under disuse conditions. In comparison to SS mice, LIPUS treated bone showed increased structural integrity with increased bone formation rates at metaphyseal endosteal and trabecular surfaces (0.104 ± 0.07 vs0.031 ± 0.30 $\mu m^3/(\mu m^2)/d$. Four-point bending tests of SS femurs showed reduced elastic modulus (53%, $p<0.05$), yield (33%, $p<0.05$), and ultimate strength (45%,$P<0.05$) at the femoral diaphysis relative to AM samples. LIPUS stimulation mitigated the adverse effects of

disuse on bone elastic modulus (42%, $p<0.05$), yield strength (29%, $p<0.05$), and ultimate strength (39%, $p<0.05$) relative to SS femurs. Analyses of contralateral control limbs from SU or NU showed that LIPUS had no systemic effects, supporting the hypothesis that LIPUS provided targeted stimulation. In summary, the data from this study indicate that LIPUS has efficacy as a non-invasive, targeted therapy for disuse osteoporosis.

3.2 Introduction

Disuse osteoporosis is a regional phenomenon, mostly concentrated at load bearing sites. Lower limbs are subjected to a high degree of mechanical stress during daily activities that result in functional static gravitational forces, ground reaction forces, and dynamic muscular contractions. Lack of mechanical stress due to long-term bed rest, brain/spinal cord injury, paralysis, and long-term exposure to microgravity can severely compromise bone microstructure and bone mineral density leading to fractures. The low stresses resulting from disuse reduce bone formation and increase bone resorption on periosteal, endocortical, and trabecular surfaces. Long-term disuse can lead to structural changes in long bones that result in the formation of rounder shaped long bones rather than the typical triangular shape, reducing moment of inertia and strength [67].

Growing and mature skeletons responded differently to disuse with bone loss concentrated in different areas of bone surfaces [68-70]. Studies done on growing dogs showed higher bone loss on periosteal surfaces, due to reductions in appositional bone formation, that resulted in smaller bones with reduced second moments of inertia [68]. In contrast, mature dogs showed increased bone loss at the endosteal surface causing an expansion of the marrow cavity and increased cortical porosity [68]. Distal bones of the forelimbs showed the highest bone loss in young and adult dogs, suggesting higher sensitivity of these sites to lack of mechanical stresses [68].

The distal most regions of bones show the highest catabolic activity during disuse and the highest anabolic response to mechanical stimulation. Long-term bed rest patients experienced the

highest rates of bone loss in bones farthest from the heart while bone formation increased in the skull due to increased interstitial pressure [72]. In a cross-section study of spinal-cord injury patients, Kiratli et al. found 27%, 25%, and 43% reductions in BMD at the femoral neck, mid-shaft, and distal femur, respectively, compared to normal controls [199]. Similar trends have been observed in astronauts, with mean BMD decreases of 5.4% in trabecular bone seen after 6 months of spaceflight [114].

Numerous anti-resorptive/anti-catabolic and anabolic agents haves been studied as treatments for osteoporosis. Anti-resorptive agents such as bisphosphonates [200, 201], RANKL inhibitors [201], and strontium ranelate [202, 203] reduce osteoclast differentiation, maturation, and activity, leading to increased bone strength and delayed remodeling. Anabolic agents such as PTH [204] and anti-sclerostin antibodies [205], increase bone formation rates, bone mass, and mechanical strength by enhancing osteoblast activity. Both anti-resorptive and anabolic agents have shown encouraging results in treating osteoporosis both in clinical (bisphosphonates, PTH) and pre-clinical studies (strontium ranelate, anti-sclerostin antibody). However, these anti-resorptive and anabolic therapies have systematic effects, while disuse osteoporosis is a more localized pathology. Therefore it is possible that these therapies can lead to undesired effects in healthy bones. As disuse osteoporosis is caused by lack of mechanical stimulation, numerous studies have evaluated the use of induced mechanical stimulation as a countermeasure for disuse osteoporosis. Several different modes of mechanical stimulation have been evaluated, namely: cyclic strain [163-166], vibrations [167-169], and LIPUS [170-174]. Cyclic strain has shown encouraging results *in vitro* but *in vivo* applications are limited by skeletal structure. Mechanical vibrations have shown promising results both *in vitro* and *in vivo* but there are questions regarding systemic effects of vibrations in whole body vibrations. LIPUS stimulation creates

acoustic vibrations that generate localized shear stress on cell membranes and has been shown to induce anabolic responses in osteoblasts [206]. Moreover, LIPUS can be readily applied *in vivo* and studies and have shown it to have anabolic effects on fresh fractures [207], delayed unions [208, 209], non-unions [208, 209], and osteoporosis [172] both in animal models [207, 208, 210] and clinical studies [211, 212]. LIPUS provides a non-invasive and targeted treatment for specific regions of interest. Furthermore, because the FDA has approved LIPUS for non-union fractures regulatory approval for its use in treating disuse osteoporosis will likely present less of a challenge than other modes of mechanical stimulation.

The objective of this study is to investigate the effects of LIPUS on the femora and tibiae of hind limb suspended mice using high resolution microCT, dynamic histomorphometry, and mechanical testing. It is hypothesized that exposure to LIPUS will provide sufficient mechanical stimulation to counteract the disuse induced bone loss in the hind limbs of these mice.

3.3 Methods and Materials:

3.3.1 Animals

Twelve-week old black B6/C57J mice were randomized into 5 groups (n=15 per group): Age match (AM), Sham non-suspended (NS), Non-suspended + LIPUS (NU), Sham suspended (SS), and Suspended + LIPUS (SU). LIPUS groups were treated with 1 kHz, 20% duty cycle, 30 mw/cm^2 pulsed ultrasound exposure for 20 min/day for 5 days per week over 4 weeks with a Sonicator 740® (Mettle Electronics, Anaheim, CA). For the duration of treatment, the animals were anesthetized with isoflurane. LIPUS was applied to the left femur and tibia in LIPUS treated animals and right legs were used as contralateral untreated controls. Sham groups were treated in same manner except that an inactive ultrasound transducer was utilized. Suspended

mice were tail suspended for a period of 4 weeks. The age match group was not exposed to suspension or treatment.

Animals were observed for signs of stress twice a day and animal weights were measured daily for the duration of the study. In cases of weight loss animals were given flavored treats and to reduce dehydration, animals were given subcutaneous injections of saline. If any animals exhibited more than 20% weight loss, infection or severe distress, veterinary staff was notified and treatment recommendations were followed. All the procedures were done in accordance with IACUC approved protocols.

After 4 weeks the animals were euthanized using CO_2 and all four limbs were harvested and stored at -80°C until analysis.

3.3.2 Microcomputed tomography

The proximal regions of the right and left tibiae were scanned at 12 micron resolution using microCT (µCT40, Scano Medical). To be consistent in analyses, a 400 slice region of the bones distal to the end of epiphysis was acquired and the microstructure was evaluated for a region beginning 20 slices below the epiphysis and continuing for 80 slices. To evaluate the region of interest, contour lines were manually drawn around the trabecular bone every 10 slices and contour lines were morphed to fit the intervening slices.

The regions of interest were then evaluated for: trabecular bone fraction (%, BV/TV), bone mineral density (mgHA/cc, Mean2), Trabecular number (1/mm, Tb.N), Trabecular Thickness (mm, Tb.Th), Trabecular separation (mm, Tb.Sp), and Bone surface/Bone volume (mm^2/mm^3, BS/BV) to determine the catabolic effects of microgravity on bone microstructure and efficacy of LIPUS treatment in preventing these effects.

Cortical bone was analyzed from the left and right tibiae at the mid-diaphysis, also at 12 micron resolution. Measurements included: cortical bone thickness (Cort.Th), cortical bone mineral density (Cort. BMD), endosteal surface (Endo S), periosteal surface (Peri S), and bone area (BA).

3.3.3 Dynamic Histomorphometry

Mice were injected with Alizarin red and Calcein. Calcein (15mg/Kg) was injected at weeks 1 and 3 and alizarin red (15mg/Kg) was injected at weeks 2 and 4. Mice were sacrificed after 4 weeks and tibias were stored at -80C. Proximal tibiae were scanned using microCT and samples were prepared for histomorphometry using poly-methyl methacrylate resin (PMMA) embedding. Briefly, the bones were serially dehydrated using 70%, 90%, and 100% isopropyl alcohol, cleaned with petroleum ether and infiltrated with PMMA in three phases. In the first infiltration, the bones were incubated in 85% methyl methacrylate + 15% N-butyl phthalate, the second infiltration was done with 85% methly methacrylate + 15% % N-butyl phthalate +1g/100ml benzoyl peroxide and in third infiltration, the bones were incubated in 85% methyl methacrylate + 14% % N-butyl phthalate +2g/100ml benzoyl peroxide. At the completion of infiltration the samples were then embedded in 85% methyl methacrylate + 14% % N-butyl phthalate +2g/100ml Benzoyl Peroxide solution at 37°C. The tibias were polished and 5µm thick coronal sections were cut using a microtome (Leica Bannockburn,IL). Osteomeausure software (Osteometrics, Decatur,GA,USA) was used to trace calcein and alizarin red labels in proximal tibia. Areas below the growth plates were contoured manually (metaphysis). The areas of evaluation were consistent with the regions scanned by microCT. Regions of interest were assessed in cortical bone, trabecular bone, voids, and double and single labels. Samples were analyzed for mineral deposition rate (Mar, µm/day), defined as the distance between double

labels divided by the interval of injections (14 days), double labels from alizarin and calcein were labeled separately and Mar values were averaged to determine average mineral deposition rate over 14 days. Mineralizing surface was obtained by adding the ratio of double label surface to 50% of the ratio of single label surface (dLS/BS + (0.5*sLS/BS). Mineralizing surface was calculated separately for alizarin red and calcein and average mineralizing area has been reported. Average bone formation rates were calculated by averaging alizarin red and calcein for BFR/BS ($\mu m^3/\mu m^2$/day) values. Data from osteomeasure was also used to calculated Bone volume / Tissue volume (BV/TV), bone surface/ bone volume (BS/BV), Trabecular Thickness (Tb.Th), and Trabecular separation (Tb.Sp).

3.3.4 *Finite Element Modeling*

Finite element modeling (FEM) was used to model the effects of uniaxial compression on proximal tibiae. MicroCT images of proximal tibia (n=7) were exported as dicom files and stacked together to form 3-D models using ScanIP software (Simpleware, UK). The slices exported were kept consistent with the slices analyzed for microCT analysis. 3-D models were meshed using ScanIP using tetrahedral elements and the total numbers of elements were kept within a range of 0.75 – 1 $x10^6$ elements. ABAQUS (Simulia, USA) was used to apply incremental uniaxial strain of 1, 5, and 10% on the top surfaces of the 3-D models with bottom surfaces restrained. Cortical and trabecular both were assigned the same Young's modulus of 10 GPa, mass density of 1500 $kg/m^3$and Poisson's ratio of 0.3 (Figure 2).

3.3.5 Mechanical Testing:

Four-point bending was performed to determine the stiffness and strength of left femora from the AM, NS, NU, SS, and SU groups. Four point bending was selected over three point

bending to minimize shear stresses. An MTS machine (585 Mini Bionix II) was used along with a 100 N force transducer (SMT1-100N, Interface). All samples were thawed slowly to room temperature. The femurs were loaded in the four-point bending jig such the mid-diaphysis of each femur was positioned in the middle of the supports (Figure 3), the posterior sides were facing upwards, and the load was applied on the posterior – anterior axis. The loading conditions were controlled by Multi Purpose TestWare software (MTS). The piston was lowered with preload of 1.5 N and then subjected to a ramp load at a rate of 0.1mm/s until complete failure occurred. Force and strain data were recorded and exported to Microsoft Excel for analyses. The Force/Strain curves, along with the mid-diaphyseal μCT scans, were used to calculate Young's modulus, stiffness, and strength using the equations listed below.

Figure 2: Finite Element Modeling

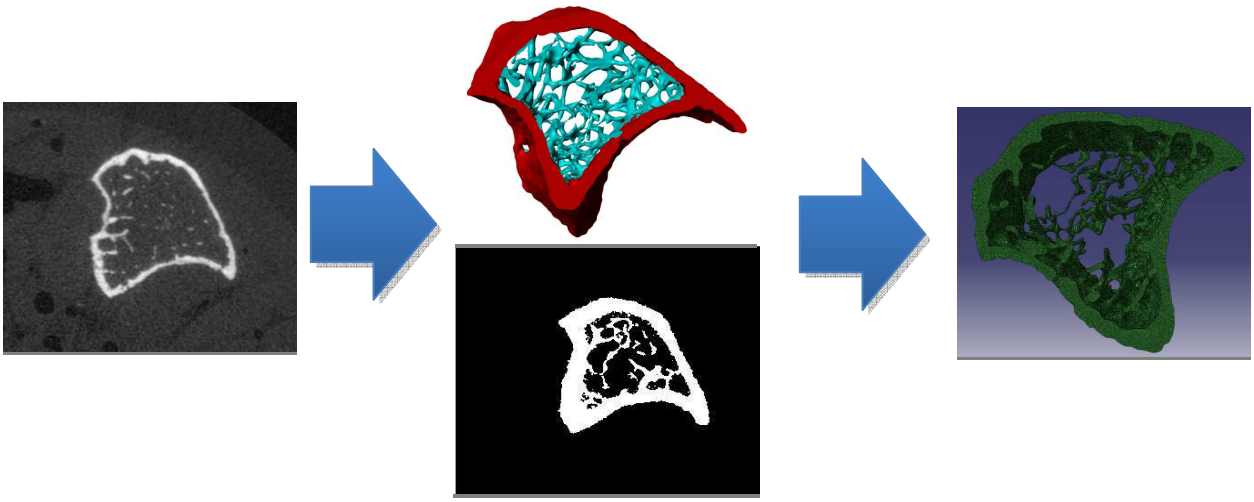

Figure 2: Finite element modeling of the proximal tibia**.** Dicom files were exported from the MicroCT and reconstructed into 3D models using ScanIP. The models were then meshed with tetrahedral elements and exported to ABAQUS (Simulia,USA) for simulated compressive loading.

\

$$I = \pi \frac{(a^3b - \acute{a}^3\acute{b})}{64} \quad (1)$$

$$E = S\left(\frac{c^2}{12I}\right)(3L - 4C) \quad (2)$$

$$E = \frac{\sigma}{\varepsilon} \quad (3)$$

$$\sigma = \frac{Fac}{4I} \quad (4)$$

$$\varepsilon = d\left(\frac{6a}{2c(3L-4c)}\right) \quad (5)$$

Moment of inertia (I) was calculated using equation 1 where a, b, a', and b' were measured using microCT images (Figure 3a). Elastic modulus (E) was calculated using stiffness (S); force over strain data obtained from four point bending; "L," defined as the distance between the bottom supports; and "c," as the distance between the upper support and the midpoint of mid-diaphysis. Stiffness was measured as the slope of the plastic region from the force vs strain graphs (Figure 3b). Elastic modulus was confirmed using equation 3, 4, and 5. Stress (σ) and strain (ε) were calculated by taking into account the applied force (F), displacement of piston (d), a, c, I, and L.

3.3.6 Statistics:

The GraphPad Prism 3.0 software was used to run statistical analyses. All of the data was presented in means ± standard deviation. One-way ANOVA with Newman Keulspost hoc was used to calculate significance within the different groups and time points; student t-test was used within contralateral controls. A *p*-value of <0.05 was considered to be significant.

Figure 3 – Four Point bending setup
a)

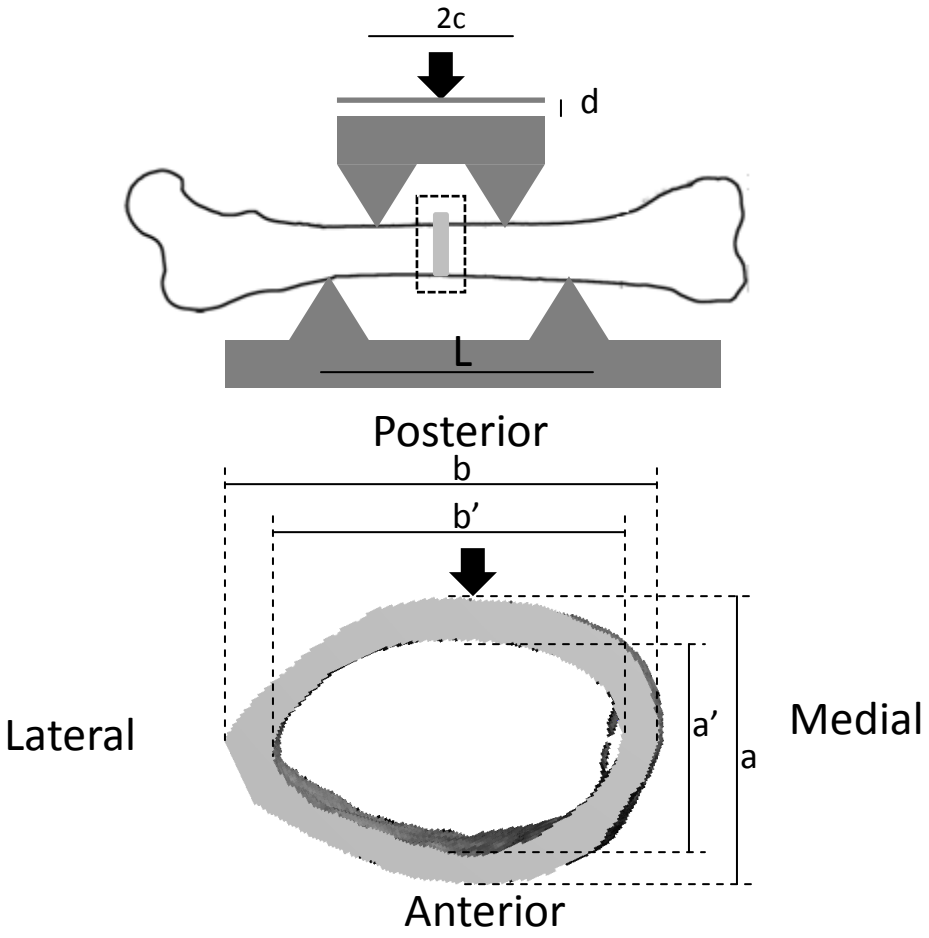

3 b)

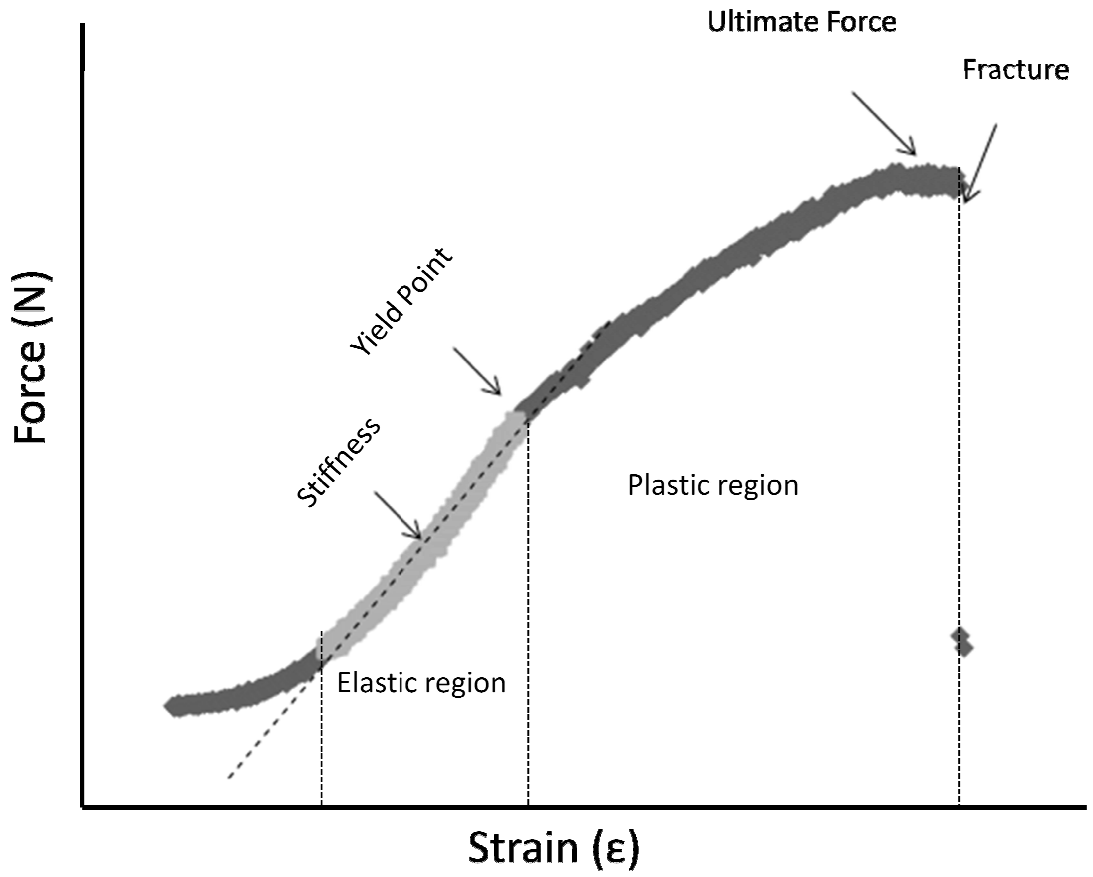

Figure 3a): Four Point bending setup, the load was applied on the posterior – anterior axis.
3b): Typical force-strain curve generated by four-point bending. Stiffness was calculated from the tangent at the elastic region. Yield and ultimate strength were calculated using the yield point and ultimate force measurements from force-strain curve.

3.4 Results:

3.4.1 Micro CT Shows Anabolic effects of LIPUS in trabecular and cortical bone

The microCT analyses of the proximal tibiae from AM mice showed dense and intact trabecular struts with no apparent differences when compared to either of the non-suspended groups (NS,NU) (Figure 4). In contrast, trabecular struts in suspended mice (SS) appear to be thinning and breaking down. LIPUS treated tibiae (SU) demonstrate more intact and denser trabecular struts relative to untreated (SS) samples. Quantification of microCT parameters showed that SS mice had a 36% decrease in trabecular BV/TV ($p<0.001$, Figure 5a), 3%in bone mineral density BMD ($p<0.05$, Figure 5b), 4% in Tb.N ($p<0.05$, Figure 5c), 12.5% in Tb.Th ($p<0.005$, Figure 5d), along with a 16% increase in BS/BV, in comparison to AM mice (Table 2). Application of LIPUS increased trabecular BMD by 3 %($p<0.05$) ,Tb.Th by 6% ($p<0.05$), and decreased BS/BV by 10% ($p<0.05$). BV/TV, Tb.N, and Conn. Den showed positive trends but no significant changes were seen following exposure to LIPUS, when compared to SS mice. Tibiae from NS and NU mice did not show any differences with AM controls, suggesting that LIPUS has no adverse effect on healthy bone while showing anabolic effects in unloaded tibia. LIPUS effects were localized to treated left tibia as no significant differences were observed in non treated NU and SU mice.

Cort.Th showed 8% decrease between the AM and SS groups ($p< 0.01$, Figure 6a), while the other parameters didnot show any significant changes between AM and SS groups. However, there were trends towards decreased Cort,BMD, Inertia, MoI, Peri S, and BA (Table 3, Figure 6 b-f). Exposure to LIPUS increased Cort.Th ($p<0.05$), Peri S ($p<0.05$), and BA ($p<0.05$) in SU animals, when compared to contralateral controls (left tibia vs right tibia, Figure 6 a-f). Differences between the left tibia of SS and SU were not significant but positive trends were

apparent. Trabecular bone was more responsive to unloading and LIPUS treatment than cortical bone. It is speculated that a longer duration of study will show significant difference for cortical bone parameters.

Table 2: MicroCT Proximal Tibia Trabecular Bone Data

	AM	NS	NU	SS	SU
BV/TV	0.086187±0.025	0.08515±0.019	0.08009±0.025	0.05475±0.023***	0.06176±0.024
	0.08657±0.028	0.08862±0.023	0.08292±0.024	0.05245±0.014***	0.05686±0.089
BMD (mmHg/cc)	771.343±23.60	762.037±21.77	758.847±19.99	747.862±26.49*	772.502±21.50†
	773.603±17.07	765.202±25.60	765.352±29.6	754.623±18.72	742.896±40.58‡
Tb.Th (mm)	0.03894±0.0026	0.03792±0.0031	0.03635±0.003	0.03407±0.0031**	0.03633±0.004†
	0.03753±0.0028	0.03782±0.0036	0.03772±0.0028	0.03322±0.0014*	0.03293±0.0042‡
Conn. Den	87.4428±48.26	83.7609±32.74	81.8453±47.15	41.4259±31.03	45.7749±41.11
	79.756±48.31	92.7583±40.83	80.6469±45.09	36.3662±24.87	44.9833±40.68
Tb.N	4.86308±0.49	4.91501±0.41	4.64126±0.47	4.18122±0.51**	4.25086±0.55
	4.82827±0.49	4.93701±0.45	4.88611±0.39	4.20087±0.46*	3.94239±0.83
BS/BV	73.5287±7.00	73.9497±5.66	76.4512±9.22	85.4138±6.97***	77.6242±6.96††
	71.7236±6.66	73.5559±7.53	74.0938±5.50	84.309±8.97**	86.4818±13.03‡

Table 2: MicroCT analyses of trabecular bone at metaphysis of proximal tibia**.** This table illustrates the effects of LIPUS on trabecular bone in suspended and non-suspended mice proximal tibiae. BV/TV (Bone Volume/ Tissue Volume), BMD (Bone Mineral Density), Tb.Th (Trabecular Thickness), Conn.Den (Connectivity Density), Tb.N (Trabecular Number) and BS/BV (Bone Surface/Bone Volume). Grey shaded rows are for treated tibia (left) and clear ones are for non-treated (right) tibiae.

* P<0.05, ** P<0.01, ***P<0.001 relative to AM

† P < 0.05, †† P< 0.01 relative to SS,

‡ P<0.05, ‡‡ P<0.01 relative to left tibia (contralateral control)

Table 2 :MicroCT Mid-Diaphysis Cortical Bone Data

Index	AM	NS	NU	SS	SU
Cort. Th (mm)	0.184293±0.008	0.182508±0.008	0.184818±0.0099	0.16905±0.008**	0.176936±0.008
	0.184117±0.010	0.183936±0.010	0.1842±0.0087	0.171663±0.007	0.168238±0.010‡
BMD (mmHg/cc)	1065.14056±23.97	1062.00229±22.30	1059.52109±17.48	1053.97±16.116	1050.53±16.23
	1007.65±21.31	1065.93114±20.38	1057.894109±18.86	1048.327±18.558	1051.641±16.64
Endo. S (mm^2)	2.841675±0.26	2.77561667±0.20	2.912536364±0.27	2.86255±0.28	2.9799±0.244
	2.741357±0.27	2.8249±0.36	2.773427273±0.19	2.8973±0.24	2.89912±0.21
Peri. S (mm^2)	4.4008±0.54	4.275±0.40	4.469244±0.48	4.1849±0.47	4.4698±0.39
	4.3609±0.36	4.3043±0.29	4.3569±0.44	4.1527±0.37	4.1412±0.32‡
Bone Area (mm^2)	0.6281±0.04	0.627±0.04	0.640847273±0.07	0.60057±0.033	0.6214±0.04
	0.6341±0.05	0.6231±0.04	0.626433636±0.05	0.59561±0.0289	0.5847±0.035‡
pMOI(mm^4)	0.2163±0.02	0.212±0.04	0.2167011±0.029	0.19122±0.035	0.2059±0.037
	0.2148±0.05	0.2112±0.04	0.21377±0.05	0.19384±0.034	0.20286±0.014

Table 3:MicroCT analyses of cortical bone at the mid-diaphysis of tibia. This table illustrates the effects of LIPUS on cortical bone in suspended and non-suspended mice proximal tibiae. Cort.Th (Cortical Thickness), BMD (Bone Mineral Density), Endo.S (Endosteal Surface), Peri.S (Periosteal Surface) and pMOI (polar Moment of Inertia).Grey shaded rows are for treated tibiae(left) and clear one are for non-treated (right) tibiae.

* P<0.05, ** P<0.01, ***P<0.001 relative to AM,

† P < 0.05, †† P< 0.01 relative to SS,

‡ P<0.05, ‡‡ P<0.01 relative to left tibia (contralateral control)

Figure 4: MicroCT images of trabecular proximal tibia

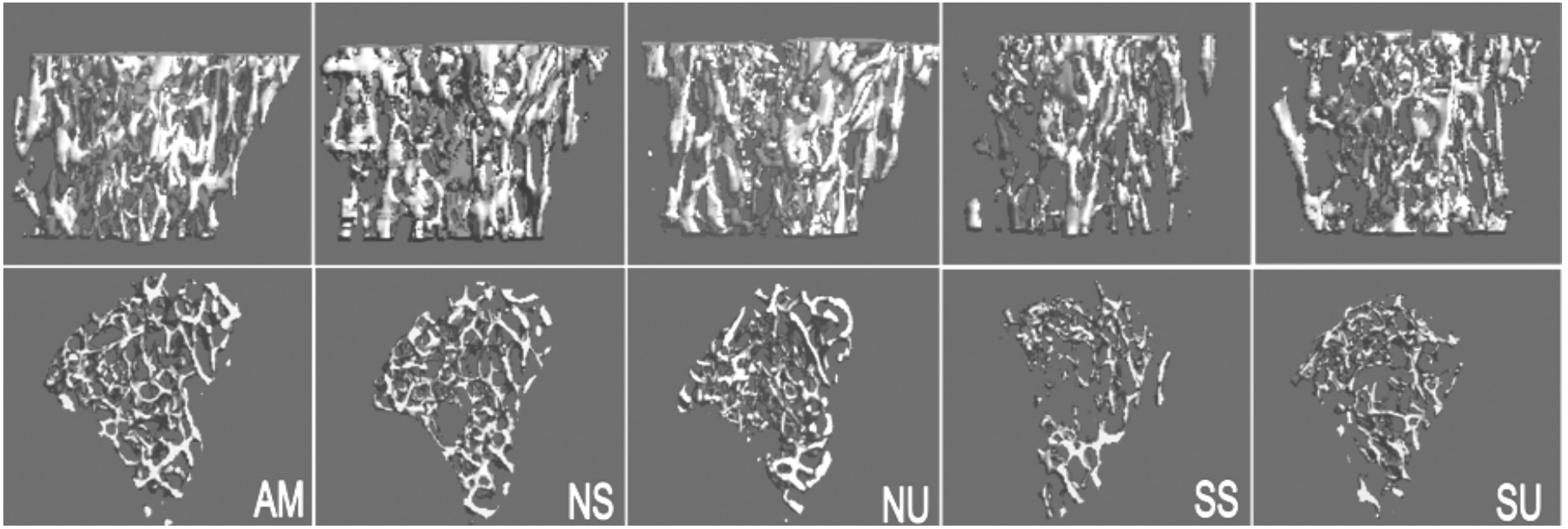

Figure 4: Representative Proximal tibiae longitudinal and cross sectional images showing intact trabecular struts in AM,NS and NU mice. SS mice show disintegrated trabecular struts in proximal tibiae, exposure to LIPUS (SU) show improved trabecular struts structure.

Figure 5: Trabecular Bone MicroCT

a)

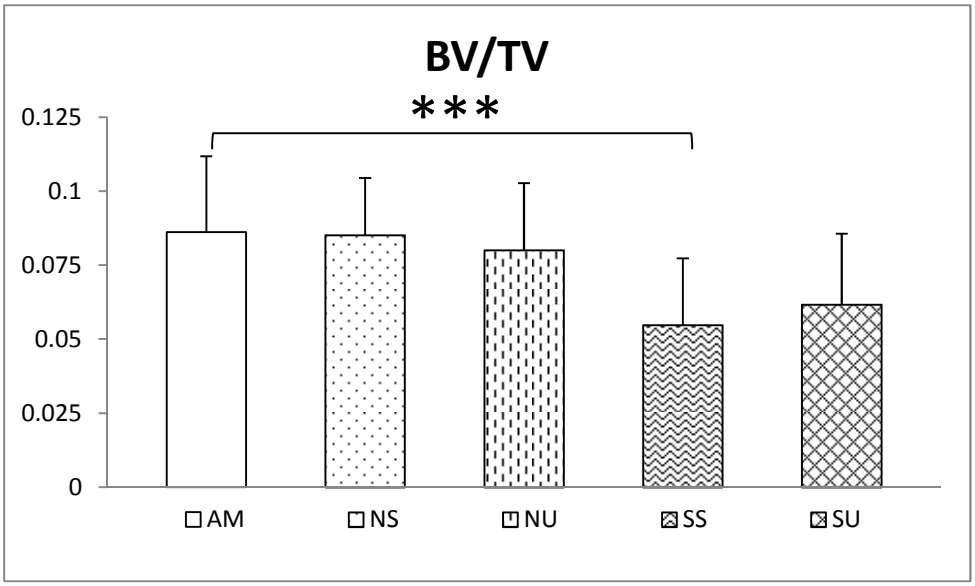

b)

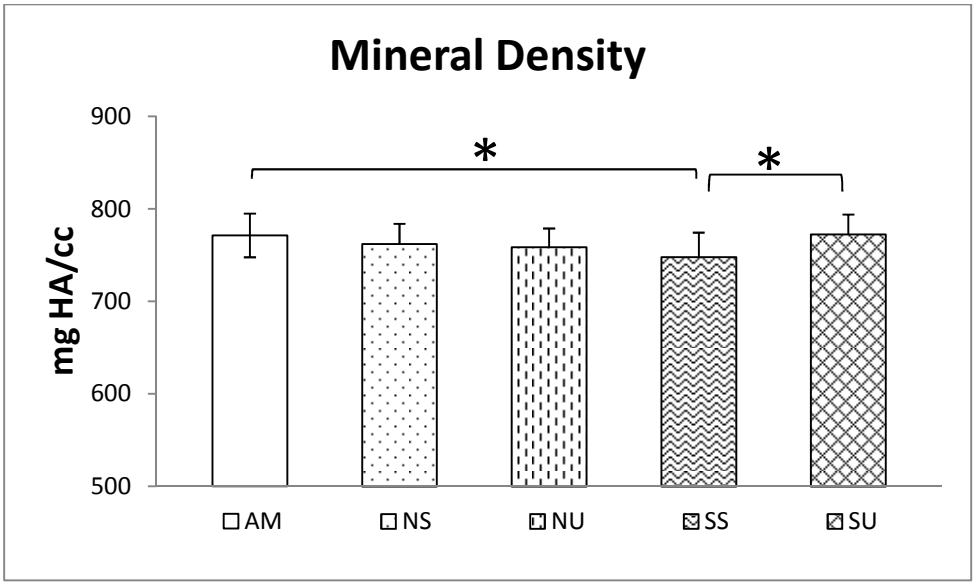

c)

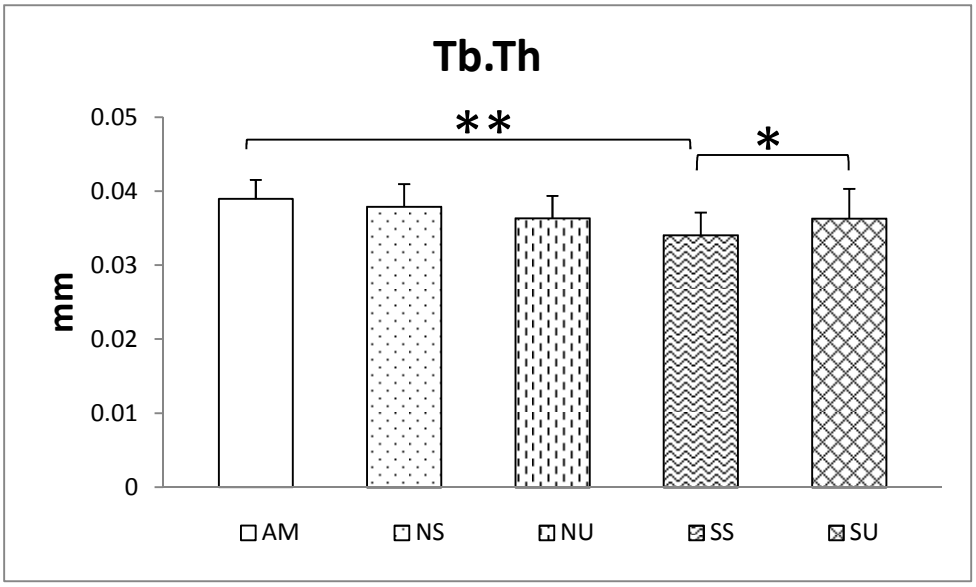
Tb.Th
0.05
0.04
0.03
0.02
0.01
0
mm
**
*
AM
NS
NU
SS
SU

d)

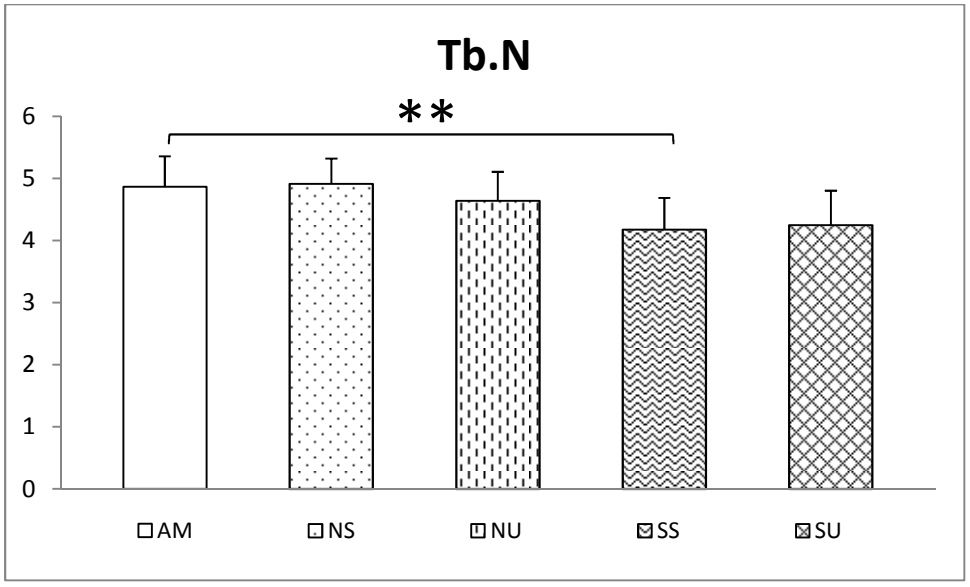
Tb.N
6
5
4
3
2
1
0
**
AM
NS
NU
SS
SU

e)

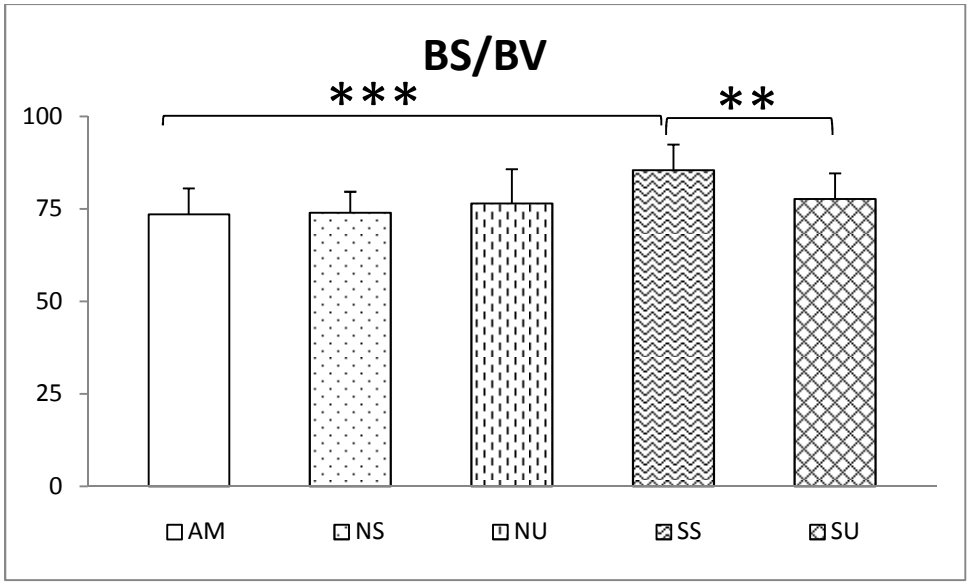

Figure 5: Series of bar graphs showing the results of microCT assessment of Trabecular Bone, showing significant changes in unloaded mice tibiae. LIPUS treatment show anabolic effects on trabecular bone by significantly increasing BMD, Tb,Th and reducing BS/BV. NS and NU tibiae didn't show any difference with AM controls, implying that LIPUS has no adverse effect on healthy bone, while showing anabolic effects in unloaded tibiae.

a) BV/TV: 36 % bone volume fraction decrease was calculated in SS mice. LIPUS doesn't increase bone volume fraction in suspended mice (SU). LIPUS exposure in non-suspended mice showed no difference.

b) BMD: Suspension (SS) significantly reduces bone mineral density in trabecular bone (app 2.5%), LIPUS treatment enhances bone mineral density in SU to nearly the level seen in age match animals.

c) Tb.Th: SS mice showed significant reduction in trabecular thickness; SU mice showed significant increase.

d) Tb.N: Trabecular number showed significant decrease in HLS animals; LIPUS expose doesn't seem to recover trabecular number

e) BS/BV: SS mice show osteopenic tendencies in bone surface area/volume ratio as it increased significantly and SU mice showed significant decrease in bone surface/volume ratio.

*P < 0.05, **P<0.01, ***P<0.001

Figure 6: Cortical Bone MicroCT

a)

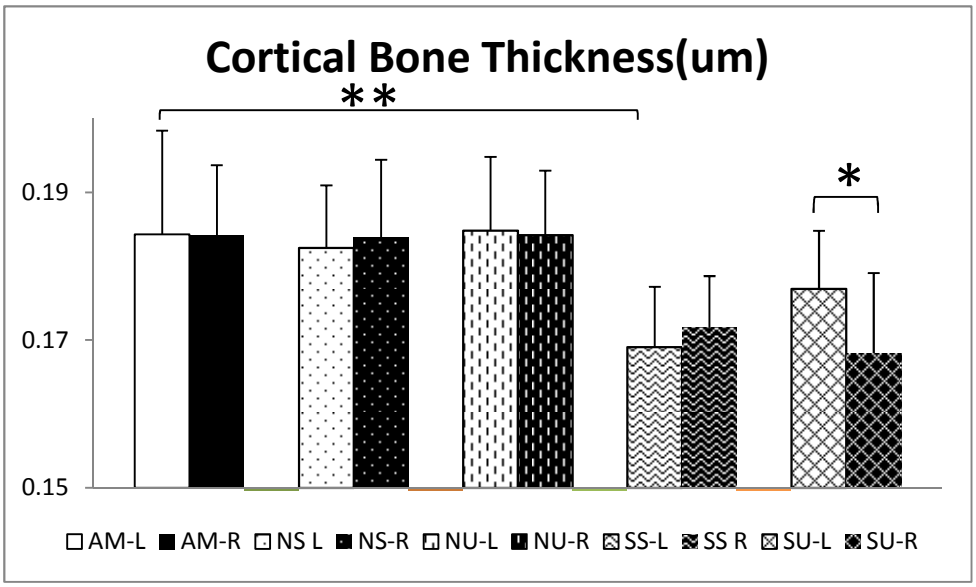

b)

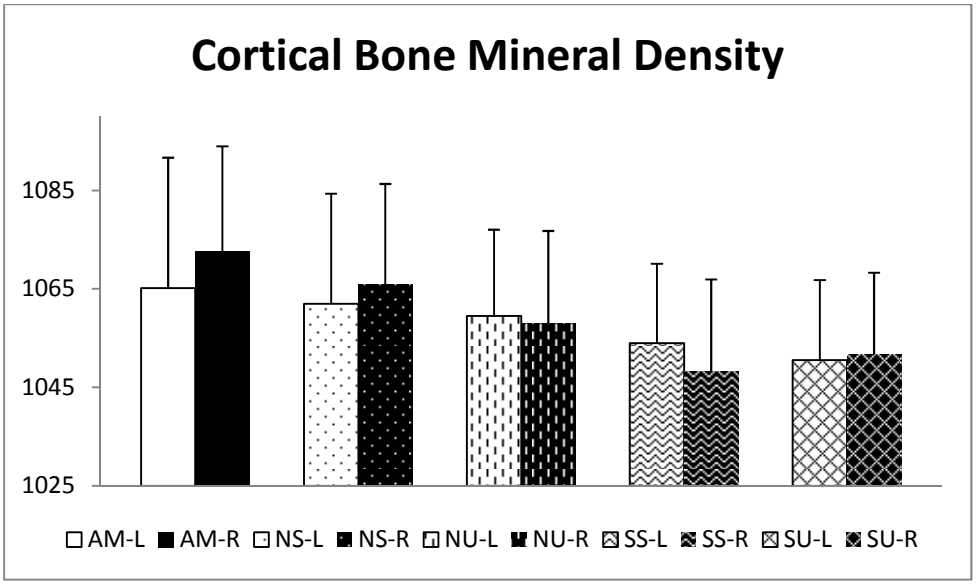

c)

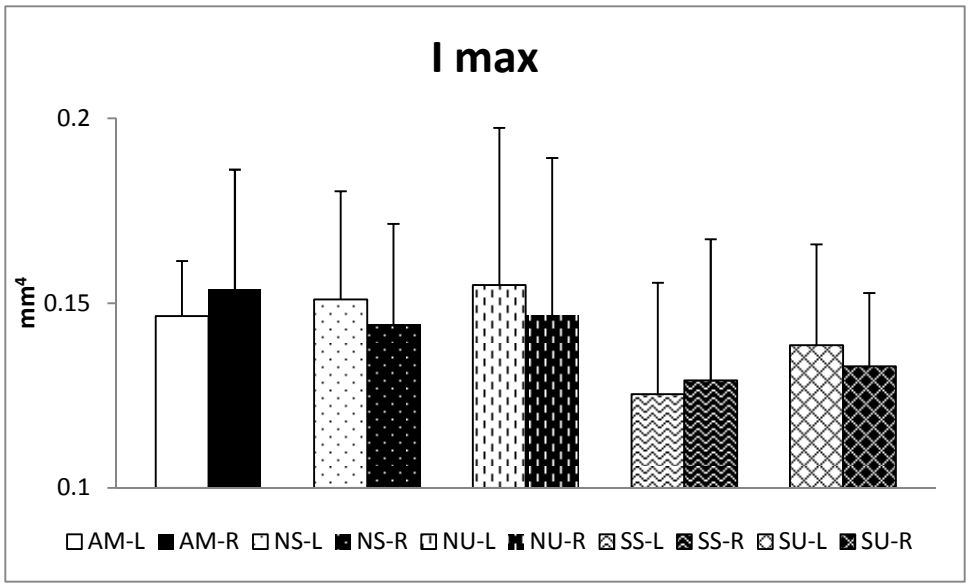
I max
0.2
0.15
0.1
mm⁴
AM-L AM-R NS-L NS-R NU-L NU-R SS-L SS-R SU-L SU-R

d)

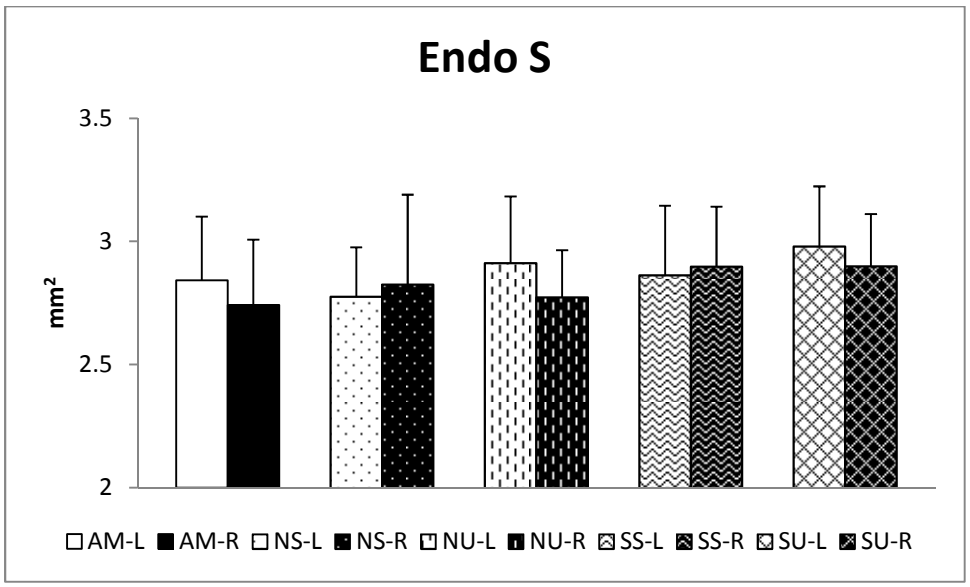
Endo S
3.5
3
2.5
2
mm²
AM-L AM-R NS-L NS-R NU-L NU-R SS-L SS-R SU-L SU-R

e)

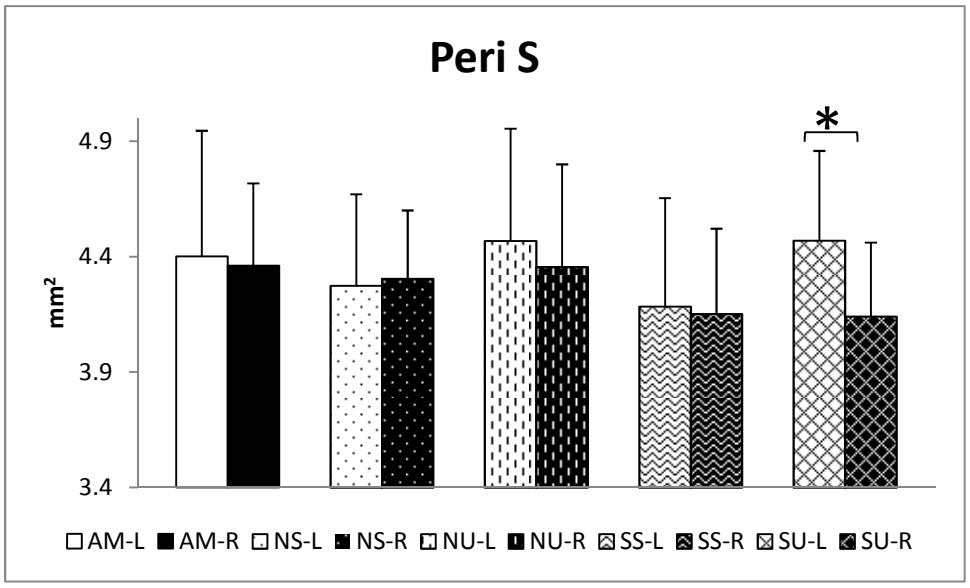
Peri S
4.9
4.4
3.9
3.4
mm²
*
AM-L AM-R NS-L NS-R NU-L NU-R SS-L SS-R SU-L SU-R

f)

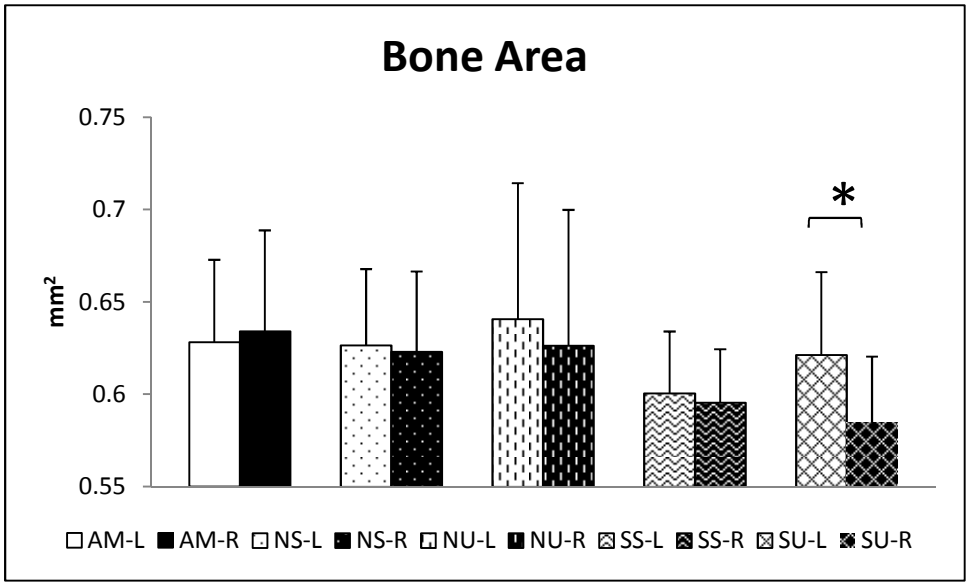
Bone Area
0.75
0.7
0.65
0.6
0.55
mm²
*
AM-L AM-R NS-L NS-R NU-L NU-R SS-L SS-R SU-L SU-R

Figure 6: Cortical bone analyses show lesser effect on cortical bone in SS mice tibia but adverse trend is apparent in inertia, Cort. BMD, MoI, BA and Peri S. LIPUS exposure show significant increase in Cort.Th, BA and Peri S when compared to contralateral controls (left vs right tibia). No significant differences were observed in NS and NU tibia when compared to AM.
a) Cort. Th: A significant decrease in SS tibia cortical thickness, LIPUS increases cort.Th significantly relative to untreated tibia of SS animals. SU/SS comparison show positive trend in SU tibia but difference is not significant.
b) Cort. BMD: Cort. BMD reduces in SS mice tibia but not significantly. LIPUS treatment show positive trend (SU).
c) Inertia: SS mice tibia show decrease in inertia but difference is not significant after 4 week of suspension. SU show positive trends.
d) Endo.S: Endosteal surface doesn't show any different in SS and SU tibia over 4 weeks of suspension.
e) Peri S. Periosteal Surface reduces in SS tibia but not significantly. LIPUS treatment increases Peri S in treated tibia relative to contralateral controls.
e) BA: Bone Area show similar trends to Peri S, with decreased BA in SS tibia and significant increase SU-L relative to SU-R.
*P < 0.05, **P<0.01, ***P<0.001

3.4.2 Dynamic Histomorphometry shows LIPUS increases bone formation in the proximal tibia under disuse

Histomorphometric analyses were only performed on samples from the AM, SS and SU groups as no significant difference were observed in non-suspended groups (NS and NU) in the microCT data. AM mice showed compact cortical bone with intact trabecular struts, along with strong single labeling most prevalent in endosteal and trabecular sites (Figure 7,AM). In contrast, SS mice showed visibly broken and disoriented trabeculae. Fluorochrome labeling was dispersed with sporadic single labels mostly confined to trabecular bone and endosteal surfaces (Figure 7, SS). LIPUS treated tibiae retained their normal bone microstructure and visible double and single labels present on the endosteal surface and trabeculae (Figure 7, SU).

The histomorphometry data were consistent with those from microCT scanning (Table 4). As compared to age match controls, SS mice had 41% less BV/TV ($p<0.05$, Figure 8a) and 31% less Tb.Th ($p<0.05$, Figure 8). LIPUS treatment had anabolic effects as SU mice showed significant increases of 38% in BV/TV ($p<0.05$) and53% in Tb.Th ($p<0.05$) in comparison to SS mice in the metaphyseal region. In addition, BS/BV and Tb.Sp showed significant increases in SS mice compared to SU, and LIPUS exposure significantly decreased BS/TV ($p<0.05$, Figure 8c). The trabecular bone formation rate decreased in SS mice, while treatment with LIPUS significantly increased BFR/BS ($p<0.05$, Figure 8d) in proximal tibia metaphysis. Furhtermore BFR/BS, MAR, and mineralization surface was reduced after 4 weeks of suspension. However, application of LIPUS significantly increased BFR/BS and mineralization surface, while MAR values showed positive trends (Figure 8e, f).

Figure 7: Dynamic Histomorphometry Images

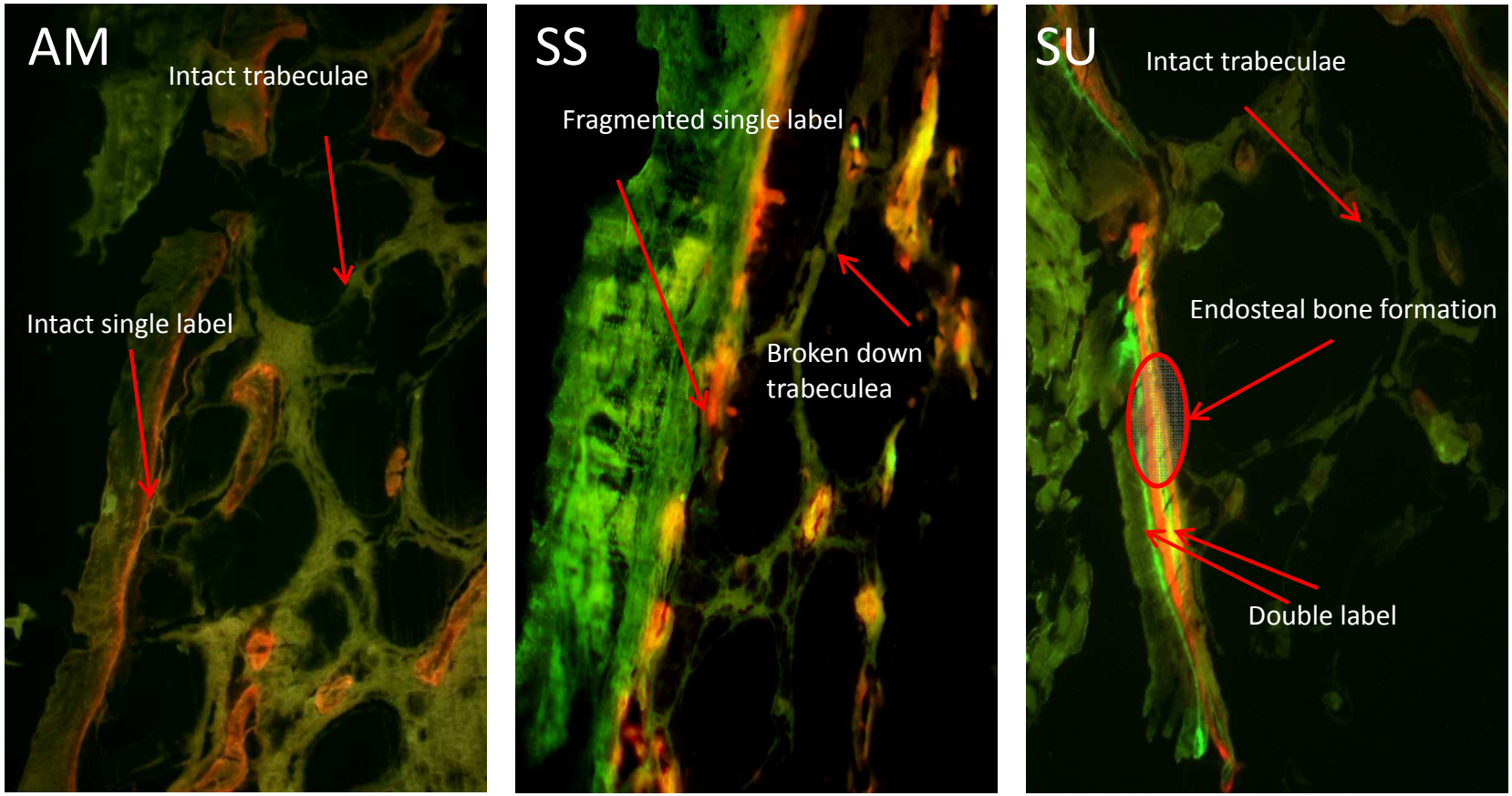

Figure 7: Histomorphometry. Mice were injected with Calcein (weeks 1 and 3) and alizarin red(weeks 2 and 4). Analyses were performed on proximal tibia metaphyseal sections. AM mice showed intact microstructure along with seamless single labeling, SS mice showed broken down microstructure with little or no labeling, and SU mice showed improved microstructure and with enhanced double labeling along endosteal and trabecular surfaces.

Table 4: Dynamic Histomorphometry Data

Index	AM	SS	SU
BV/TV	19.04±4.54	7.81±4.24*	12.72±3.21†
Tb.Th(μm)	84.70±25.91	26.58±22.02*	56.64±18.75†
BS/BV	25.42±7.43	128.78±112.09*	35.46±16.19†
Tb.Sp(μm)	317.21±67.50	427.42±211.35*	369.88±160.71
BFR/BS ($\mu m^3/(\mu m^2)/d$)	0.052±0.024	0.031±0.30*	0.104±0.07†
MS	4.01±1.42	3.00±0.84	5.90±2.37
MAR (μm/day)	1.41±1.01	0.75±0.55	1.57±0.92†

Table 4**:** Histomorphometry analyses of proximal tibiae metaphysis. This table shows significantly decreased trabecular BV/TV, Tb.Th, MS and BFR/BS and increase BS/BV and Tb.Sp in SS mice relative to AM mice. SU mice showed significantly increased BV/TV, Tb.Th, MA and BF/BS and decreased Bs/BV and Tb.Sp in comparison to SS mice.

* $P<0.05$ compared to age match

† $p< 0.05$ compare to SS

Figure 8: Dynamic Histomorphometry

a)

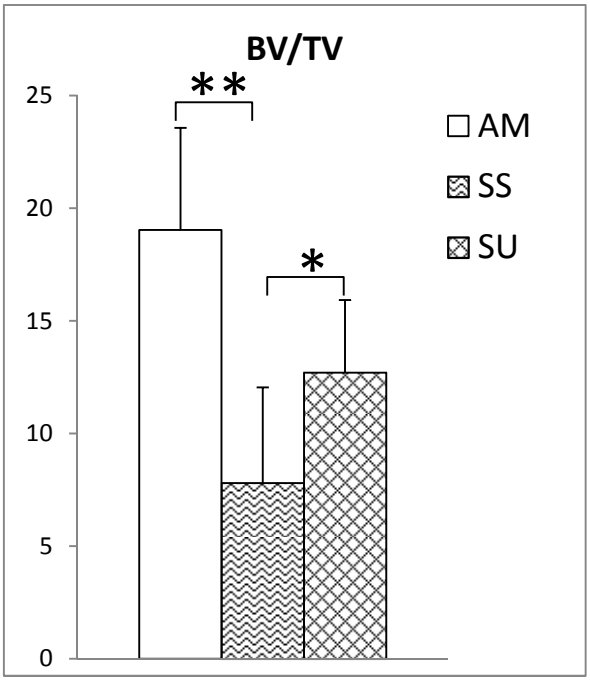

b)

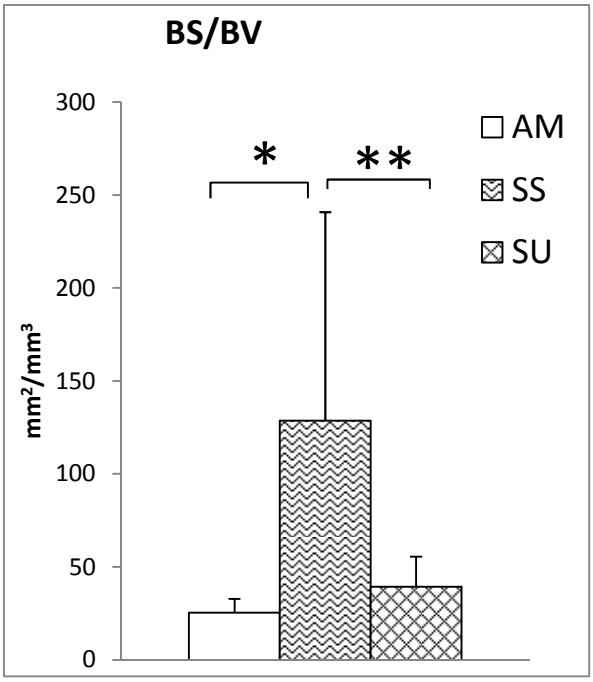

c)

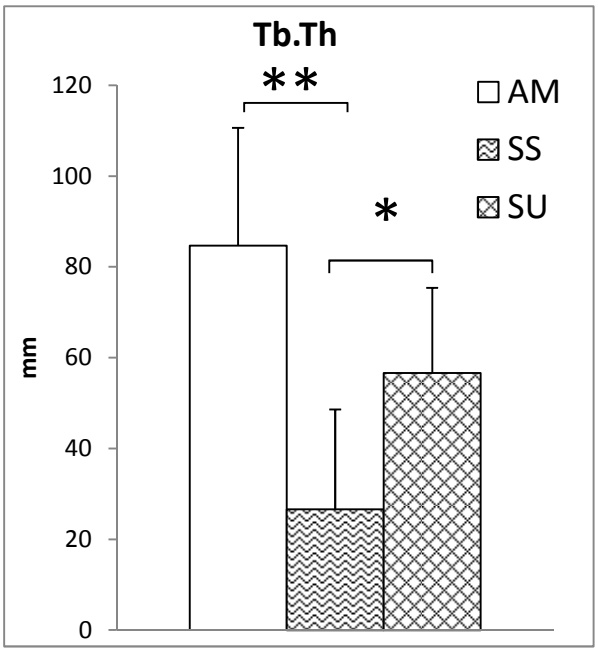

d)

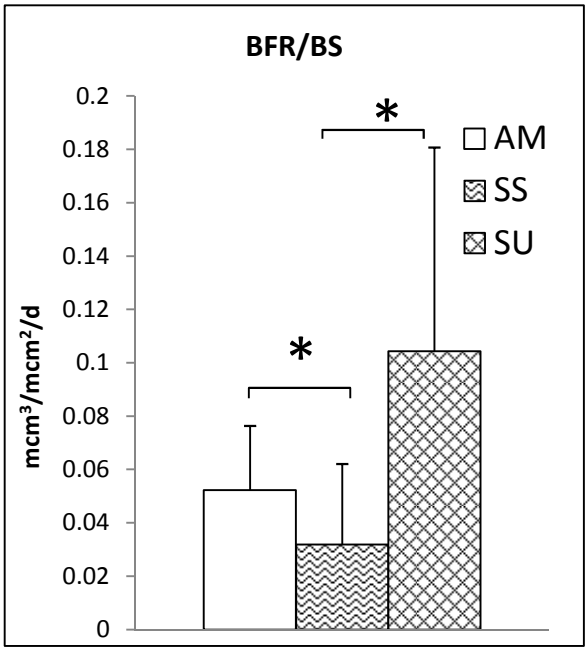

e)

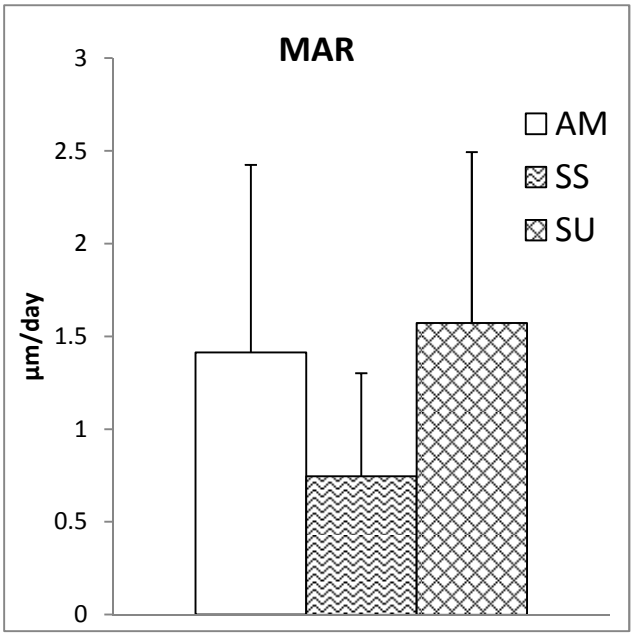

f

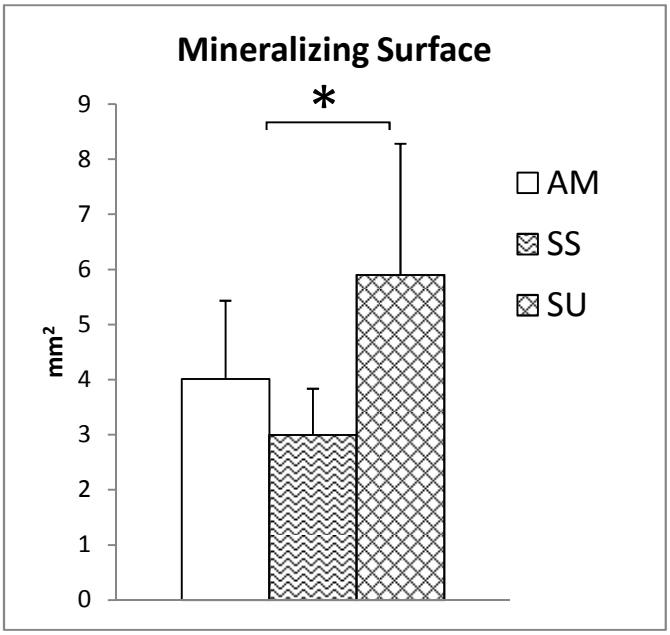

Figure 8: Histomorphometry results. Histomorphometric analyses were performed using Osteomeasure. Bar graphs showing the results of this analysis for a,b,c,d are shown. SS mice proximal metaphysis show significant decreases in BV/TV, Tb,T h and BFR/BS. LIPUS treatment practically retains BV/TV and Tb.Th while significantly enhancing BFR and mineralization surface.

a) BV/TV: 41% decreases in SS tibia metaphysis, application of LIPUS reduces (SU) BV/TV by 38% relative to SS mice

b) BS/BV: increases in SS mice, SU metaphysis show significant reduction in BS/BV ratio.

c) Tb.Th reduces by 31% in SS mice relative to AM animals. Application of LIPUS metaphysis retains ~53% more Tb.Th then SS mice.

d) BFR/BS: significant decrease in rate of bone formation in SS mice, LIPUS exposure induces increase in rate of bone formation in SU metaphysis.

e) Rate of Mineral deposition reduces in suspended mice (SS) and show approximately full recovery on application of LIPUS(SU)

f) Mineralization surface increases significantly in response to LIPUS (SU mice)

*P < 0.05, **P<0.01, ***P<0.001

3.4.3 Finite element modeling shows that LIPUS protects proximal tibial strength during disuse

Application of incremental strain showed higher stress levels in disuse proximal tibias (SS), with most of stresses concentrated at the cortical shell due to the large number of disconnected trabecular struts (Figure 9a, SS). Application of LIPUS resulted in an increased number of trabecular struts which reduced the concentration of stresses on the cortical shell and also led to a more even distribution of stresses throughout the trabecular network.

Proximal tibia from SS showed increased Von Mises' stress with the highest average stress ($7.42x10^7$Pa) calculated at 10% strain, (Table 5). However, application of LIPUS reduced average Von Mises' stress by 11% (Table 5, $p<0.05$) relative to disuse proximal tibias.

	1% (MPa)	5% (MPa)	10% (MPa)
AM	7.17 ± 0.48	35.98± 2.38	71.79±4.75
SS	7.94 ± 0.36 *	39.30 ± 1.94*	78.61 ±3.86†
SU	7.03 ± 0.63†	35.16 ±3.17†	70.34 ±6.33†

Table 5: This table shows the FEM derived Average Von Misses stress in AM, SS and SU proximal tibias. Disuse tibiae (SS) show significantly increased stress relative to AM. LIPUS treatment restores structural integrity of bone and reduces ave. stress on proximal tibia in state of compression/strain.
* $p< 0.05$ relative to AM
† $p < 0.05$ relative to SS

Figure 9: Finite Element Modeling

a)

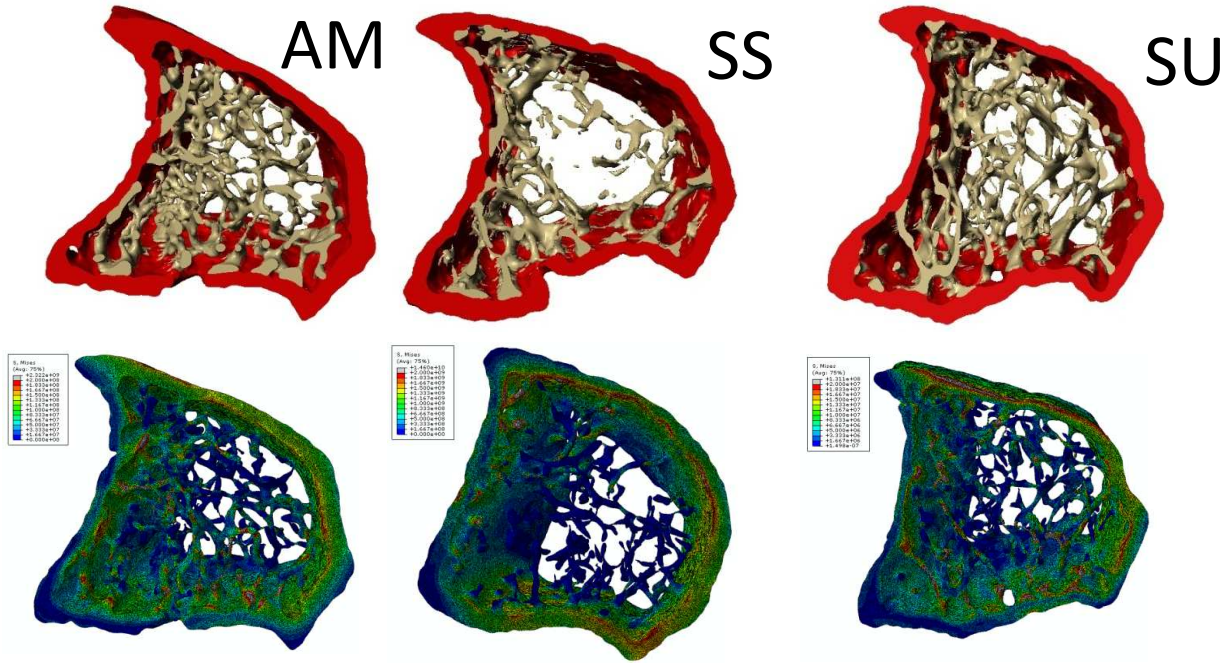

b)

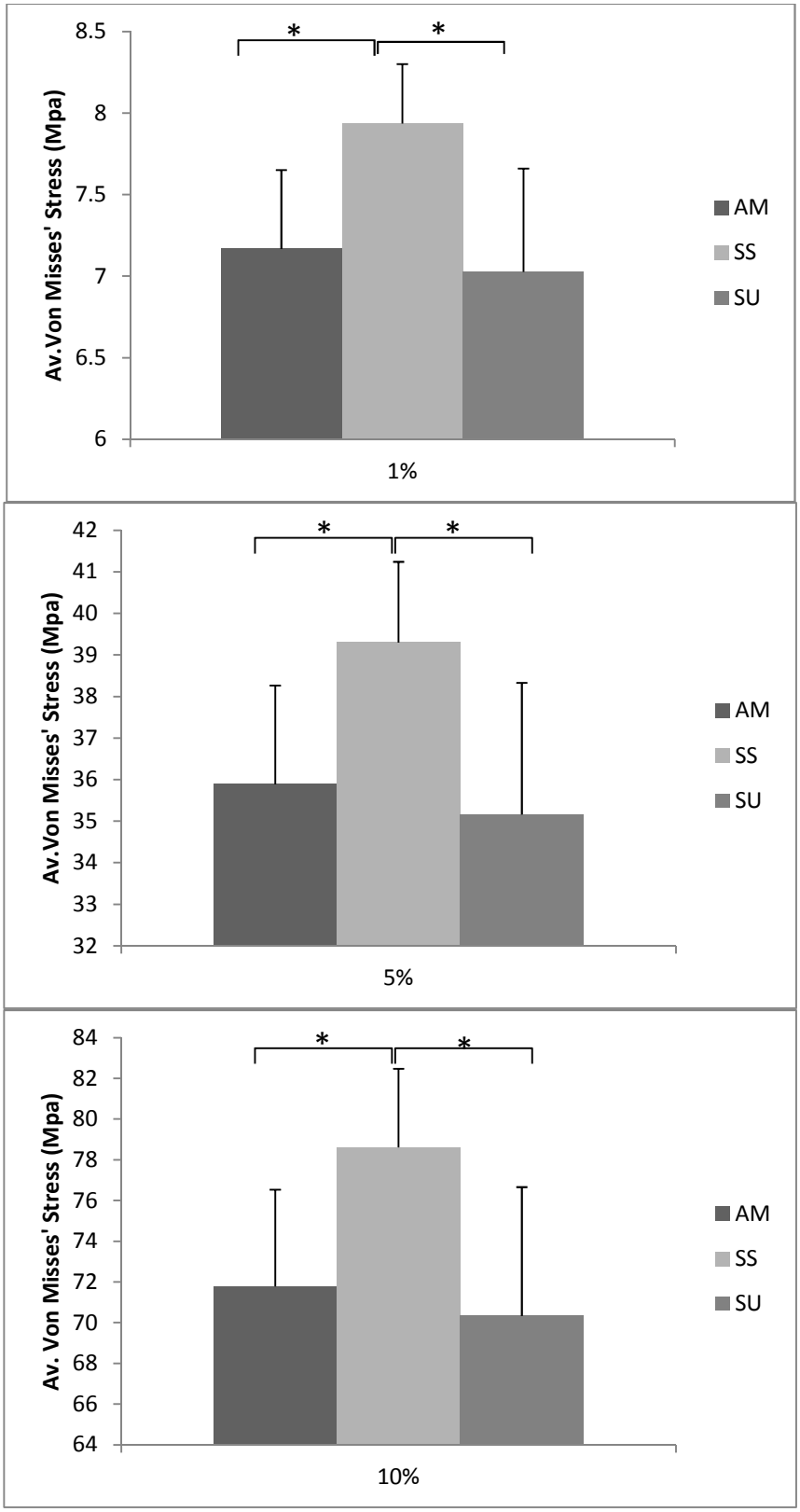
8.5
8
7.5
7
6.5
6
Av.Von Misses' Stress (Mpa)
*
*
AM
SS
SU
1%
42
41
40
39
38
37
36
35
34
33
32
Av.Von Misses' Stress (Mpa)
*
*
AM
SS
SU
5%
84
82
80
78
76
74
72
70
68
66
64
Av. Von Misses' Stress (Mpa)
*
*
AM
SS
SU
10%

Fig 9: FEM results a) Image showing Average Von Mises' stress at proximal tibiae under incremental strain (1, 5, and 10 %). Disuse proximal tibiae showed significantly increased von Mises' stress mostly confined at cortical shell. b) Disused tibiae showed app 10% increase average von Mises' stress at 1, 5 and 10% strain ($p<0.05$). LIPUS treatment reduced av. von Mises' stress by 11% ($p<0.05$) and restored it to AM levels.

3.4.4 LIPUS improves femoral mechanical properties under disuse

Although microCT analyses of femoral mid-diaphysis showed no significant decreases in cortical thickness in SS mice compared to AM mice, significant differences in elastic modulus, yield strength, and ultimate strength were seen for the SS mice in comparison to AM, NS, and NU mice (Table 6). Suspension significantly compromised femoral mechanical properties as SS femurs had a 53% decrease in elastic modulus ($p<0.05$, Figure 10a), 33% decrease in yield strength, ($p<0.05$, Figure 10b) and 45% decrease in ultimate bone strength when compared to AM femurs (Figure 10). LIPUS treatment significantly improved the mechanical properties of the mid-diaphysis. Femoral elastic modulus increased by 42% ($p< 0.05$), yield stress increased by 29% ($p<0.05$), and ultimate strength increased by 39% ($p<0.05$), in SU compared to SS. Contralateral femora of SU mice confirmed the increase in elastic modulus, yield strength, and ultimate strength in LIPUS treated femurs. Finally, compared to AM mice, SU mice showed an 18% decrease in elastic modulus, 6% decrease in yield strength, and 10 % decrease in ultimate strength. Table 6, shows the comparison between the groups and contralateral controls.

Table 6: Mechanical Testing Data

Index	AM	NS	NU	SS	SU
Cortical Thickness (mm)	0.149017±0.008	0.14381±0.009	0.14182±0.007	0.13205±0.012*	0.13295±0.008
	0.146117±0.009	0.14824±0.017	0.14039±0.014	0.13553±0.010*	0.13997±0.012
BMD (mmhg/cc)	1102.703±22.82	1099.54±54.05	1091.68±11.70	1088.49±32.83	1092.29±19.68
	1084.59±24.29	1089.04±28.46	1073.99±26.16	1069.35±17.36	1075.57±25.57
Elastic Modulus (GPa)	1730.66± 631.94	1581.32±737.71	1578.52±712.35	811.86±344.52*	1407.64±581.01†
	1772.12±682.38	1793.27±619.87	1881.03±642.78	726.48±316.18	792.76±310.41‡‡
Yield Strength (MPa)	69.79 ± 25.77	74.94±37.65	75.28±27.86	46.41±18.99*	65.44±26.98†
	74.38±25.27	75.52±30.98	69.12±12.99	33.07±12.20	34.18±12.67‡
Ultimate Strength (MPa)	86.66±31.22	88.68±32.45	91.19±35.80	47.49±25.02*	78.07±38.78†
	92.03±35.22	90.40±44.66	81.21±22.01	36.42±13.29	45.45±15.60‡‡

Table 6– Four Point Mechanical testing analyzing bone elastic modulus and strength under disuse conditions and anabolic effects of LIPUS on femoral mid-diaphysis. Gray row represent treated (left) tibiae, Clear rows represent un-treated (right) tibia

* P<0.05, ** P<0.01, ***P<0.001 relative to AM

† P < 0.05, †† P< 0.01 relative to SS, ‡ P<0.05,

‡‡ P<0.01 relative to left tibia (contra-lateral control)

Figure 10: Mechanical Testing

a)

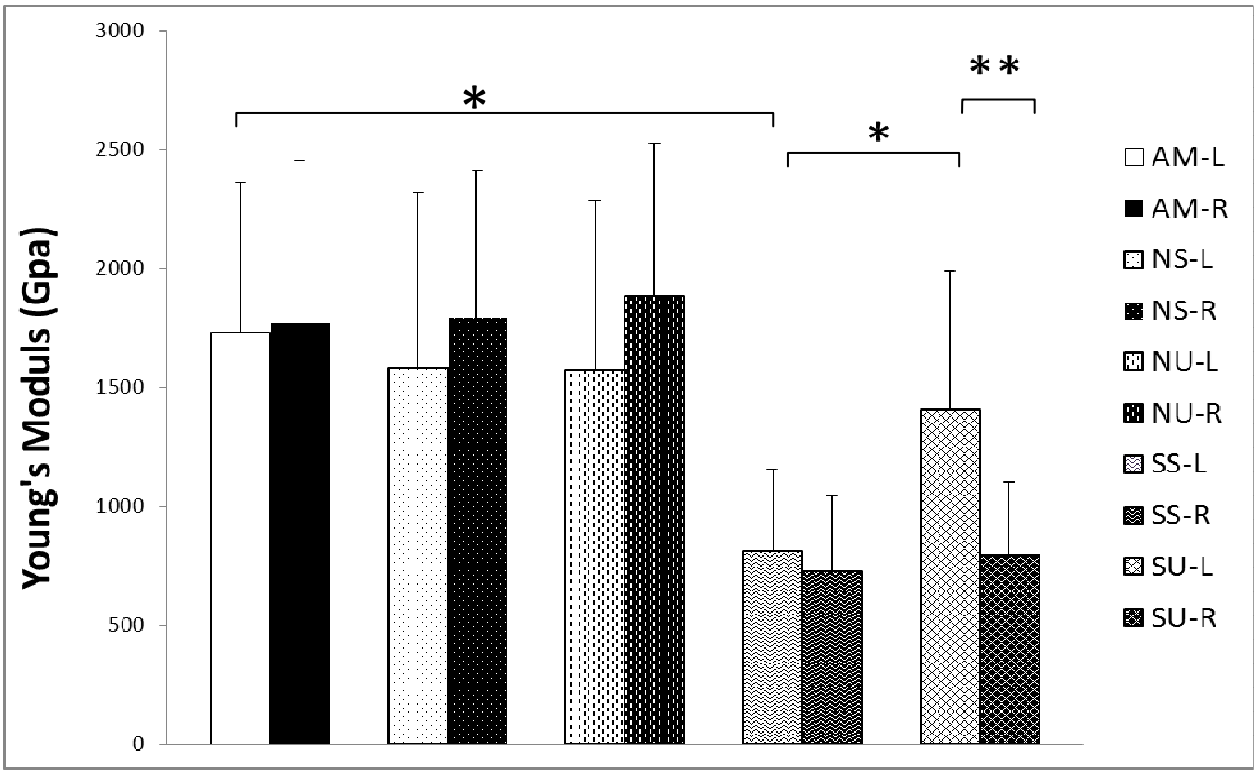

b)

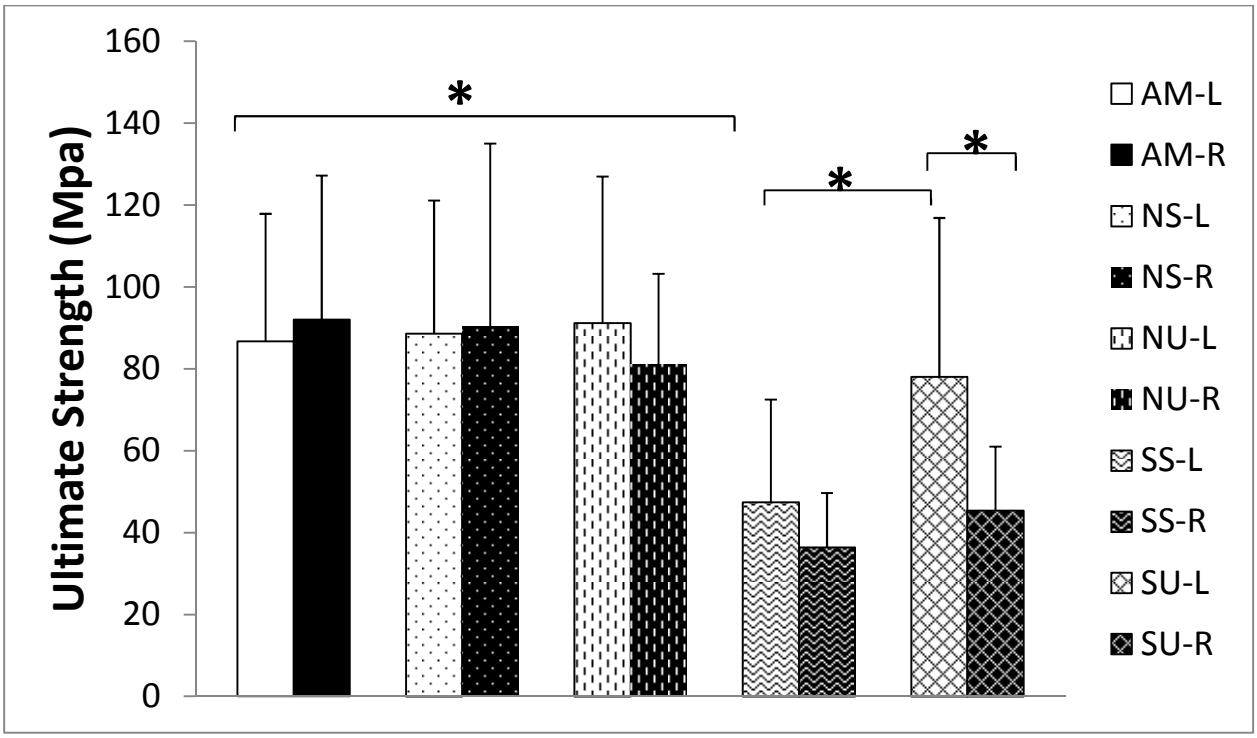

c)

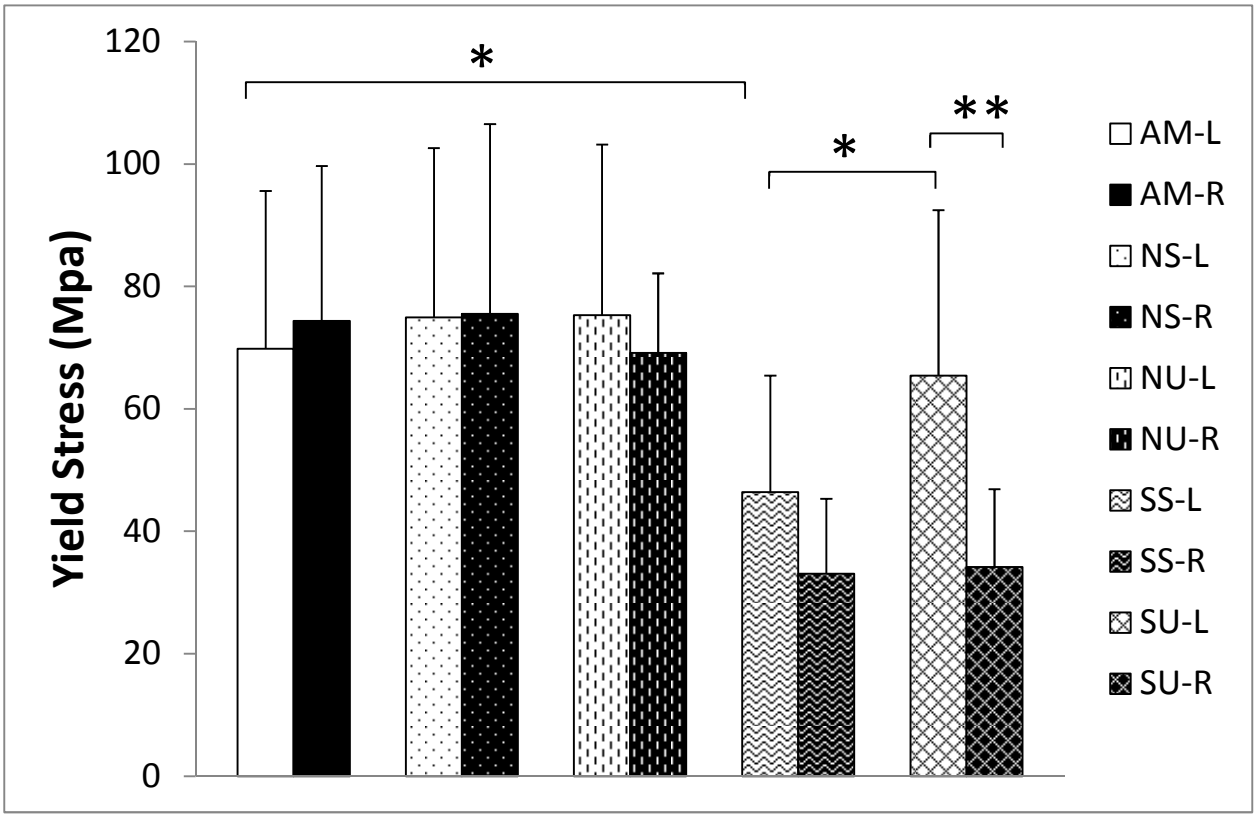

Fig 10) Mechanical Testing- four point bending bar charts showing significantly decrease in mechanical properties of SS mice femur (Elastic modulus, yield and ultimate strength). LIPUS exposure retains mechanical integrity of femoral bone.
a) Elastic modulus: SS mice showed a significant decrease in elastic modulus relative to AM. LIPUS exposure increased elastic modulus in SU mice.
b) Ultimate strength: decreased significantly in SS femurs in comparison to AM mice. SU showed a significant increase in ultimate strength relative to SS mice.
c) Yield stress: significantly decreased in SS mice. LIPUS exposure increased yield stress relative to SS mice.

3.5 Discussion:

Disuse osteoporosis is a degenerative bone disease that compromises bone strength and leads to a high risk for fractures. This type of bone loss is concentrated on weight bearing limbs. The localized pathology of disuse osteoporosis favors a targeted and non-invasive approach to treatment, which can provide the essential mechanical stimuli required to maintain bone quality. Since LIPUS has shown encouraging results in providing an anabolic stimulus that promotes bone healing, this study examined LIPUS as a potential countermeasure for disuse induced bone loss. The microCT results confirmed the detrimental effects of disuse on trabecular and cortical bone, with trabecular bone showing more sensitivity to disuse than cortical bone. Trabecular bone showed significant decreases in BV/TV, BMD, Tb.Th, and Tb.N along with an increase in BS/BV. Cortical bone showed significant losses in thickness with lesser effects on BMD, BA, MOI, Endo S, and Peri S. Application of LIPUS mitigated the decreases in trabecular BMD, Tb.Th, and showed increases in BS/BV with no effects seen for BV/TV. LIPUS treatment partially mitigated the losses in cortical thickness and bone area. The contralateral untreated tibiae (SU) and non-suspended LIPUS treated (NU) tibiae did not show significant changes in bone microstructure relative to treated left tibiae indicative of the targeted nature of LIPUS stimulation.

Histomorphometry results confirmed those from microCT, showing that LIPUS treated mice retained bone microstructural integrity and had increased bone formation rates. Furthermore, the histomorphometry data showed a significant increase in proximal tibiae BV/TV, which was not apparent in the microCT analyses. This is likely due to the higher sensitivity of histomorphometry compared to microCT. In addition, the histomorphometry images showed fluorochrome labels concentrated on endosteal and trabecular bone surfaces with

little or no labeling at the periosteal surface. As the endosteal and trabecular surfaces are lined with osteoblasts, increased labeling is indicative of increased rates of bone formation by osteoblasts. Previous studies have shown increased bone loss on the endosteal surface and reduced trabecular thickness in response to disuse due lack of bone formation [68, 70], our data indicate that LIPUS treatment can induce bone formation on endosteal and trabecular surfaces to counteract the adverse effects of disuse.

Femoral mechanical properties were severely compromised in SS animals despite no differences being found for BMD and cortical thickness of AM and SS. This suggests that other factors such as collagen alignment, collagen cross-linking, porosity, microcracks etc. may play an important role in determining bone mechanical properties. Application of LIPUS partially restored the mechanical properties of bone without significantly affecting cortical thickness and BMD. *In vitro* studies have shown that application of LIPUS improves collagen cross-linking in calcified matrix by increasing prostaglandin E_2 activity in osteoblast cell cultures [213]. It is speculated that the absence of mechanical stimulus when under disuse may similarly adversely affect collagen cross-linking, leading to compromised mechanical properties, and LIPUS stimulation partially mitigates this effect to improve biomechanical function.

The results of this study indicate that LIPUS has the strong potential to be used as a targeted, non-invasive and non pharmacological countermeasure for disuse induced bone loss. Increased calcein and alizarin red staining on endosteal and trabecular surfaces indicated that LIPUS was increasing bone formation, but the current study did not examine the effects of LIPUS on osteoclast activity and/or numbers. Bone homeostasis is preserved by the synergistic activities of osteoblasts and osteoclasts. Increased osteoblast activity can reduce osteoclast activity and differentiation. Studies have shown that LIPUS stimulation increases osteoblast

activity, resulting in increased production of TGF-β3 and reduced levels of TNF-α and IL-6 [178], which combine to decrease osteoclast activity [214, 215]. Furthermore, LIPUS decreases RANKL expression in osteoblasts, which is essential for osteoclast differentiation (unpublished data). Considering the effects of LIPUS stimulation from *in vitro* studies it is possible that LIPUS decreases osteoclastogenesis and osteoclast activity, leading to reduced bone resorption. However, more detailed *in vivo* studies are required to fully determine the effects of LIPUS on osteoclast activity and differentiation.

These results indicate localized anabolic effects of LIPUS in disuse induced bone loss. LIPUS has the potential to be used in clinical settings as in non-invasive, targeted therapy for age related, post menopausal and long term bed rest induced osteopenia and osteoporosis. Furthermore, LIPUS provides a portable and easy-to-comply-with therapy for microgravity induced bone loss in astronauts and can be a pivotal therapy to increase the duration of time astronauts can spend in microgravity, a well as speeding rehabilitation upon returning to earth. Data from contralateral controls showed no effects due to LIPUS treatment thus indicating localized and targeted stimulation of bone cells without any adverse effects on healthy bone tissue.

The exact mechanism through which LIPUS enhances osteoblast activity and increases the rate of bone formation remains unknown. Ultrasound is speculated to induce acoustic streaming in interstitial fluid and localized mechanical vibrations in the extracellular matrix [185]. This results in local deformation of cell membrane and the induction of shear stresses and strains in osteoblasts [163, 164, 186-189]. These mechanical deformations activate receptors on the cell membrane such as integrins, mechanosensitive-calcium channels, G-proteins, IGF, TGF-

β/BMP, and gap junctions, all of which activate different downstream pathways [181, 188, 190-193].

This study explored the potential of LIPUS as a non-invasive, non- pharmacological targeted therapy for disuse osteoporosis. The results suggest that LIPUS has very strong potential as a non-invasive and targeted anabolic agent for disuse osteoporosis. The study did not evaluate the effects of LIPUS on osteoclast and osteocytes activity *in vivo* and futures studies will be required to study these responses as well as perform in-depth analyses of alterations in bone matrix and gene expression in order to begin to understand the underlying mechanism.

Chapter 4

LIPUS Enhances Osteogenic Differentiation of Human Mesenchymal Stem Cells in Simulated Microgravity

Specific Aim 2*: Determine the effects of LIPUS on human mesenchymal stem cell differentiation in simulated microgravity in vitro.*

4.1 Abstract

Adult stem cells can differentiate into multiple lineages depending on their exposure to differing biochemical and biomechanical inductive factors. Lack of mechanical signals due to disuse can inhibit osteogenesis and induce adipogenesis of MSC. Long-term bed rest due to brain/spinal cord injury and space travel can lead to disuse osteoporosis that is in part caused by a reduced number of osteoblasts. To induce osteogenesis under disuse conditions, it is essential to provide proper mechanical stimulation. The objective of this study was to examine the effects of low intensity pulsed ultrasound (LIPUS) on the osteogenic differentiation of adipose-derived human stem cells (Ad-HMSC). Cells were cultured in a 1D clinostat to simulate microgravity (SMG) and treated with LIPUS at 30mW/cm^2 for 20 min/day. It was hypothesized that the application of LIPUS to SMG cultures would restore osteogenesis in Ad-HMSCs. The results showed significant increases in ALP, OSX, RANKL, RUNX2, and decreases in OPG in LIPUS treated SMG cultures compared to non-treated cultures. SMG significantly reduced ALP positive cells by 70%, $p<0.01$and ALP activity by 22% ($p<0.05$), while LIPUS treatment restored ALP positive cell number and activity to equivalence with normal gravity controls. Extracellular matrix (ECM) collagen and mineralization was assessed by Sirius red and Alizarin red staining, respectively. SMG cultures showed little or no collagen or mineralization, but LIPUS treatment restored collagen content to 50% ($p<0.05$) and mineralization by 45% ($p<0.05$) in LIPUS treated-SMG cultures relative to SMG-only cultures. The data suggests that LIPUS treatment can restore normal osteogenic differentiation of MSCs.

4.2 Introduction

Adult mesenchymal stem cells (MSC) are multi-potent stem cells capable of self-renewal and differentiation into osteoblastic, adipogenic, myogenic, and chondrogenic lineages. Recent studies have examined the effects of the presence or absence of mechanical stimuli on commitment of MSCs to different lineages [216-218]. Mechanical vibrations, stress, and shear forces can all enhance osteogenic differentiation of MSCs while the lack of mechanical stimuli can induce adipogenesis [217, 219]. Luu et al. have shown that low magnitude mechanical stimulation (LMMS) induces osteogenesis and inhibits adipogenesis [220, 221] and MSCs extracted from LMMS treated mice show increased expression of RUNX2 relative to PPARγ [220]. A recent study by Yang et al. has shown that cyclic tensile strain increased RUNX2 expression while inhibiting PPARγ in rat MSCs [222]. In contrast, lack of mechanical stress can induce adipogenesis and inhibit osteogenesis [155, 223]. Loss of gravity in space or lack of physical activity due to spinal/brain injury can significantly reduce mechanical stresses thus leading to decreased rates of osteogenesis and increased rates of adipogenesis [221]. The lack of mechanical stress during spaceflight induces bone loss of 1-2 % per month which can eventually lead to disuse osteoporosis [224].

MSCs are progenitor cells to osteoblasts, and the detrimental effects of disuse on MSCs can significantly reduce their rates of proliferation and differentiation into osteoblasts [223]. Microarray analysis of MSC cultures in simulated microgravity (SMG) have shown reductions in expression of genes controlling the cell cycle, cytoskeleton, proliferation, and differentiation along with increased expression of apoptotic genes [155]. Furthermore, MSCs cultured in SMG had disorganized microfilaments and reduced F-actin polymerization [47, 223]. Huang et al. have shown that this is in part due to inhibition of the ERK1/2 and AKT pathways, leading to

reductions in proliferation, RUNX2, and ALP concomitant with increased PPARγ levels [47]. In general, lack of mechanical stimulus appears to force MSCs into a state of quiescence.

To restore MSC self-renewal and osteogenic differentiation, it is essential to provide an anabolic mechanical signal, ideally one which can provide a localized mechanical stimulus. LIPUS produces pressure waves which induce biochemical events in bone cells [175-177]. The effects of LIPUS on intercellular activity, cytokine release [178], gene expression [179], calcium mineralization [180], Akt signaling [181], potassium influx [182], angiogenesis [183], adenyl cyclase activity, and TGF-b synthesis[184] have all been studied.

LIPUS induced mechanical deformations activate receptors on cell membranes such as integrins, mechanosensitive-calcium channels, G-proteins, IGF, TGF-β/BMP and gap junctions, activating different downstream pathways [181, 188, 190-193].These studies, and many others show that rates of bone formation are increased in the presence of LIPUS.

A number of studies have specifically evaluated the effects of ultrasound on mechanotransductive pathways. Tang et al. reported on activation of the Akt pathway and p-13 kinase, through aggregation of integrin expression, which resulted in induction of nitric oxide, hypoxia inducible factor-1, and increased activity of cox-2 in osteoblast cells [191, 192]. Similarly, LIPUS treated osteoblasts show higher nuclear localization of β-catenin and activation of Wnt signaling [194]. A microarray study done on LIPUS treated osteoblasts showed enhanced gene expression of integrins, cytoskeletal components, TGF-β family members, IGF family members, MAPKs pathway, ATP-related, Guanine nucleotide binding protein family, lysyl genes, and apoptosis-associated gene families as compared to non-treated osteoblast [195-198].These cellular level studies indicate that ultrasound treatment can activate

mechanotransductive pathways and significantly increase osteogenic differentiation in progenitor cells and promote osteogenic maturity in differentiated osteoblasts. Recent studies have also shown increased RUNX2, ALP, Collagen type 1, and integrin beta 1 expression in LIPUS treated MSCs [225]. Finally LIPUS exposure has been shown to enhance cell adhesion, focal adhesion formation, and increase proliferation in MSCs [225].

The catabolic effects of disuse are driven by inactivation of mechanotransductive pathways and they also severely affect MSC activity. As LIPUS exposure has mechanotransductive properties, it has the potential to induce mechanical stress in MSCs and promote osteogenic differentiation in microgravity or disuse conditions. This study was performed to test the hypothesis that LIPUS exposure restores the osteogenic differentiation of SMG cultured MSCs.

4.3 Materials and Methods

4.3.1 Rotation Microgravity Simulation

A *one-dimensional clinostat (1-D Clinostat)* was developed to keep cells in continuous 1-D rotation at a speed of 15 rpm around the horizontal axis. This resulted in an averaging out the net gravitational forces (Figure 11). Lee Silver et al. explained in detail the effects of 1-D rotation on cells and sub-cellular organelles with respect to gravity, showing that continuous rotation along the horizontal axis disables cells ability to respond to gravitational force and induces a lack of orientation. In our clinostat, the rotation resulted in a radial force less than 0.045N. Further, the rotator is controlled by a variable speed motor and the holder is 80 mm (radius = 40mm) in width allowing it to holding 8 Opticell® (Nunc, VWR, Bridgeport, NJ.USA) cartridges.

Each Opticell cartridge is 2 mm thick and MSCs were seeded on their gas-permeable polystyrene membranes. Each cartridge was filled with 10 ml of media and, to prevent fluid shear stress, all air bubbles were carefully removed. The clinostat was kept under sterile conditions at $37^{o}C$ in $5\%CO_2$ in a standard humidified incubator (Thermo scientific, Asheville, NC, USA) for the duration of all experiments.

Figure 11: 1-D Rotation and clinostat setup

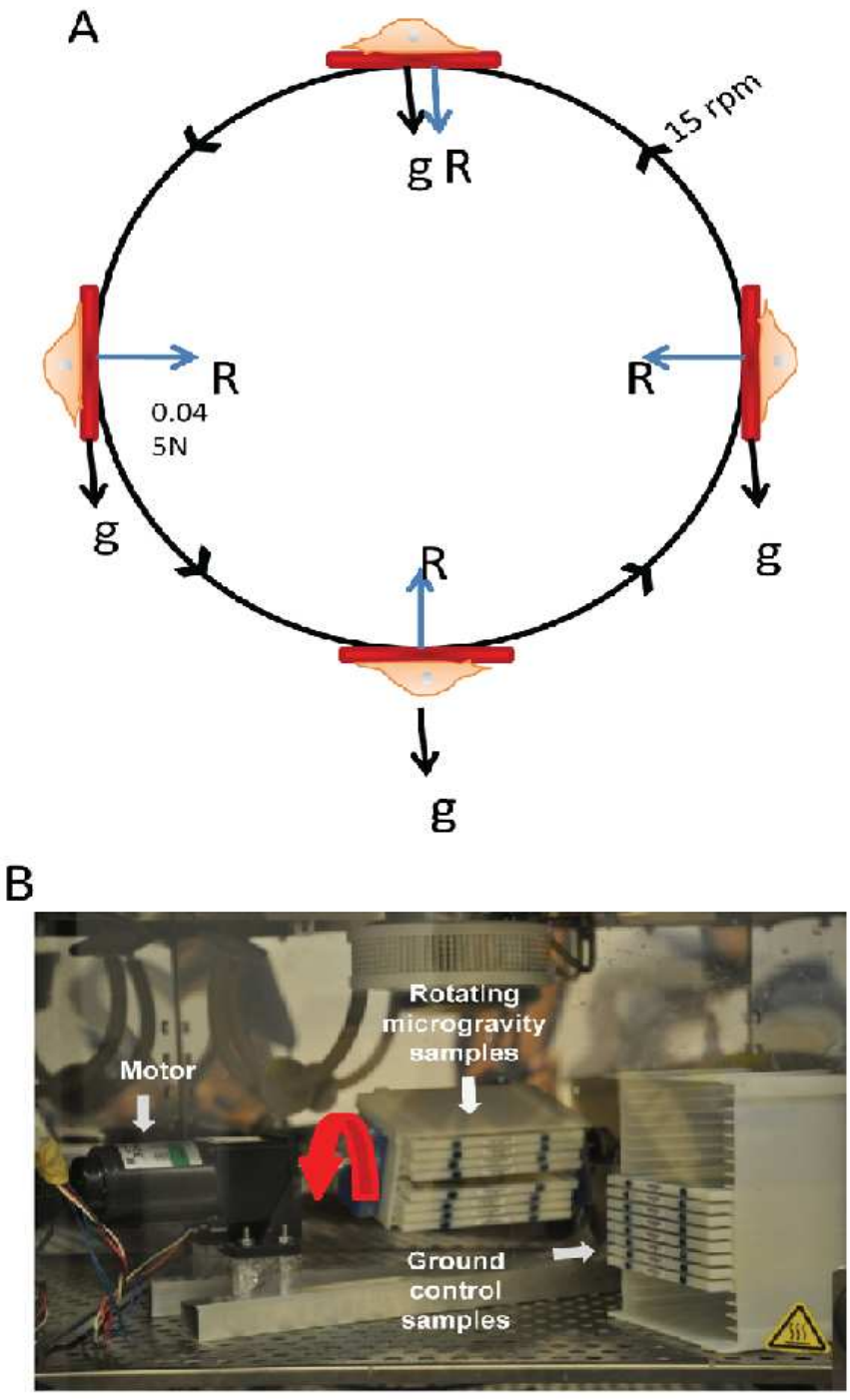

Figure 11: Simulated microgravity (SMG) bioreactor. A) One dimensional rotation results in net gravity vector of magnitude zero, thus producing simulated microgravity B) SMG bioreactor setup inside incubator with experimental and control samples setup.

4.3.2 Ultrasound Exposure:

LIPUS stimulation was applied using an acoustic device, Sonicator® 740 (Mettler Electronics, Anaheim, CA) with a $10cm^2$ transducer (35mm diameter) utilizing a modified repetitive frequency at 100 Hz pulse, an ultrasound characteristic frequency of 1MHz and a pulse width of 200μs repeated at 100 Hz at an intensity of 30 mW/cm^2 for 20 minutes/day. This type of LIPUS application at a modified low repetitive comparable dynamic frequency may lead to a new approach for noninvasive stimulation of bone turnover. The region of LIPUS treatment was marked with a 10cm diameter circle before the start of each experiment. All stimulations targeted the same region of each Opticell and only those cells that were growing in the Region of Stimulation (RoS) were harvested and analyzed. The 3-5mm distance between the transducer and Opticell was filled with degassed water.

4.3.3 Cell Culture:

Adipose derived human Mesenchymal stem cells (Ad-hMSC, LifeLine, CA) were cultured in StemLife media (LifeLine, CA) at an initial seeding density of 250,000 cells/Opticell. Cells were distributed into five groups (n=4/group): 1) Control; 2) Gravity (G); 3) Gravity + LIPUS (GU); 4) SMG (M); and 5) SMG + LIPUS (MU). All the groups were initially cultured in proliferation media (StemLife media) until 90% confluency was reached. After 90%,GU,M, and MU groups were supplemented with osteogenic factors (50ug/ml ascorbic acid, 10mM beta-glycerolphosphate), while the control group was maintained in proliferation media to serve as a negative control for osteogenesis. Microgravity simulation of M and MU groups was started after initiation of osteogenic induction. GU and MU samples were stimulated with LIPUS for 20 min per day 5 days a week, for the duration of the experiments while the G and M samples were placed on a switched-off transducer for the same duration. All cells were maintained at 37^oC and

5% CO_2 and the culture medium was changed every other day.

4.3.4 Quantitative Real-Time PCR

After 24 hours of SMG, MU and GU samples were exposed to LIPUS and immediately lysed with lysing buffer for RNA collection. The RNA from the control, G, and M was collected in similar fashion. Total RNA was extracted using RNeasy Mini Kit (Qiagen) and reverse transcribed using random primers and a High capacity RNA-to-cDNA kit (Applied Biosystems). The cDNA was then amplified using a StepOnePlus Real-time PCR system (Applied Biosystems). QPCR analyses were then performed for ALP, RUNX2, OSX, RANKL and OPG.

4.3.5 ALP Activity:

After 7 days of SMG, samples from all groups were washed twice with double distilled water and lysed using sonification. Cell lysates were incubated with p-nitrophenol phosphate (Sigma) at 37ºC for 1 hr. The enzymatic reaction was stopped using 1 M sodium hydroxide and absorbance was measured at 540nm (Bio-Tek EL800, Winooski, VT.USA)

4.3.6 Fluorescence-activated cell sorting – FACS:

Ad-HMSCs were trypsinized, washed with PBS, and stained with primary anti-bone alkaline phosphatase (abcam, ab17272) and secondary goat-anti mouse lgG1 heavy chain (FITC) antibodies (abcam, ab97239). After staining, the cells were washed, fixed with 1% formalin, and analyzed for ALP positive cells using flow cytometry.

4.3.7 Collagen Staining:

After 12 days of treatment, the RoS were cut out of the Opticells and fixed in 4% paraformaldehyde for 30 min at room temperature. The samples were then stained with 1% pico-sirius red for 1 hr and the cells were washed with acidified water (0.5 % acetic acid water) and

dehydrated with serial ethanol washes: 70%, 90%, and 100% (5 min each). Digital images were taken using polarized light microscopy (Nikon Diaphot 200, Melville, NY. USA) at 2.5X magnification. After imaging, staining was eluted using sodium hydroxide and quantified at 540nm optical density

4.3.8 Matrix Mineralization:

After 12 days of treatment, the RoS were cut out of the Opticells and the cells were fixed in 70% ethanol for 1 hr at room temperature. They were stained with 40mM alizarin red (pH 4.2) for 10 min, afterward washed with tap water, allowed to dry at room temperature and imaged using an Axiovert 2000M Inverted Microscope (Carl Zeiss, Axiocam MRC, Thornwood,NY). Following imaging, the stain was eluted off the cells in a solution of 10% cetylpyridinium chloride in 10mM sodium phosphate for 15 min. The eluted stain was then measured at 562nm in a spectrophotometer (Bio-Tek EL800, Winooski, VT, USA). All samples were quantified against an alizarin red standard curve in 10% cetylpyridinium and normalized to the total number of cells.

4.3.9 Statistics:

The GraphPad Prism 3.0 software was used to run statistical analyses. All of the data is presented in average ± standard deviation. One-way ANOVA with Newman Keuls Post -hoc was used to calculate significance within the different groups and time points. The p-values of <0.05 were considered to be significant.

4.4 Results

4.4.1 LIPUS increases expression of osteogenic genes in Ad-HMSC

PCR analyses were completed to assess the effects of SMG and LIPUS on the expression of osteogenic genes. SMG significantly reduced expression of all the genes analyzed (ALP, RUNX2, OSX, RANKL, and OPG) (Figure12). Application of LIPUS increased gene expression of ALP, RUNX2, OSX, RANKL (Figure 2a-d), and reduced expression of OPG (Figure 12e). MU samples showed significant increases in expression of ALP, RUNX2, OSX and RANKL relative to M samples, and restored the expression of these genes to levels seen in G samples (Figure12a-d). In the GU samples, LIPUS exposure showed positive correlations with osteogenic gene expression but no significant differences were found relative to G cultures. OPG expression levels went down significantly with application of LIPUS in the GU and MU samples (Figure 12e). When combined with RANK-L expression, an increased RANKL/OPG ratio was seen following application of LIPUS with the highest ratio seen in GU and MU samples. This finding suggests that LIPUS stimulation favors bone formation over bone resorption (Figure 12 f).

Figure 12: Ad-MSCs Gene Expression

a)

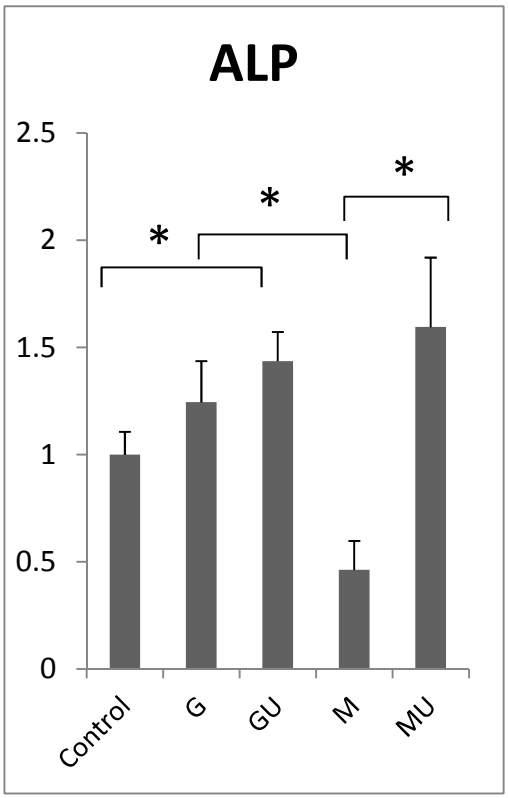

b)

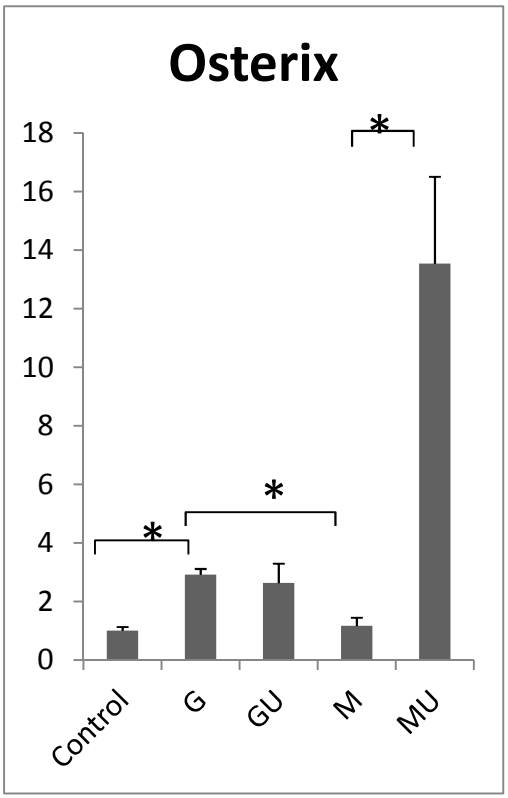

c)

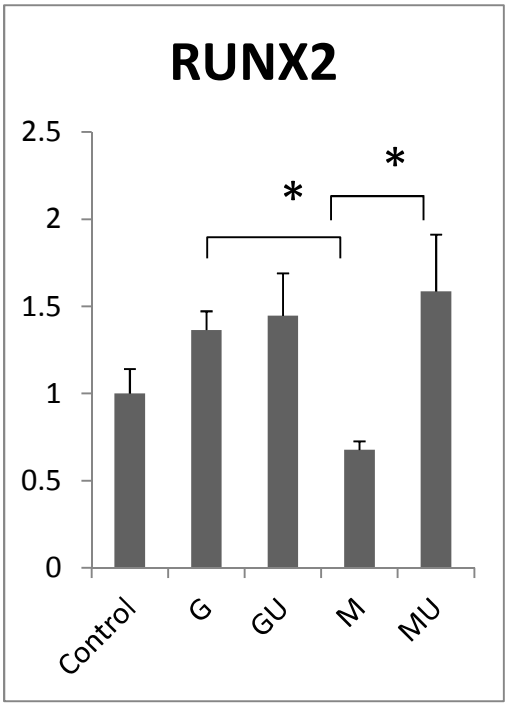

d)

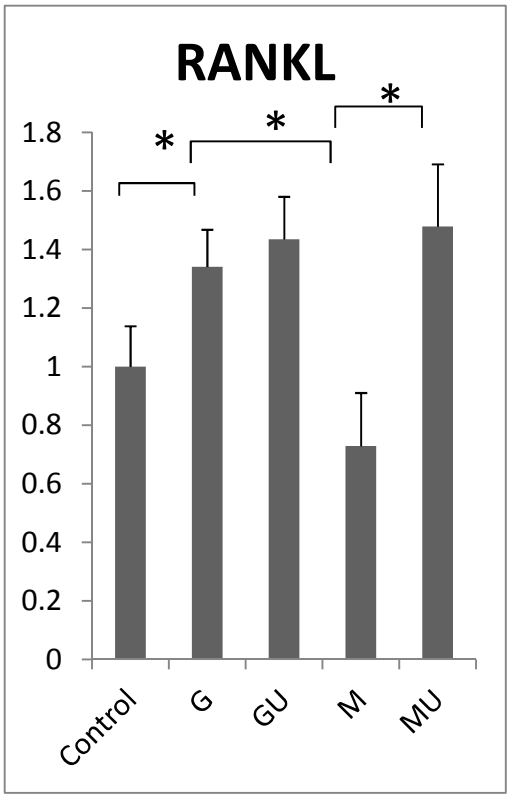
RANKL
1.8
1.6
1.4
1.2
1
0.8
0.6
0.4
0.2
0
Control
G
GU
M
MU
*
*
*

e)

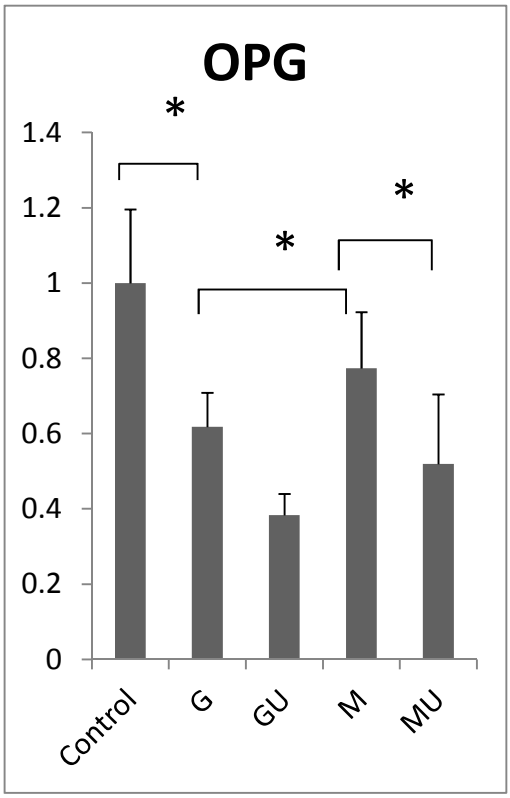
OPG
1.4
1.2
1
0.8
0.6
0.4
0.2
0
Control
G
GU
M
MU
*
*
*

f)

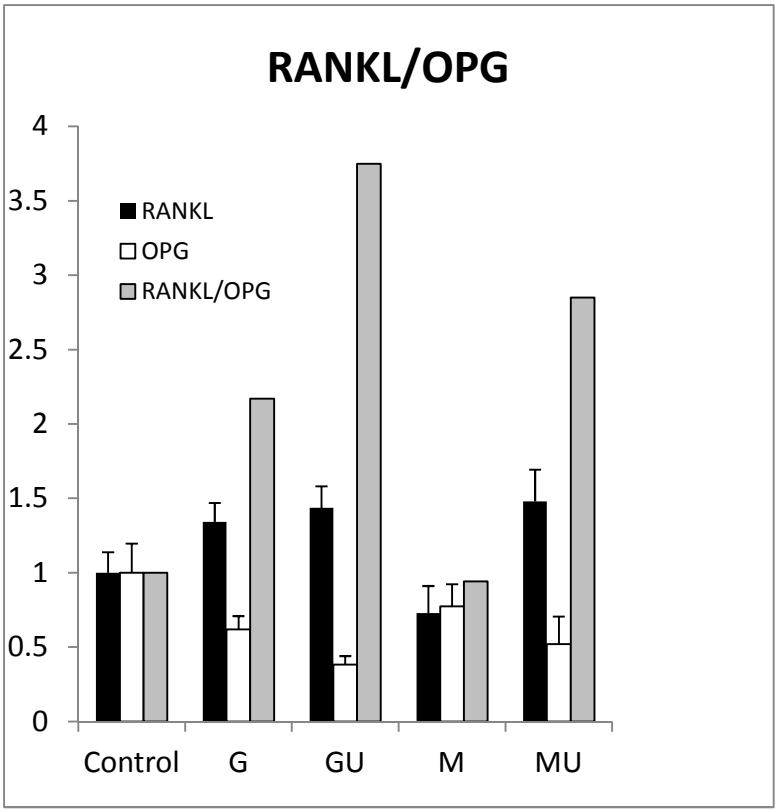
RANKL/OPG
4
3.5
3
2.5
2
1.5
1
0.5
0
RANKL
OPG
RANKL/OPG
Control
G
GU
M
MU

Fig 12: PCR analyses of osteogenic genes in response to SMG and LIPUS exposure.
a) ALP expression decreases in SMG and application of LIPUS significantly increases ALP expression; highest expression observed in MU samples.
b) OSX gene expression significantly reduces in SMG and LIPUS exposure induces significant increase in MU samples relative to M samples. GU Samples show little effect on OSX expression relative to G samples.
c) RUNX2 shows similar expression patterns as in ALP And OSX MU samples show significant increase compared to M samples and LIPUS exposure restores RUNX2 expression in HMSC.
d) RANKL expression levels significantly reduce in M samples but not significantly compared to control.
e) M samples showed significantly higher OPG expression than G, GU and MU samples. Exposure of LIPUS further reduces OPG expression ad-HMSC.
f) RANKL/OPG ratio is indicative of osteogenic commitment: M samples show same ratio as Controls and LIPUS exposure significantly increased RANKL/OPG ratio.

4.4.2 LIPUS restores ALP positive population and ALP activity in Ad-HMSC

ALP, a membrane bound enzyme is considered to be the initial marker of osteogensis as MSCs differentiate into osteoblasts. We looked at both the percentage of ALP positive cells and total AMP activity levels in ad-MSC under SMG with and without LIPUS exposure. SMG reduced the ALP positive population in M group, 70% less then G, resulting in levels similar to control (Figure 13). Exposure of LIPUS significantly increased the percentage of ALP positive cells in GU samples by 3% and restored ALP positive cells in MU samples in comparison to gravity controls (G).

ALP positive cells and ALP activity were significantly reduced in M cultures relative to gravity controls (G)(Figure 13b).However, LIPUS stimulation increased ALP activity in GU samples by 45% and completely restored ALP activity in MU samples relative to G samples (Figure 13b).

Figure 13: ALP Positive Cells and activity

a)

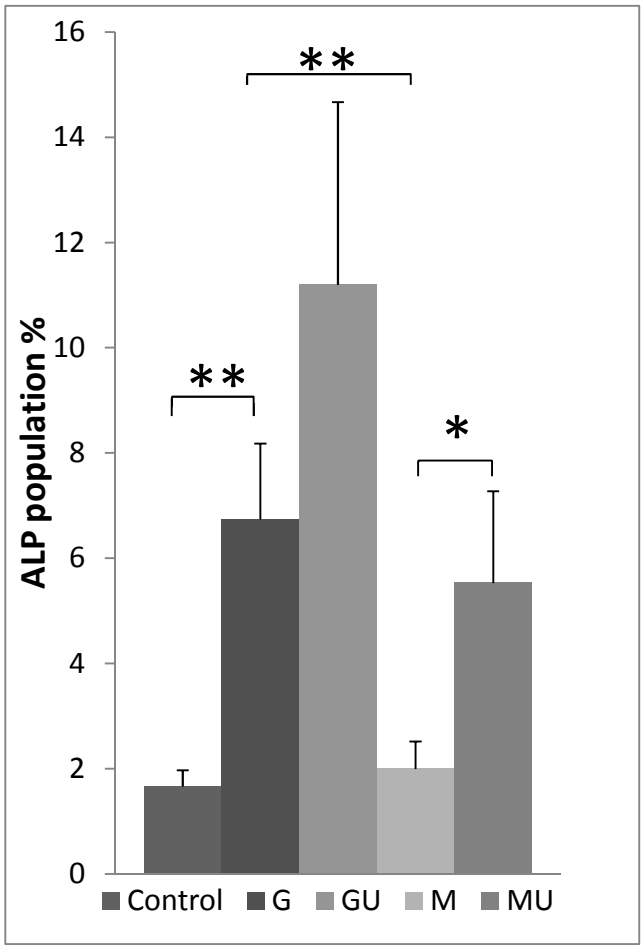

b)

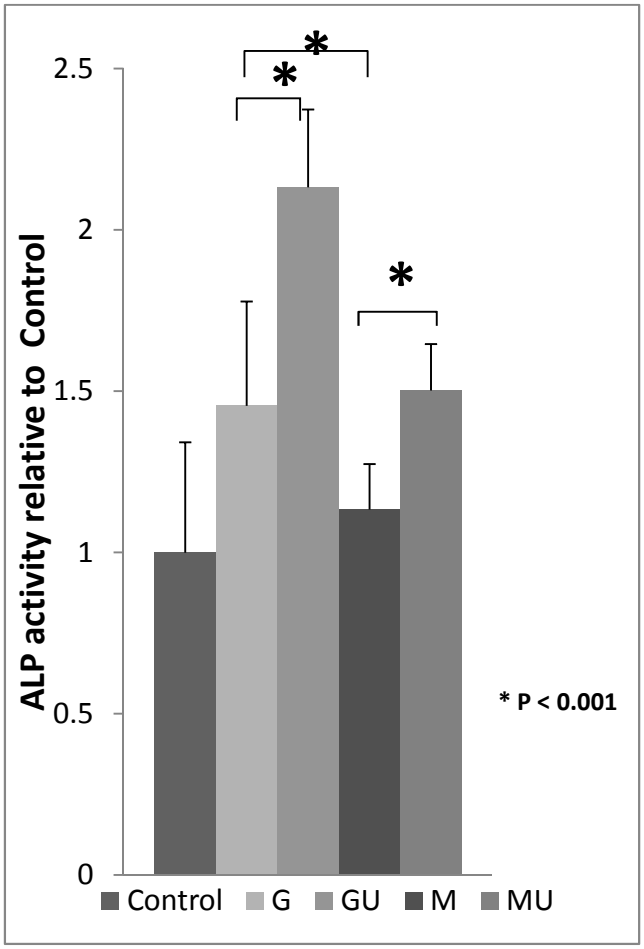

Figure 13. ALP positive popultion and activity.
a) ALP positive popultion signigicantly goes down to levels of control in M cultures. Application of LIPUS restores the ALP postive population in MU samples and signifcantly increases in GU samples relative to G samples.
b) ALP Activity showed same pattern as ALP postive population, as ALP activity in M sampels was signifcantly reduced and application of LIPUS restored ALP acitivity in differentiating cells. Application of LIPUS increases ALP acitvity in GU cultures.

4.4.3 LIPUS exposure significantly reverses SMG-induced decreases in collagen production:

Collagen deposited by osteoblasts was measured using Sirius red (stains collagen, predominantly type I and III fibers). Histological/qualitative analyses showed a reduction in collagen level in the SMG exposed samples (M) and significant recovery due to stimulation with LIPUS (MU) as evidenced by dark red clusters of collagen evenly distributed throughout the RoS (Figure 14a). The application of LIPUS on the GU samples resulted in a significant increase in collagen secretion as compared to the control (G) (Figure 14a). In addition, while all three cultures, G, GU and MU showed variable collagen density (with scattered areas of lower and denser clusters of collagen), the M cultures showed weaker staining and overall low collagen density throughout the cultures, almost resembling the collagen levels in the G group (Figure 14a). Further, quantitative measurement of the intensity of Sirius Red staining in these cultures identified a significant reduction of 21% of collagen secretion in the presence of SMG in comparison to the G samples (Figure 14b). In contrast, LIPUS stimulation reversed this trend and restored collagen levels to those observed in the G samples and actually enhanced collagen content in GU samples by 24% (Figure 14b).

Figure 14: Ad-MSC Collagen Content

a)

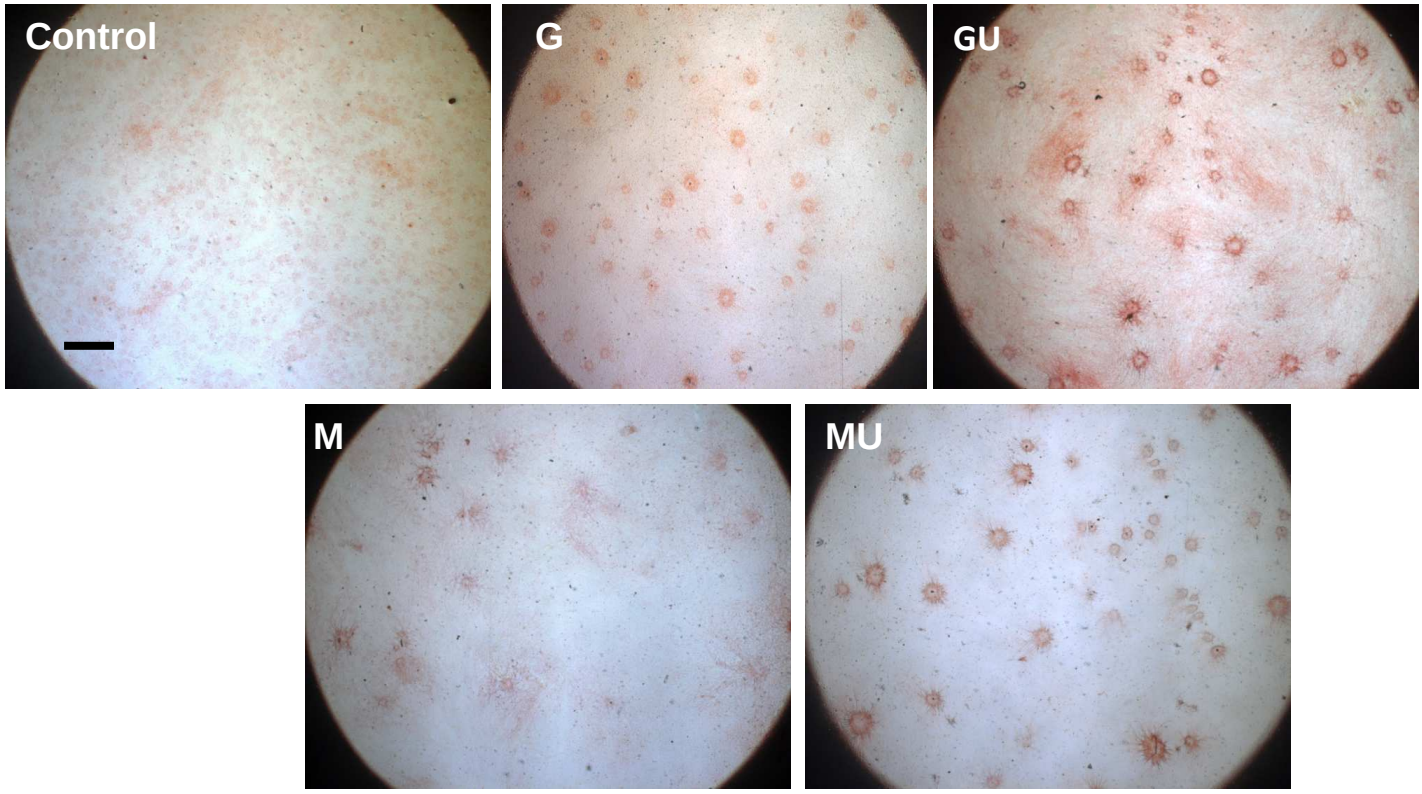

b)

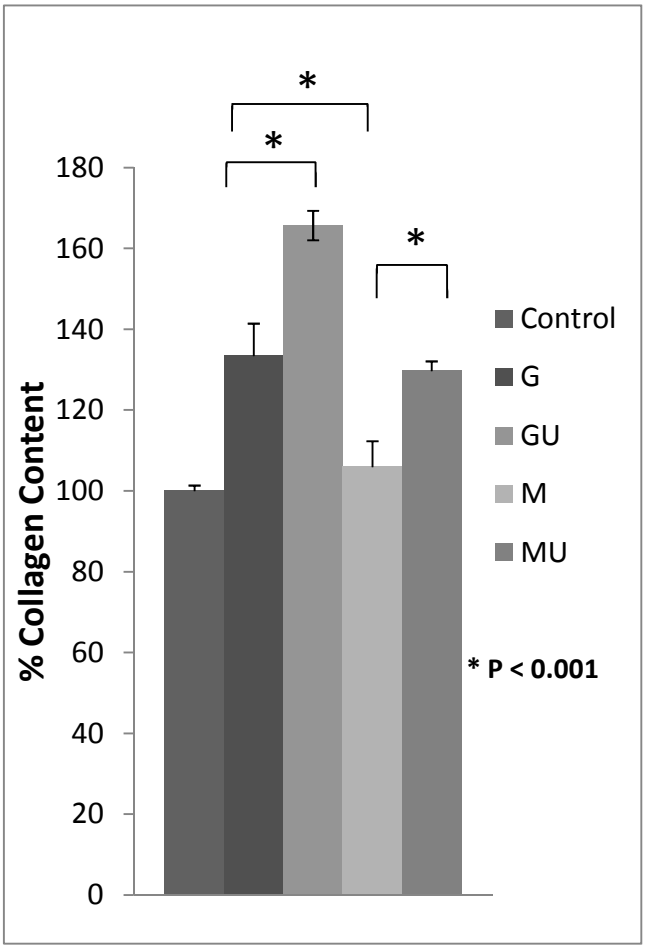

Figure 14**:** Collagen Content and Quantification.
a) Sirius Red stain showing collagen clusters forming in extracellular matrix. Control samples show little or no collagen and Gravity (G) samples showed evenly distributed collagen clusters over the ECM. Simulated microgravity (M) samples showed little or no collagen clusters and much more comparable to control cultures. Application of LIPUS to simulated microgravity + LIPUS (MU) samples apparently increased collagen content, making them more comparable to G samples. Gravity + LIPUS (GU) samples showed denser collagen clusters and formation of thick collagen fibers (scale bar 500um).
b) Sirius red quantification showed a significant decrease in collagen content in M cultures to the levels of control. Application of LIPUS restores collagen content in MU cultures, making them more comparable to G samples. LIPUS exposure significantly increases collagen in MU and GU samples.

4.4.4 LIPUS exposure significantly reverses SMG-induced decreases in calcification:

To further probe the positive effects of LIPUS stimulation on SMG-exposed cells, matrix calcification was investigated using Alizarin Red staining. Results from these experiments showed even distribution of calcium phosphate in G cultures, but with LIPUS stimulation, a much denser and wider pattern of calcification was observed in ECM. (Figure 15a, GU). M cultures showed decreased levels of Alizarin Red staining comparable to the control samples (Figure 15a, M). LIPUS exposure in SMG (MU) samples showed increased distribution of calcium phosphate nodules resembling that seen with G (Figure 15a, G). LIPUS exposure also enhanced alizarin red staining in GU cultures, leading to the formation of denser positively stained clusters. Further, after quantitatively measuring the concentration of the eluted dye, a 75% decrease in matrix calcification was observed in M compared to G but with LIPUS stimulation it was increased by 45% in the MU cultures. Furthermore, there was a significant increase of 56% in the GU cultures in comparison to G (Figure 15b).

Figure 15: Ad-MSC-Matrix Calcification

a)

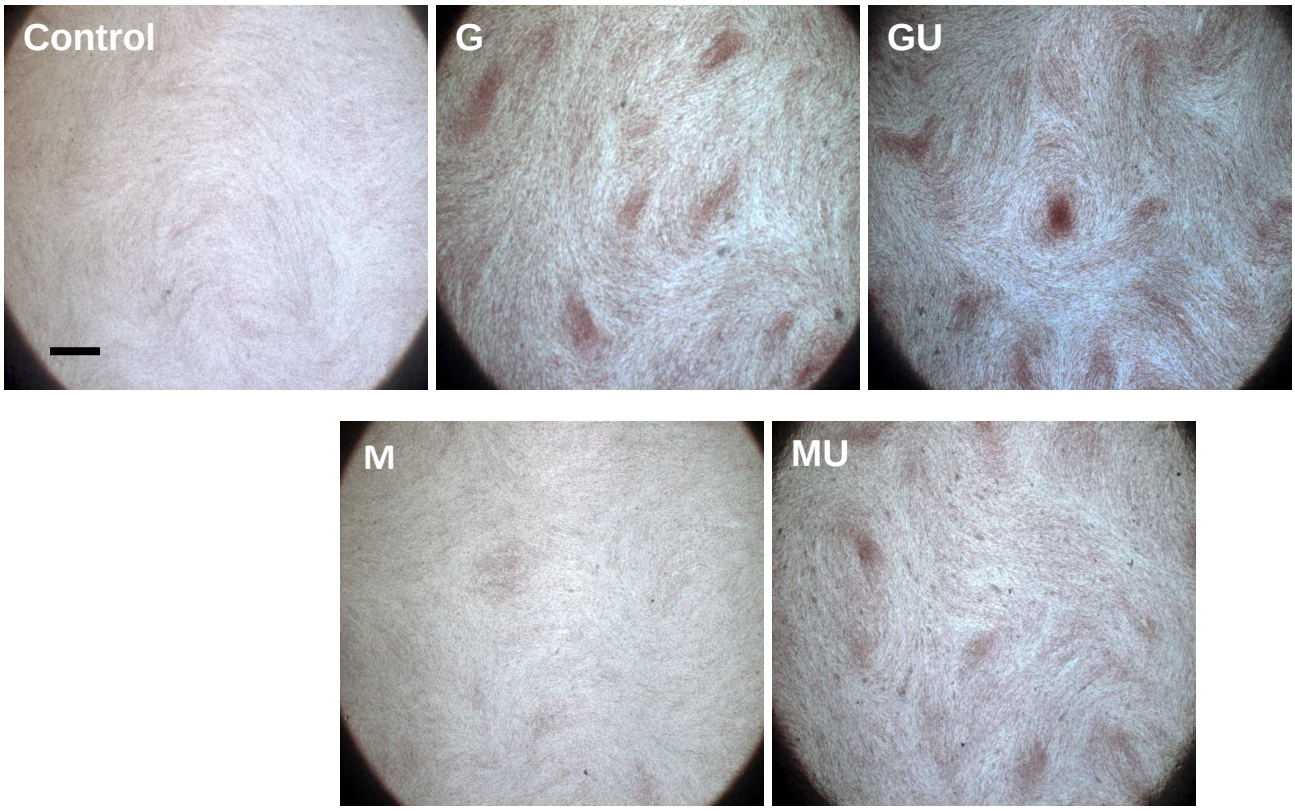

b)

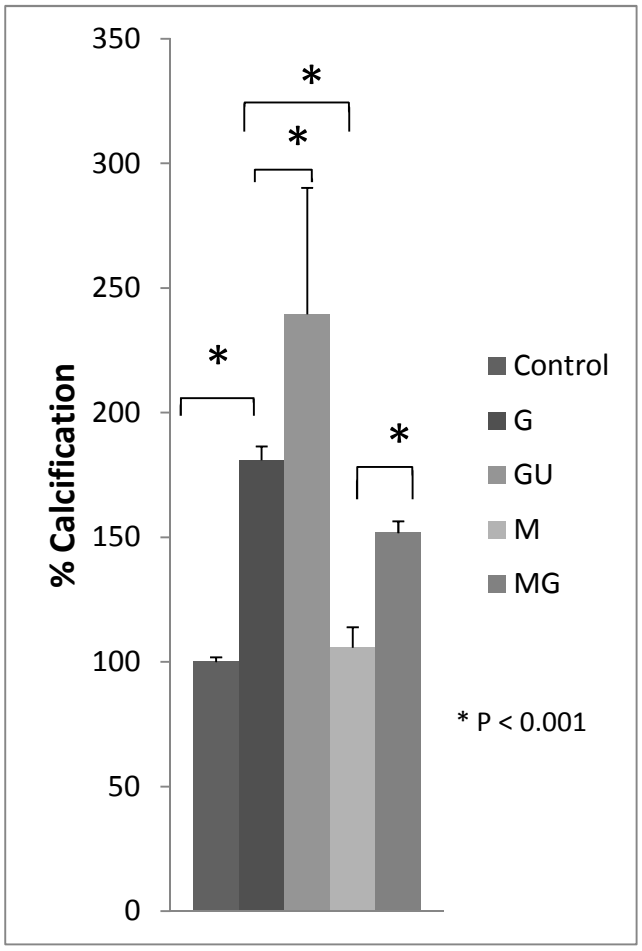

Figure 15) Matrix mineralization and Alizarin Red Quantification
a) No or little mineralization was apparent in Control samples. Gravity samples showed formation of mineralized clusters distributed evenly over the area of ECM. M samples showed no visible clusters and ECM morphology comparative to Controls. Application of LIPUS in MU samples induced mineralization as calcium clusters are apparent in ECM and morphology was more comparable to G samples.GU cultures showed denser calcium cultures and with higher frequency (scale bare 500um).
b) Alizarin red quantification showed significant decrease of ECM calcification in M cultures almost to the level of the control group. LIPUS exposure restored mineralization of ECM. Application of LIPUS significantly increased calcification in MU cultures relative to M and GU cultures relative to G.

4.5 Discussion:

Mesenchymal stem cells are multipotent cells that play an important role in tissue repair and regeneration in adult humans. Recent studies have shown that both mechanical and biochemical stimuli are important for differentiation of stem cells into different lineages. Yamazaki et al. showed that a lack of mechanical stress can inhibit osteogenesis and induce adipogenesis in bone marrow MSC [223]. MSC play an important role in bone remodeling being the progenitor cells to osteoblast cells and also affecting, osteoclastogenesis by the regulation of OPG. Disuse conditions due to brain/spinal injury or space travel can severely affect MSCs ability to differentiate into osteoblasts and alter the balance of the bone remodeling process leading to disuse osteoporosis. This study looked at the effects of LIPUS as a potential mechanotransductive stimulus to induce osteogenesis in SMG-MSCs cultures.

In the presence of biochemical and mechanical stimuli MSCs differentiate into bone matrix secreting osteoblasts, characterized by elevated expression of ALP, Runx2, OSX, and RANKL along with secretion of matrix proteins. The present study confirmed the inhibitory effects of SMG on osteogenic differentiation of MSCs; SMG cultures showed reduced expression of ALP, RUNX2 , OSX, RANKL and increase in OPG. In addition, SMG cultured MSCs showed fewer ALP positive cells and reduced ALP activity, which was more comparable to the non-induced MSCs (control). SMG cultured MSCs also showed little or no collagen production or matrix mineralization after 12 days of culture in osteogenic media. The data show that SMG-MSC (M)are drastically hampered from osteogenesis after 12 days of culturing in osteogenic media and instead resemble non-induced MSC cultures. These results confirm that lack of gravity or mechanical stress severely affects MSC osteogenic differentiation. Meyers et al. have reported similar results with ALP and RUNX2 expression and collagen content under

SMG [226]. The same study reported inactivation of the MAPK-ERK pathway due to reduced expression of collagen 1 in extracellular matrix leading to inhibition of Runx2 expression and osteogenesis [226]. Furthermore, Sheyn et al. have shown that SMG down-regulates genes regulating cell proliferation, differentiation, adhesion, cytoskeletal proteins, and cell communication and upregulates stress related genes in human MSCs [227].

LIPUS exposure increased expression of ALP, OSX, RUNX2, and RANKL and decreased OPG gene expression in SMG cultures and restored it to levels similar to normal gravity grown control samples. RANKL and OPG are proteins secreted by osteoblasts and MSCs to control osteoclastogenesis. As MSCs differentiate into osteoblasts, the level of RANKL increases while that of OPG decreases. LIPUS exposure increased the RANKL/OPG ratio in normal and SMG cultures, thus enhancing osteogenic differentiation of MSCs. Similarly, recent studies by Liu et al. have shown that static and dynamic pressure can increase the RANKL/OPG ratio in early osteogenesis [228]. These findings correlate well with our study as LIPUS is an acoustic pressure wave providing localized and targeted stimulation. On the contrary, Rubin et al. has reported that cyclic strain reduces RANKL expression in murine marrow stem cells [229]. It is speculated that different mechanical stimuli can induce different responses in MSCs. Detailed study of mechanical stimuli relative to corresponding mechanotransductive pathways is required to understand MSC role in osteoclastogenesis and osteogenesis.

ALP positive population and activity increased with exposure to LIPUS stimulation. SMG cultures had little or no ALP positive cells; application of LIPUS restored ALP positive cells. ALP, a membrane bound enzyme, functions to catalyze phosphate addition to calcium ions resulting in the formation of hydroxyapatite crystals and matrix mineralization. Since ALP expression is known as an early osteogenic marker, increases in ALP positive cell numbers and

ALP activity is indicative of MSC osteogenic differentiation as seen in the LIPUS treated cultures.

Collagen and matrix mineralization also increased with the application of LIPUS. Collagen is an extracellular matrix protein that facilitates cellular adhesion, mineralization, and mechanotransduction through integrin alpha 2 and beta 1[226]. The reduction of collagen content inhibits integrin α2β1 activation, formation of focal adhesion complexes and MAP-ERK pathways, which are essential from osteogenic induction. LIPUS exposure restores collagen in ECM resulting in increased cellular adhesion, matrix mineralization and activation of MAPK-ERK pathway.

The lack of mechanical stimulus can severely impair the ability of MSCs to differentiate into osteoblasts. Studies have shown downregulation of the focal adhesion complex, MAPK and TGFβ signaling pathways in MSCs under SMG. LIPUS is known to induce acoustic streaming in interstitial fluid and localized mechanical vibrations in the ECM [185] resulting in the local deformation of cell membranes and shear stresses and strains to osteoblasts [163, 164, 186-189]. These mechanical deformations subsequently activate integrin, mechanosensitive-calcium channels, G-proteins, IGF, TGF-β/BMP and gap junctions, activating different downstream pathways [181, 188, 190-193]. As such, these studies indicate that the LIPUS treatment can activate mechanotransductive pathways and significantly increase osteogenic differentiation in stem cells.

The objective of this study was to investigate the effects of LIPUS on osteogenic differentiation of MSCs in disuse conditions. Application of LIPUS increased the expression of osteogenic genes along with increasing ALP activity and expression. LIPUS treated SMG cultures had higher collagen content in ECM and more matrix calcification. Further studies are

needed to understand underlying mechanotransductive pathways and the effect of LIPUS on early osteoclastogenesis/osteogenesis in MSCs. Taken together, we conclude that LIPUS provides the essential mechanical stimulus to induce osteogenesis in a SMG environment and has the potential to be used as a therapy for disuse osteoporosis due to space travel, long-term bed rest, and brain/spinal cord injuries.

Chapter 5

LIPUS Induces Osteoblastic Activity in Simulated Microgravity Cultures

Specific Aim 3: *Evaluate the effects of LIPUS on osteoblast activity during simulated microgravity in vitro*

5.1 Abstract:

Microgravity (MG) is known to induce bone loss in astronauts during space travel. The bone loss is caused by a lack of mechanical stress due to the absence of gravity. Mechanical stimulation can be used to provide essential signals to bone cells and potentially serve as countermeasure to the catabolic effects of MG. The objective of this study was to examine the effects of low intensity pulsed ultrasound (LIPUS) on osteoblasts in a simulated microgravity (SMG) environment (created using a 1D clinostat bioreactor).Specifically, we evaluated the hypothesis that osteoblasts' (human fetal osteoblastic [Hfob] cell line) exposure to LIPUS for 20 min per day at 30 mW/cm^2will significantly reduce the detrimental effects of SMG. Effects of SMG and LIPUS were analyzed using the MTS assay for proliferation, Phalloidin for F-actin staining, Sirius red stain for collagen and Alizarin red for mineralization. Our data show that osteoblast exposure to SMG results in significant decreases in proliferation (38% and 44% at day 4 and 6, respectively, $p<0.01$), collagen content (22%, $p<0.05$) and mineralization (37%, $p < 0.05$) and actin stress fibers. In contrast, LIPUS stimulation under SMG conditions significantly increases the rate of proliferation (24% by day, $p<0.05$), collagen content (52%, $p < 0.05$) and matrix mineralization (25%, $p<0.001$) along with restoring formation of actin stress fibers in the SMG-exposed osteoblasts. These data suggest that the acoustic wave can potentially be used as a countermeasure for MG-induced bone loss.

5.2 Introduction

Microgravity (MG) induced during extensive space-flight can significantly reduce bone mineral density (BMD). Overall, 1-2% monthly loss of BMD is observed during a typical 3-6 month space mission, in which, greater bone loss was observed in the weight-bearing sites, especially in the low extremity and lumbar spine [224, 230]. Further, ~20-30% total bone loss is expected in a 30-month manned mission to Mars [142, 231], which will significantly hamper the astronauts bone's structural and physiological function. Thus, it is important to understand the effects of MG on skeletal remodeling, both on local osteoblast/osteoclast coupling and on systemic hormones (PTH, calcitonin, etc.) and how they may influence bone metabolism. To make long term space exploration possible, it is imperative that an effective countermeasure against the catabolic effects of MG can be developed. This countermeasure should be able to maintain the integrity of the skeleton's mechanical and physiological, as well as have the capacity to meet the technical challenge in space, e.g., noninvasive, lightweight, and portable. To address such a challenge, astronauts usually spend ~2.5 hrs/day exercising (running and weight lifting while in space flight), but this is still not sufficient enough to attenuate their bone loss. Promising studies have shown anabolic effects using drugs and growth factors, but long-term effects of pharmacological agents are still unclear. Furthermore, drugs have mostly systemic effects, are not as effective in space, and can become prohibitively expensive over an extended period of time [158].

To understand the underlying biological processes behind the observed bone loss, *in vitro* studies were conducted at the International Space Station using various types of bone cells. For example, osteoblasts cultured in space showed significant reduction in glucose utilization, rate of

proliferation and mineralization [140-143] and severely affecting cytoskeletal organization and cell adhesion [232].

Conducting *in vitro* studies at the Space Station is greatly limited by access and can be expensive with many technical difficulties. Therefore, to address these disadvantages, different ground base SMG models have been developed and utilized. The two most commonly used SMG models are the Rotating Wall Vessel (RWV) [150, 151] and Random Position Machine (RPM) [152]. Studies conducted using these SMG models showed down-regulation of a number of bone related genes including alkaline phosphatase (ALP), runt-related transcription factor 2 (RUNX2), parathyroid hormone receptor 1 (PTHr1), bone morphogenetic protein 4 (BMP4), procollagen and osteoglycin, as well as significant reductions in the formation of calcium nodules and collagen matrix formation [151, 155]. Lastly, osteoblasts grown in SMG also show similar effects on morphology, cytoskeleton, apoptosis and gene expression as those cultured during space flight [151, 155].

In the past decade researchers have also explored the anabolic effects of various mechanical stimulatory signals, namely vibration, fluid flow, and ultrasound on the skeleton. Specifically, low-intensity pulsed ultrasound (LIPUS) was applied *in vivo* and showed reversal of osteopenia and bone fracture healing [170-172]. Additionally, LIPUS exposure induced anabolic events in bone cells [175-177, 233], cytokine release [178], increased mRNA expression of RUNX2. ALP, Osterix (OSX) and collagen 1[179], calcium mineralization of ECM [180], Akt pathway activation[181], potassium influx[182], angiogenesis[183], adenyl cyclase activity and TGF-β synthesis, resulting in increased osteogenesis of bone stromal cells [184].

Despite these effects, the exact mechanism through which LIPUS enhances bone cell properties and increases the rate of bone formation remains unknown. As such, we attempted to further explore the effects of LIPUS by testing the hypothesis that LIPUS serves as aneffective countermeasure for the detrimental effects of SMG on osteoblast activity and morphology. Herein, we show that LIPUS positively regulates actin stress fiber polymerization, proliferation, and matrix mineralization in human osteoblasts.

5.3 Materials and Methods

5.3.1 Rotation Microgravity Simulation

A *one-dimensional clinostat (1-D Clinostat)* was used as described in section 4.3.1.

5.3.2 Ultrasound Exposure:

Ultrasound exposure and setup were kept identical to setup described in 4.3.2.

5.3.3 Cell Culture:

Human fetal Osteoblasts (Hfob 1.19, ATCC, Manassas,VA.USA) were cultured in DMEM:F12 media supplemented with 15% FBS, 0.3mg/ml G418with an initial seeding density of 250,000 cells/Opticell. Cells were distributed into four groups (n=4/group):1) Gravity (G); 2) Gravity + LIPUS (GU); 3) SMG (M); and 4) M + LIPUS (MU). GU and MU samples were stimulated with LIPUS for 20 min/day for the duration of the experiments while G and M samples were placed on a switched-off transducer. All cells were maintained at 37^{o}C and 5% $CO_2$and the culture medium was changed every other day.

5.3.4 Cell layer Deformation:

Hfob cells were allowed to reach confluency and form a monolayer in Opticells (visually inspected using a light microscope). Cells were kept under simulated MG for 7 days and the cell layer was observed for structural integrity using bright field microscopy (Axiovert 200, Carl Zeiss, Thornwood, NY, USA).

5.3.5 Proliferation Assay:

Hfob cells were cultured at 250,000/opticell and were allowed to adhere to the Opticell surface for 24 hr before being subjected to the clinostat. Daily LIPUS was applied after 24 hr of MG. Samples were collected at Day 2, 4 and 6 and each RoS was cut out of the Opticell and

processed with an MTS reagent (Invitrogen) in serum-less DMEM per manufacturer's instructions. Briefly, the cells were incubated for 4 hours at 37^{o}C, 5% CO_2 with the MTT reagent followed by lysis with DMSO for 10 min. Finally, the supernatant was analyzed at 540nm in a spectrophotometer *(Bio*-Tek EL800, Winooski, VT.USA*).*

5.3.6 Collagen Staining:

Staining protocol details were kept identical to one described in section 4.3.6

5.3.7 F-Actin Staining:

Hfob cells were seeded at initial density of 100,000 cells/opticell and were allowed to adhere for 24 hr. The cells were cultured in MG for 3 days and then fixed in 10% formaldehyde buffer for 15 min at room temperature and washed with PBS. The cell membrane was permeabilized using 1% Triton-X100 for 10 min followed with three, 5 min PBS washes. The cells were then blocked with 1% BSA and incubated with Rhodamine-conjugated Phalloidin for 20min and mounted using Vectashield mounting medium containing DAPI (Vector labs, Burlingame,CA). Finally, the cells were imaged at 100x using an Axiovert 2000M Inverted Microscope (Carl Zeiss, Thornwood, NY, USA).

5.3.8 Matrix Mineralization:

Experimental procedure and methods were kept identical to section 4.3.7

5.3.9 Real Time Quantitative PCR

Experimental methods were kept consistent with section 4.3.4. Gene expression was analyzed for RUNX2, OSX and RANKL.

5.3.10 *Statistics:*

GraphPad Prism 3.0 software was used to run statistical analyses. All data is presented in ± standard deviation. One-way ANOVA with Newman Keuls Post hoc was used to calculate significance within the different groups and time points. A p value of <0.05 was considered to be significant.

5.4 Results

5.4.1 Simulated microgravity disrupts the cellular monolayer:

As osteoblast function is highly dependent on the ECM, any deficiency in the quality of the ECM will negatively affect osteoblast activity. As such, we investigated the effects of MG and LIPUS on the integrity of the cellular monolayer. During SMG cells were observed daily and after 7 days of SMG, M samples displayed dark areas that represent disruptions in the cell monolayer (Figure 16, M, arrows). In contrast, the gravity control samples (G) maintained a uniform and intact cell monolayer (Figure 16, G).

Figure 16: Osteoblast – Cell Layer Deformation

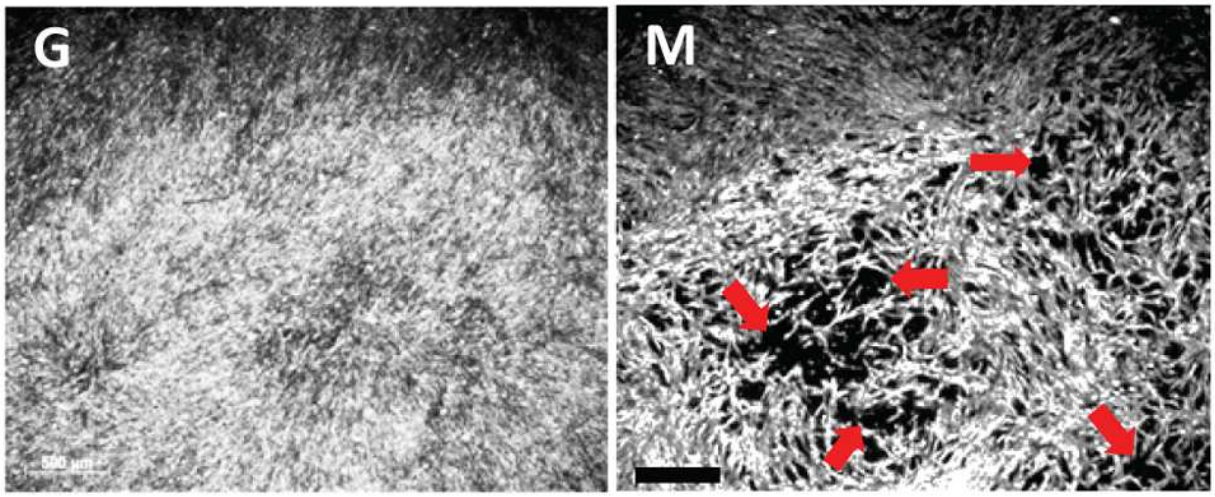

Figure 16: SMG induces gaps in cellular layer. Bright field microscopy was conducted on Day 7, bright field microscopy of primary osteoblasts in the presence of SMG (M) and Gravity (G). Images clearly show gaps within the cell monolayer of the M cultures (arrows) as compared to the G. Scale Bar = 100µm

5.4.2 LIPUS exposure significantly reverses SMG-induced decreases in osteoblast proliferation:

The observed non-uniform cell layers in M samples are indicative of either a reduced rate of proliferation or a compromised ECM. Thus, we decided to examine these possibilities starting with cell proliferation. Results from these experiments showed that the rate of proliferation is significantly reduced in samples exposed to SMG (M) by 38% ($p<0.01$) and 45% ($p<0.01$), on day 4 and 6 samples, respectively (Figure 17). The application of LIPUS reversed this trend and in fact, it increased cell proliferation by 24% ($p<0.05$) and 19% ($p<0.001$), when compared to the M samples at day 4 and 6, respectively (Figure 17). In contrast, LIPUS stimulation had no major effect on cell proliferation in the gravity samples (GU) as compared to the control (G)(Figure 17).

Figure 17: Osteoblast Proliferation

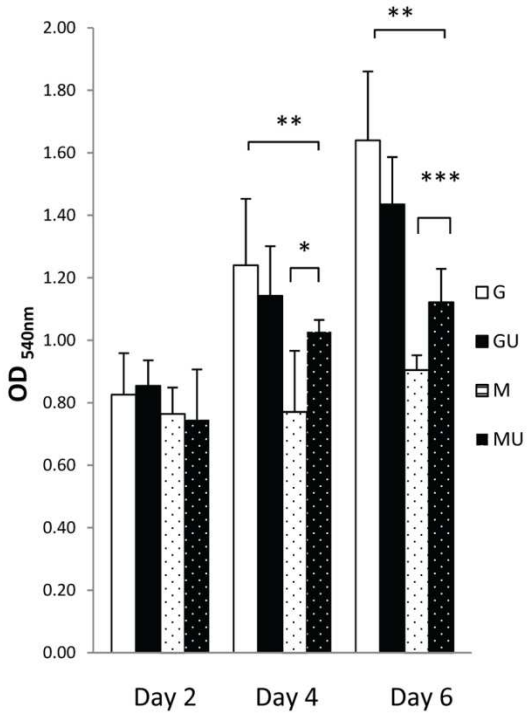

Figure 17: LIPUS exposure significantly reverses SMG-induced decreases in Osteoblast proliferation. Osteoblast proliferation (n=4) is shown in the various conditions (G, GU, M, MU) and time (Day 2, 4 and 6). G cultures show a steady rate of proliferation whereas SMG significantly reduces osteoblast proliferation. LIPUS exposure increases proliferation rate in SMG (* $P<0.05$, ** $p<0.01$,***$p<0.001$). Osteoblasts show significant growth between day 2 to 4 and 6($p<0.01$). SMG cultured cells show no significant proliferation between days 2-4 and 4-6 ($p>0.05$). LIPUS stimulation induces significant proliferation between days 2-4 and 2-6 ($p<0.05$).

5.4.3 LIPUS exposure significantly reverses SMG-induced decreases in collagen production:

As we postulated earlier, disruption of the cell monolayer in the presence of SMG may also be due to a compromised ECM. Thus, we sought to measure the amount of secreted collagen by osteoblasts using Sirius red (stains collagen, predominantly types I and III fibers). Histological/qualitative analyses show a reduction in collagen staining in the SMG exposed samples (M) and significant recovery when stimulated with LIPUS (MU) (dark red patches of collagen distributed evenly in extracellular matrix, Figure 18a). The application of LIPUS on the G samples (GU) did not result in any significant increase in collagen secretion as compared to the control (G) (Figure 18a). In addition, while all three cultures, G, GU and MU showed variable collagen density (with scattered areas/loci of lesser and denser collagen patches), the M cultures showed weaker and overall very low collagen density throughout the culture (Figure 18a).Further, when we quantitatively measured the intensity of the staining in these cultures we detected a significant reduction (22%, $p<0.05$) of collagen secretion in the presence of SMG in comparison to the G cells (Figure 18b).In contrast, LIPUS stimulation reversed this trend and in fact, restored collagen levels to those observed with the G and GU samples (Figure. 18b). Specifically, LIPUS stimulation decreased the loss of collagen in the presence of SMG by 52% ($p<0.05$) (Figure 18b).

Figure 18: Osteoblast – Collagen ECM Content

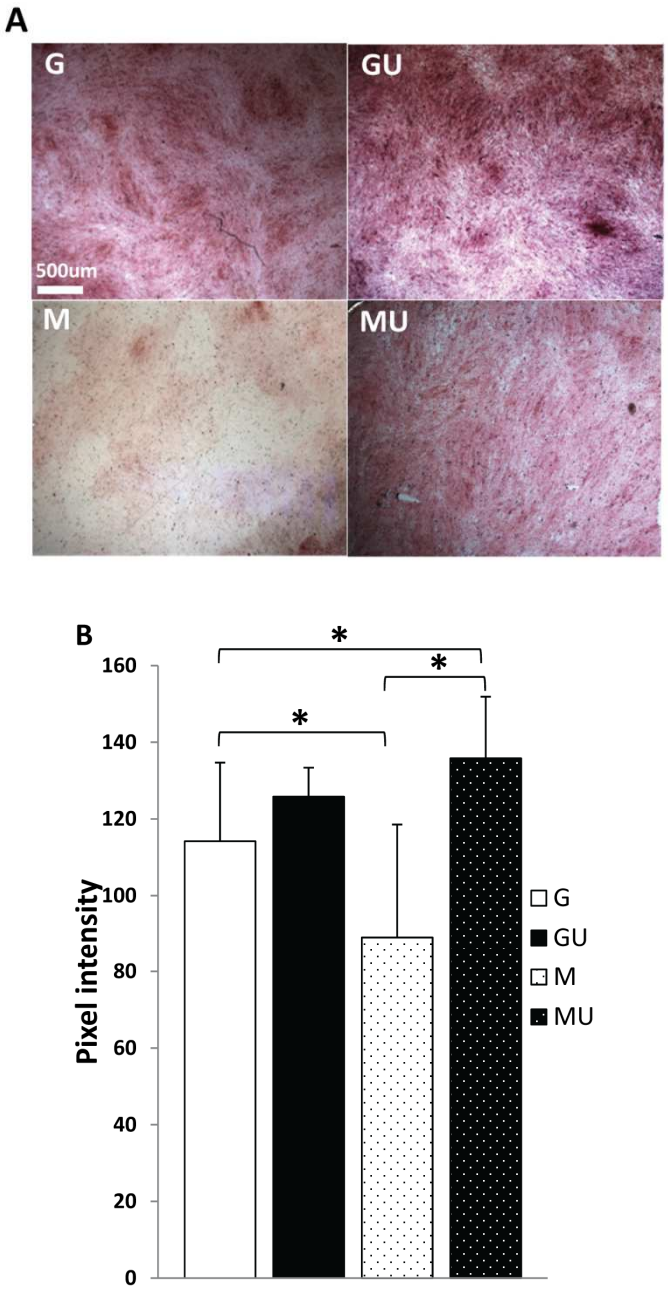

Figure 18: LIPUS exposure significantly reverses SMG-induced decreases in collagen production.
A) Sirius Red Staining: G samples show evenly distributed collagen fibers. LIPUS stimulation (GU) increased the stain intensity of collagen fibers in the ECM. Cell cultures in SMG (M) show minimal collagen fibers, whereas exposure of LIPUS increases collagen staining. MU samples show uneven collagen distribution. Scale Bar = 500µm
B) Quantitative measurement of Sirius Red stain as a function of collagen content: Significant decrease in collagen in SMG; LIPUS treatment recovers collagen content in the ECM (* $p < 0.01$).

5.4.4 LIPUS exposure significantly reverses SMG-induced decreases in calcification:

To further probe the positive effects of LIPUS stimulation on SMG-exposed cells, we investigated matrix calcification using alizarin red staining. Results from these experiments showed an even distribution of calcium phosphate in G cultures, but with LIPUS stimulation, we observed a much denser and wider presence of stained patches of calcified matrix (Figure 19A, GU). Alizarin red staining was less evenly distributed in the M cultures with apparent areas of no staining, probably due to the reduced number of cells and collagen (Figure 19A, M). This was again reversed in the presence of LIPUS (MU) whereby the formation of calcium phosphate nodules resembled that seen with GU (Figure 19a, GU). Further, when we quantitatively measured the concentration of the eluted dye, we found a 37% ($p<0.05$) decrease in matrix calcification in M as compared to G but with LIPUS stimulation it was increased by 25% ($p<0.01$) in the M cultures. Although there was a slight increase (16%) in the GU cultures in comparison to G, it was not statistically significant.

Figure 19: Osteoblast –Matrix Mineralization

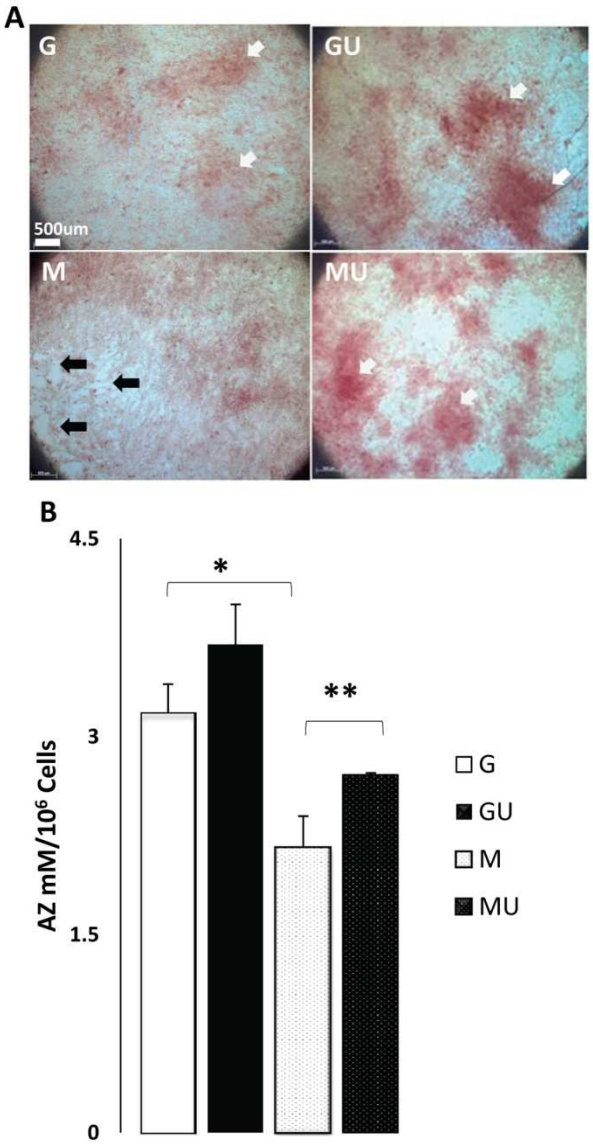

Figure 19: LIPUS exposure significantly reverses SMG-induced decreases in Osteoblast matrix calcification.
A) Calcification of ECM: G cultures shows evenly distributed calcified matrix and with LIPUS stimulation denser patches (white arrows GU) are visible. In contrast, M cultures show a dispersed calcification pattern with areas of no calcification (black arrow M). LIPUS exposure increases the area of calcified matrix and formation of denser calcium nodules (MU).Scale Bar = 500µm
B)Quantification of ECM Calcification: SMG induced osteoblasts show 47% less matrix calcification than G controls. LIPUS restores matrix calcification significantly by 25%. (*p <0.05, **p<0.01). GU cultures show positive calcification trends after 14 days of LIPUS exposure.

5.4.5 LIPUS exposure increased expression of osteogenic genes while reducing expression of osteoclastogenic genes.

PCR analyses were done to investigate the effect of LIPUS on osteogenic gene, specifically RUNX2, OSX and RNAKL, on ostoeblasts cultured under SMG conditions. RUNX2 and OSX expression showed downregulation after 24 hours of SMG. MU samples showed significant increases in RUNX2 and OSX immediately after LIPUS stimulation. GU samples showed little to no increase in RUNX2 and OSX expression levels after LIPUS stimulation.

RANKL expression was studied to see the effects of LIPUS on osteoclastogensis when exposed to SMG conditions. RANKL expression didn't show significant change due to SMG, however LIPUS exposure significantly decreased RANKL expression (Figure 20, $p<0.0.5$) in MU cultures relative to G and M.

Figure 20: Osteoblast PCR Results

a) b)

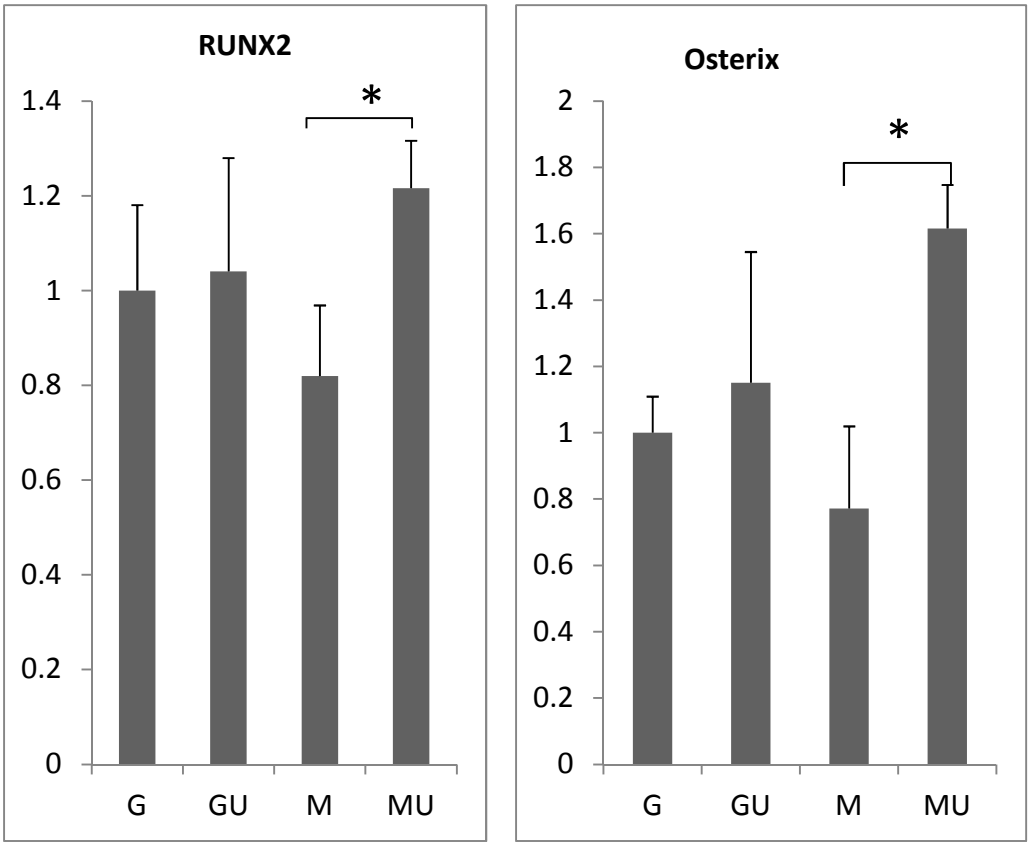

c)

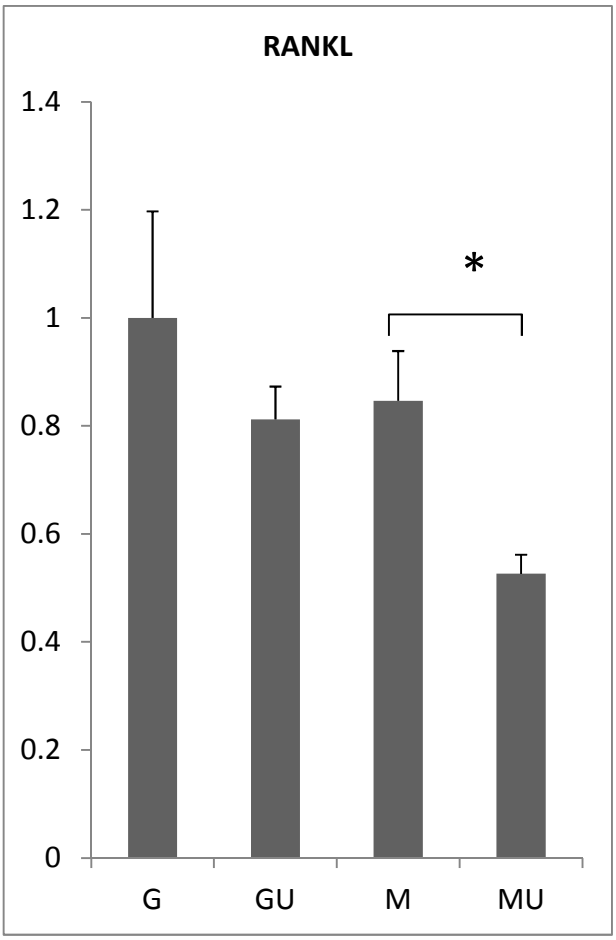

Figure 20: LIPUS increases osteogenic genes expression and reduces osteoclastogenic gene expression.
a) RUNX2 showed no change in GU but was significantly reduced in M cultures. Application of LIPUS increased RUNX2 expression significantly relative to M cultures.
b) OSX decreased significantly in M cultures and application of LIPUS increased OSX expression significantly in MU but didn't show any significant changes in Gravity samples.
c) RANKL expression showed decreases M; exposure of LIPUS further decreased RANKL expression in MU cultures and showed little reduction in GU cultures.

5.5 Discussion

The experiments, reported herein using the 1-D clinostat to generate simulated MG, confirm previous *in vitro* experiments conducted both in space and under SMG conditions on the ground[146, 147, 230] that this experimental setup is capable of inducing SMG. Further, it enabled us to test the hypothesis that LIPUS can serve as a countermeasure for MG-induced bone loss.

Application of LIPUS significantly restored the functional and morphological changes in human osteoblasts as induced by SMG. The observed disruption in the cell monolayer in the presence of SMG resulted from both, the reduction in the rate of proliferation and decreased ECM leading to reduced cell adherence. Initially, we showed that SMG inhibited osteoblast proliferation which was fully restored in the presence of LIPUS but not to the level of the control cells. It is well known that mechanical stimuli enhance the differentiation of osteoblasts, which can lead to a reduced rate of proliferation [234].The same observation has been made by Pre et al. (2009) with low-amplitude high frequency mechanical vibrations [235].In contrast, other studies have shown increased osteoblast proliferation during LIPUS exposure [236, 237]. While Chen et al. used signals of 50, 100 and 150 mW/cm^2 for 3 min per day, our study used $30mW/cm^2$ for 20 min per day, and perhaps it is possible that the difference in intensity and time resulted in the observed changes in cell proliferation. Raucci et al. (2008) have argued that the relative activation of the ERK and AKT pathways determines the tendency of osteoblasts towards differentiation or proliferation [234]. Specifically, high ERK expression induced osteoblast proliferation and increased expression of AKT enhanced differentiation. In addition, Ultrasound stimulation is known to upregulate the ERK1/2-MPAK pathways through activation of integrins [159, 238, 239] andvarious studies have shown activation of the AKT pathway after

LIPUS exposure [240, 241]. Thus, it is possible that different intensities and durations of treatment may affect different mechanotransductive pathways. Unfortunately, it is still unclear how and if LIPUS regulates the synergy between ERK-MPAK and AKT pathways. Alvarenga et al. showed increased proliferation at days 5 and 7 in primary osteoblast cultures when stimulated with LIPUS (30mw/cm^2, 20 min per day, 1.5 MHz) and as such it was speculated that different cell types and stimulation frequency can potentially affect the cellular response to LIPUS. More in depth studies are required to fully understand the exact LIPUS effects on rate of proliferation relative to different signal parameters.

SMG has also been found to reduced the amount of collagen in the ECM leading to decreased osteoblast adhesion and even induced cell death [242].This is consistent with our data where we showed that LIPUS exposure restored the amount of collagen in MU compare to the M cultures showing areas with little or no staining, probably due to a reduced number of cells as a result of apoptosis (but this was not experimentally verified). Interestingly, LIPUS stimulation did increase collagen content in the GU cultures, indicating that the ultrasound signal is capable of stimulating collagen production, under normal conditions.

LIPUS stimulation also increased the SMG-induced reduction in matrix mineralization. Specifically, the LIPUS treated SMG samples showed a 25% increase in mineralization in comparison to the untreated M cultures, but this is significantly lower than the controls (G). Our mineralization study was conducted over 14 days and it is possible that extended exposure of LIPUS can continue to increase mineralization in the GU samples. The LIPUS-induced increase in mineralization in the cultures exposed to SMG conditions is probably due to an increase in the number of osteoblasts, higher content of collagen secretion and an overall increase in osteoblastic activity. This study extends the findings of other studies using LIPUS as anabolic

stimuli in bone cells. For example, Suzuki et al. showed that daily application of LIPUS for 14 days increased the expression of RUNX2, ALP, Dlx5, BMP-2 and OSX, as well as the matrix calcification in rat osteoblast cells. The anabolic effects of LIPUS were also reported in various animal models of bone fracture healing and ovaricectomy [243, 244]. These studies, along with our data, suggest that LIPUS can potentially be used to reverse the detrimental effects of MG on the mammalian skeleton.

This study showed that LIPUS stimulation induced increased F-actin polymerization, which is known to play an critical role in both the tensegrity and mechanosome concepts of mechanotransduction[245]. Tensegrity is based on the transmission of applied forces on a cell membrane to chromosomes resulting in chromosomal deformations and changes in transcription [246]. This is highly dependent on the continuous transfer of forces from the plasma membrane to chromosomes through intact connections of the cytoskeletal actin stress fibers to the plasma and nuclear membranes [246, 247]. The mechanosome theory is based on localized changes on the plasma membrane, specifically, the induction of conformational changes on cell surface proteins leading to activation of different signaling pathways and resulting in transcriptional changes [248]. Thus, actin plays an important role in the conduction of mechanical conformational changes of cell surface receptors to the activation of downstream signaling pathways. Further, it is also known that acoustic vibrations caused by LIPUS lead to conformational changes in integrin receptors and activate downstream mechanotransductive pathways [249]. Yang et al. has shown increased integrin expression after ultrasound stimulation in osteoblast cells [193], thereby activating the ERK1/2-MAPK downstream pathways [192]. Kook et al. has also shown that the ERK pathway plays an important role in collagen expression [250]. Since osteoblasts are known to mineralize bone matrix along collagen fibers [251-253]),

any decrease in collagen content will lead to a reduction in osteoblast adhesion to the ECM as well as a reduction in matrix mineralization. On the other hand, reduced numbers of F-actin stress fibers in MG can inhibit the integrin mediated ERK1/2 pathway, resulting in a reduced rate of proliferation and ultimately resulting in low collagen production and overall matrix mineralization (as observed with the SMG exposed samples). It would be interesting in future studies, to determine whether the structural properties of collagen and calcium phosphate crystals are altered in SMG conditions.

SMG significantly reduced the expression of RUNX2, OSX and RANKL. LIPUS exposure restored RUNX2 and OSX expression but further reduced expression of RANKL.RUNX2 and OSX are established osteogenic markers and increased levels of RUNX2 and OSX indicates anabolic effects due to LIPUS treatment. Conversely, RANKL is known to induce osteoclastogenesis and osteoclast activity, thus the reduced RANKL expression seen in LIPUS treated groups (MU & GU) is indicative of the anti-resorptive effects of LIPUS stimulation in osteoblast cultures. Gene expression analysis confirmed LIPUS as an anabolic and anti-resorptive stimulus for osteoblast cells.

The objective of this study was to test the hypothesis that LIPUS serves as an effective countermeasure for the detrimental effects of SMG on osteoblast activity and morphology. We found that application of LIPUS significantly increased the rate of osteoblast proliferation and restored F-actin polymerization. Further, the collagen content was fully restored and mineralization showed significant increase with LIPUS exposure relative to SMG cultures. Taken together, we conclude that LIPUS can successfully serve as a countermeasure to the detrimental effects of MG on osteoblasts. LIPUS can potentially provide a non-invasive and targeted therapy for astronauts in space as ultrasound transducers or arrays can be designed such

that they adhere to the region of interest (i.e. limbs and spine) and operated by rechargeable batteries. Regardless, further studies are required to completely understand the molecular mechanism(s) by which LIPUS induces mechanotransduction in osteoblasts before it can be accepted as a “true” countermeasure for microgravity-induced bone loss.

Chapter 6

Conclusion

6.0 Conclusion

The objective of this study was *to study the effects of ultrasound as a countermeasure to the catabolic effects of MG on osteoblast and mesenchymal stem cells in an in vitro simulated microgravity system and on bone quality and architecture in a HLS model.* The study was designed in three specific aims, the first specific aim examined the effects of LIPUS on disuse bone structural integrity and mechanical properties, the second specific aim was designed to investigate LIPUS effects on osteogenic differentiation in MSG conditions; and lastly, the third specific aim targeted osteoblastic activity in SMG with and without LIPUS stimulation. The *in vivo* study showed LIPUS partially restored bone structural integrity in a disuse model, as evidenced MicroCT and histomorphometry data, showing significant increases in BV/TV, BMD and trabecular thickness. Detailed analysis of histomorphometry data also revealed increased bone formation rate in the endosteal surface of the proximal tibia. Furthermore, LIPUS did not show any adverse effects on non-suspended nice, indicating that LIPUS only targeted area of bone loss and did not negatively affect healthy bone tissue. The endosteal surface is enriched with MSCs and osteoblasts, which plays a pivotal role in bone formation. Increased bone formation in the endosteal surface indicated LIPUS effecting bone formation and thus differentiation of MSCs and osteoblast activity. LIPUS exposure increased ALP activity, matrix collagen content and mineralization. LIPUS treated MSCs showed increased expression of RUNX2, OSX and ALP. LIPUS also increased the RANKL/OPG ratio; RANKL is predominantly excreted by pre-osteoblast and osteoblast lineage cells, thus an increase in RANKL indicates an increase in osteogenesis. That said, RANKL is essential also for osteoclastogenesis and osteoclast maturation, thus, increasing osteoclast number and activity. Further studies are required to understand the underlying role of early MSC osteogenic differentiation in osteoclastogenesis. LIPUS exposed osteoblasts showed an increase in osteogenic activity in SMG as well as an increase in osteoblast proliferation, matrix collagen and mineralization. LIPUS restored expression of RUNX2 and OSX in osteoblast and further decreased RANKL expression, indicating a decrease in osteoclastogenesis.

Collectively, the data suggest LIPUS has the strong potential to provide an essential mechanotransductive anabolic stimulus to counter measure disuse-induced bone loss while showing no adverse effect on healthy bone. This study showed increased structural and mechanical integrity in LIPUS treated disuse bones. Furthermore, LIPUS increased MSCs osteogenic differentiation and osteoblastic activity in SMG. RANKL expression decreased in LIPUS treated osteoblast cells, indicating decreased osteoclastogenesis but on the contrary, the RANKL/OPG ratio increased in LIPUS treated disused MSCs. RANKL is highly expressed in osteoblasts while OPG is predominately excreted by MSCs, thus an increased RANKL/OPG ratio is more indicative of increased osteogenesis but detailed studies are required to examine this in further.

Chapter 7

Limitations and future studies

7.0 Limitation and Future Studies

Bone remodeling is regulated by bone formation and resorption which in turn controlled by osteoblasts, osteocytes and osteoclasts coupled with the differentiation potential of their respective progenitors, MSCs and HSCs. This study focused on the bone formation aspects of bone remodeling. Previous studies have shown increased osteoclastogenesis and osteoclast activity during microgravity or disuse conditions [232, 254]. Results from this study showed LIPUS decreased osteoblast RANKL expression in SMG conditions but increased RANKL in MSCs. Thus it is not clear if LIPUS will increase or reduce osteoclastogenesis. Experiments need to be designed to study the effects of early osteogenic differentiation on osteoclastogenesis. Furthermore, co-culture experiments should be designed to see the effects of MSC osteogenesis and/or osteoblast activity on osteoclast differentiation and activity, both with and without LIPUS stimulation.

The *in vivo* study also focused on bone formation and the changes brought about due to disuse and application of LIPUS, but did not consider bone resorption/osteoclastogensis/osteoclastic activity, which is the other half of the bone remodeling equation. Future studies are needed to investigate osteoclast numbers and activity under disuse conditions, and this could be done by analyzing bone for BMU units and microfractures. The current study showed a significant decrease in mechanical properties at the mid diaphysis but micro CT data didn't show a corresponding decrease in cortical BMD. It is speculated that disuse can affect matrix collagen alignment and structure but further research is required to thoroughly examine collagen content and alignment in cortical bone. The data from this study showed that LIPUS can be used as a countermeasure for disuse induced bone loss; That LIPUS reduced bone loss partially, considering the treatment was limited to 20 min per day 5 days a week, while animals were in suspension continuously over the period of 4 weeks, it is speculated that increasing the number of stimulations per day may reduce bone loss further.

This study focused on the anabolic effects of LIPUS on bone in disuse conditions, and further investigated MSCs differentiation and osteoblast activity in SMG conditions, with and without LIPUS. To optimize the anabolic effects of LIPUS it is important to study the cellular and molecular mechanisms. This study didn't look at mechanotransductive pathways with respect to LIPUS stimulation. The ideal next step for this study will be to study LIPUS and different mechanotransductive pathways.

In summary, LIPUS has the potential to be an anabolic agent to induced bone formation in disuse, both *in vivo* and *in vitro* disuse models. LIPUS reduced bone loss in HLS mice over 4 weeks of suspension, specifically reducing loss of trabecular BV/TV, Tb.Th, BMD and increasing BS/BV. Dynamic histomorphometry confirmed MicroCT data and showed an increased bone formation rate in LIPUS treated disuse bone, with most of that bone formation limited to the endosteal surface. Cortical bone showed improved biomechanical properties, as LIPUS increased Young's modulus and ultimate strength of disuse bone. LIPUS increased osteogenic differentiation of MSCs in SMG. It also increased ALP positive cells and ALP activity along with increasing matrix collagen content and mineralization. LIPUS treated MSCs showed increased expression of the osteogenic genes RUNX2, ALP, and OSX. Osteoblast activity was severely compromised in SMG conditions and LIPUS exposure increased osteoblast proliferation and matrix collagen and mineralization. LIPUS increased expression of RUNX2 and OSX expression in SMG osteoblast cultures.

References:

1. Crockett, J.C., et al., *Bone remodelling at a glance.* J Cell Sci. **124**(Pt 7): p. 991-8.
2. Rey, C., et al., *Bone mineral: update on chemical composition and structure (vol 20, pg 1013, 2009).* Osteoporosis International, 2009. **20**(12): p. 2155-2155.
3. Clarke, B., *Normal Bone Anatomy and Physiology.* Clinical Journal of the American Society of Nephrology, 2008. **3**: p. S131-S139.
4. Parfitt, A.M., *The mechanism of coupling: a role for the vasculature.* Bone, 2000. **26**(4): p. 319-23.
5. Ducy, P., et al., *Osf2/Cbfa1: a transcriptional activator of osteoblast differentiation.* Cell, 1997. **89**(5): p. 747-54.
6. Otto, F., et al., *Cbfa1, a candidate gene for cleidocranial dysplasia syndrome, is essential for osteoblast differentiation and bone development.* Cell, 1997. **89**(5): p. 765-71.
7. Robledo, R.F., et al., *The Dlx5 and Dlx6 homeobox genes are essential for craniofacial, axial, and appendicular skeletal development.* Genes Dev, 2002. **16**(9): p. 1089-101.
8. Barnes, G.L., et al., *Osteoblast-related transcription factors Runx2 (Cbfa1/AML3) and MSX2 mediate the expression of bone sialoprotein in human metastatic breast cancer cells.* Cancer Res, 2003. **63**(10): p. 2631-7.
9. Bendall, A.J. and C. Abate-Shen, *Roles for Msx and Dlx homeoproteins in vertebrate development.* Gene, 2000. **247**(1-2): p. 17-31.
10. Morsczeck, C., *Gene expression of runx2, Osterix, c-fos, DLX-3, DLX-5, and MSX-2 in dental follicle cells during osteogenic differentiation in vitro.* Calcif Tissue Int, 2006. **78**(2): p. 98-102.
11. Bianco, P., et al., *Bone sialoprotein (BSP) secretion and osteoblast differentiation: relationship to bromodeoxyuridine incorporation, alkaline phosphatase, and matrix deposition.* J Histochem Cytochem, 1993. **41**(2): p. 183-91.
12. Nakashima, K., et al., *The novel zinc finger-containing transcription factor osterix is required for osteoblast differentiation and bone formation.* Cell, 2002. **108**(1): p. 17-29.
13. Henrichsen, E., *Alkaline phosphatase in osteoblasts and fibroblasts cultivated in vitro.* Exp Cell Res, 1956. **11**(1): p. 115-27.
14. Glass, D.A., 2nd, et al., *Canonical Wnt signaling in differentiated osteoblasts controls osteoclast differentiation.* Dev Cell, 2005. **8**(5): p. 751-64.
15. Hu, H., et al., *Sequential roles of Hedgehog and Wnt signaling in osteoblast development.* Development, 2005. **132**(1): p. 49-60.
16. Wetterwald, A., et al., *Characterization and cloning of the E11 antigen, a marker expressed by rat osteoblasts and osteocytes.* Bone, 1996. **18**(2): p. 125-32.
17. Feng, J.Q., et al., *The Dentin matrix protein 1 (Dmp1) is specifically expressed in mineralized, but not soft, tissues during development.* J Dent Res, 2003. **82**(10): p. 776-80.
18. Zhang, G.X., et al., *Regulation of mRNA expression of matrix extracellular phosphoglycoprotein (MEPE)/ osteoblast/osteocyte factor 45 (OF45) by fibroblast growth factor 2 in cultures of rat bone marrow-derived osteoblastic cells.* Endocrine, 2004. **24**(1): p. 15-24.
19. Nampei, A., et al., *Matrix extracellular phosphoglycoprotein (MEPE) is highly expressed in osteocytes in human bone.* J Bone Miner Metab, 2004. **22**(3): p. 176-84.

20. van Bezooijen, R.L., et al., *Sclerostin is an osteocyte-expressed negative regulator of bone formation, but not a classical BMP antagonist.* J Exp Med, 2004. **199**(6): p. 805-14.
21. Winkler, D.G., et al., *Sclerostin inhibition of Wnt-3a-induced C3H10T1/2 cell differentiation is indirect and mediated by bone morphogenetic proteins.* J Biol Chem, 2005. **280**(4): p. 2498-502.
22. Yoshida, H., et al., *The murine mutation osteopetrosis is in the coding region of the macrophage colony stimulating factor gene.* Nature, 1990. **345**(6274): p. 442-4.
23. Franzoso, G., et al., *Requirement for NF-kappaB in osteoclast and B-cell development.* Genes Dev, 1997. **11**(24): p. 3482-96.
24. Matsuo, K., et al., *Nuclear factor of activated T-cells (NFAT) rescues osteoclastogenesis in precursors lacking c-Fos.* J Biol Chem, 2004. **279**(25): p. 26475-80.
25. Wang, Z.Q., et al., *Bone and haematopoietic defects in mice lacking c-fos.* Nature, 1992. **360**(6406): p. 741-5.
26. Partington, G.A., et al., *Mitf-PU.1 interactions with the tartrate-resistant acid phosphatase gene promoter during osteoclast differentiation.* Bone, 2004. **34**(2): p. 237-45.
27. Takayanagi, H., et al., *Induction and activation of the transcription factor NFATc1 (NFAT2) integrate RANKL signaling in terminal differentiation of osteoclasts.* Dev Cell, 2002. **3**(6): p. 889-901.
28. Yasuda, H., et al., *Osteoclast differentiation factor is a ligand for osteoprotegerin/osteoclastogenesis-inhibitory factor and is identical to TRANCE/RANKL.* Proc Natl Acad Sci U S A, 1998. **95**(7): p. 3597-602.
29. Lacey, D.L., et al., *Osteoprotegerin ligand is a cytokine that regulates osteoclast differentiation and activation.* Cell, 1998. **93**(2): p. 165-76.
30. Hsu, H., et al., *Tumor necrosis factor receptor family member RANK mediates osteoclast differentiation and activation induced by osteoprotegerin ligand.* Proc Natl Acad Sci U S A, 1999. **96**(7): p. 3540-5.
31. Anderson, D.M., et al., *A homologue of the TNF receptor and its ligand enhance T-cell growth and dendritic-cell function.* Nature, 1997. **390**(6656): p. 175-9.
32. Simonet, W.S., et al., *Osteoprotegerin: a novel secreted protein involved in the regulation of bone density.* Cell, 1997. **89**(2): p. 309-19.
33. Yasuda, H., et al., *Identity of osteoclastogenesis inhibitory factor (OCIF) and osteoprotegerin (OPG): a mechanism by which OPG/OCIF inhibits osteoclastogenesis in vitro.* Endocrinology, 1998. **139**(3): p. 1329-37.
34. Lee, S.K. and J.A. Lorenzo, *Parathyroid hormone stimulates TRANCE and inhibits osteoprotegerin messenger ribonucleic acid expression in murine bone marrow cultures: correlation with osteoclast-like cell formation.* Endocrinology, 1999. **140**(8): p. 3552-61.
35. Woodward, D.F., et al., *Radioligand binding analysis of receptor subtypes in two FP receptor preparations that exhibit different functional rank orders of potency in response to prostaglandins.* J Pharmacol Exp Ther, 1995. **273**(1): p. 285-7.
36. Hofbauer, L.C., et al., *Interleukin-1beta and tumor necrosis factor-alpha, but not interleukin-6, stimulate osteoprotegerin ligand gene expression in human osteoblastic cells.* Bone, 1999. **25**(3): p. 255-9.
37. Hofbauer, L.C., et al., *Osteoprotegerin production by human osteoblast lineage cells is stimulated by vitamin D, bone morphogenetic protein-2, and cytokines.* Biochem Biophys Res Commun, 1998. **250**(3): p. 776-81.

38. Hofbauer, L.C., et al., *Stimulation of osteoprotegerin ligand and inhibition of osteoprotegerin production by glucocorticoids in human osteoblastic lineage cells: potential paracrine mechanisms of glucocorticoid-induced osteoporosis.* Endocrinology, 1999. **140**(10): p. 4382-9.
39. Makrygiannakis, D., et al., *Intraarticular corticosteroids decrease synovial RANKL expression in inflammatory arthritis.* Arthritis Rheum, 2006. **54**(5): p. 1463-72.
40. Kim, C.H., K.H. Kim, and C.R. Jacobs, *Effects of high frequency loading on RANKL and OPG mRNA expression in ST-2 murine stromal cells.* BMC Musculoskelet Disord, 2009. **10**: p. 109.
41. Bandow, K., et al., *Low-intensity pulsed ultrasound (LIPUS) induces RANKL, MCP-1, and MIP-1beta expression in osteoblasts through the angiotensin II type 1 receptor.* J Cell Physiol, 2007. **211**(2): p. 392-8.
42. Maddi, A., et al., *Long wave ultrasound may enhance bone regeneration by altering OPG/RANKL ratio in human osteoblast-like cells.* Bone, 2006. **39**(2): p. 283-8.
43. Takahashi, K. and S. Yamanaka, *Induction of pluripotent stem cells from mouse embryonic and adult fibroblast cultures by defined factors.* Cell, 2006. **126**(4): p. 663-76.
44. Okita, K., N. Nagata, and S. Yamanaka, *Immunogenicity of induced pluripotent stem cells.* Circ Res. **109**(7): p. 720-1.
45. Zhao, T., et al., *Immunogenicity of induced pluripotent stem cells.* Nature. **474**(7350): p. 212-5.
46. Tonlorenzi, R., et al., *Isolation and characterization of mesoangioblasts from mouse, dog, and human tissues.* Curr Protoc Stem Cell Biol, 2007. **Chapter 2**: p. Unit 2B 1.
47. Huang, Y., et al., *Gravity, a regulation factor in the differentiation of rat bone marrow mesenchymal stem cells.* J Biomed Sci, 2009. **16**: p. 87.
48. Friedenstein, A.J., et al., *Heterotopic of bone marrow. Analysis of precursor cells for osteogenic and hematopoietic tissues.* Transplantation, 1968. **6**(2): p. 230-47.
49. Dominici, M., et al., *Minimal criteria for defining multipotent mesenchymal stromal cells. The International Society for Cellular Therapy position statement.* Cytotherapy, 2006. **8**(4): p. 315-7.
50. Kearney, E.M., et al., *Tensile strain as a regulator of mesenchymal stem cell osteogenesis.* Ann Biomed Eng. **38**(5): p. 1767-79.
51. Wagner, D.R., et al., *Hydrostatic pressure enhances chondrogenic differentiation of human bone marrow stromal cells in osteochondrogenic medium.* Ann Biomed Eng, 2008. **36**(5): p. 813-20.
52. Gang, E.J., et al., *Skeletal myogenic differentiation of mesenchymal stem cells isolated from human umbilical cord blood.* Stem Cells, 2004. **22**(4): p. 617-24.
53. Fukuda, K. and J. Fujita, *Mesenchymal, but not hematopoietic, stem cells can be mobilized and differentiate into cardiomyocytes after myocardial infarction in mice.* Kidney Int, 2005. **68**(5): p. 1940-3.
54. Vescovi, A.L. and E.Y. Snyder, *Establishment and properties of neural stem cell clones: plasticity in vitro and in vivo.* Brain Pathol, 1999. **9**(3): p. 569-98.
55. Castillo, A.B. and C.R. Jacobs, *Mesenchymal stem cell mechanobiology.* Curr Osteoporos Rep. **8**(2): p. 98-104.
56. Haudenschild, A.K., et al., *Pressure and distortion regulate human mesenchymal stem cell gene expression.* Ann Biomed Eng, 2009. **37**(3): p. 492-502.

57. Sen, B., et al., *Mechanical strain inhibits adipogenesis in mesenchymal stem cells by stimulating a durable beta-catenin signal.* Endocrinology, 2008. **149**(12): p. 6065-75.
58. Doyle, A.M., R.M. Nerem, and T. Ahsan, *Human mesenchymal stem cells form multicellular structures in response to applied cyclic strain.* Ann Biomed Eng, 2009. **37**(4): p. 783-93.
59. Huang, C.H., et al., *Interactive effects of mechanical stretching and extracellular matrix proteins on initiating osteogenic differentiation of human mesenchymal stem cells.* J Cell Biochem, 2009. **108**(6): p. 1263-73.
60. Ruiz, S.A. and C.S. Chen, *Emergence of patterned stem cell differentiation within multicellular structures.* Stem Cells, 2008. **26**(11): p. 2921-7.
61. McBeath, R., et al., *Cell shape, cytoskeletal tension, and RhoA regulate stem cell lineage commitment.* Dev Cell, 2004. **6**(4): p. 483-95.
62. Feng, Z., et al., *Effect of cytoskeleton inhibitors on deadhesion kinetics of HepG2 cells on biomimetic surface.* Colloids Surf B Biointerfaces. **75**(1): p. 67-74.
63. Riddle, R.C., et al., *MAP kinase and calcium signaling mediate fluid flow-induced human mesenchymal stem cell proliferation.* Am J Physiol Cell Physiol, 2006. **290**(3): p. C776-84.
64. Wolf, J.H., *[Julis Wolff and his "law of bone remodeling"].* Orthopade, 1995. **24**(5): p. 378-86.
65. Riggs, C.M., L.E. Lanyon, and A. Boyde, *Functional associations between collagen fibre orientation and locomotor strain direction in cortical bone of the equine radius.* Anat Embryol (Berl), 1993. **187**(3): p. 231-8.
66. Noble, B.S., et al., *Mechanical loading: biphasic osteocyte survival and targeting of osteoclasts for bone destruction in rat cortical bone.* Am J Physiol Cell Physiol, 2003. **284**(4): p. C934-43.
67. Lanyon, L.E., *The Influence of Function on the Development of Bone Curvature - an Experimental-Study on the Rat Tibia.* Journal of Zoology, 1980. **192**(Dec): p. 457-466.
68. Jaworski, Z.F., M. Liskova-Kiar, and H.K. Uhthoff, *Effect of long-term immobilisation on the pattern of bone loss in older dogs.* J Bone Joint Surg Br, 1980. **62-B**(1): p. 104-10.
69. Jaworski, Z.F. and H.K. Uhthoff, *Reversibility of nontraumatic disuse osteoporosis during its active phase.* Bone, 1986. **7**(6): p. 431-9.
70. Uhthoff, H.K. and Z.F. Jaworski, *Bone loss in response to long-term immobilisation.* J Bone Joint Surg Br, 1978. **60-B**(3): p. 420-9.
71. Turner, C.H., *Site-specific skeletal effects of exercise: importance of interstitial fluid pressure.* Bone, 1999. **24**(3): p. 161-2.
72. Leblanc, A.D., et al., *Bone mineral loss and recovery after 17 weeks of bed rest.* J Bone Miner Res, 1990. **5**(8): p. 843-50.
73. Burr, D.B. and R.B. Martin, *Calculating the probability that microcracks initiate resorption spaces.* J Biomech, 1993. **26**(4-5): p. 613-6.
74. Burr, D.B., et al., *Bone remodeling in response to in vivo fatigue microdamage.* J Biomech, 1985. **18**(3): p. 189-200.
75. Sipos, W., et al., *Pathophysiology of osteoporosis.* Wien Med Wochenschr, 2009. **159**(9-10): p. 230-4.
76. Kalu, D.N., *The ovariectomized rat model of postmenopausal bone loss.* Bone Miner, 1991. **15**(3): p. 175-91.

77. Edwards, M.W., et al., *17 beta estradiol stimulation of endosteal bone formation in the ovariectomized mouse: an animal model for the evaluation of bone-targeted estrogens.* Bone, 1992. **13**(1): p. 29-34.
78. Martin, R.B., et al., *Effects of ovariectomy in beagle dogs.* Bone, 1987. **8**(1): p. 23-31.
79. Snow, G.R., M.A. Cook, and C. Anderson, *Oophorectomy and cortical bone remodeling in the beagle.* Calcif Tissue Int, 1984. **36**(5): p. 586-90.
80. Cochrane, R.L. and R.L. Holmes, *Unilateral ovariectomy and hypophysectomy in the rhesus monkey.* J Endocrinol, 1966. **35**(4): p. 427-8.
81. Lundon, K. and M. Grynpas, *The long-term effect of ovariectomy on the quality and quantity of cortical bone in the young cynomolgus monkey: a comparison of density fractionation and histomorphometric techniques.* Bone, 1993. **14**(3): p. 389-95.
82. Sigrist, I.M., et al., *The long-term effects of ovariectomy on bone metabolism in sheep.* J Bone Miner Metab, 2007. **25**(1): p. 28-35.
83. Leung, K.S., et al., *Goats as an osteopenic animal model.* J Bone Miner Res, 2001. **16**(12): p. 2348-55.
84. Siu, W.S., et al., *A study of trabecular bones in ovariectomized goats with micro-computed tomography and peripheral quantitative computed tomography.* Bone, 2004. **35**(1): p. 21-6.
85. Mosekilde, L., et al., *Evaluation of the skeletal effects of combined mild dietary calcium restriction and ovariectomy in Sinclair S-1 minipigs: a pilot study.* J Bone Miner Res, 1993. **8**(11): p. 1311-21.
86. Jee, W.S.S., Y.F. Ma, and X.J. Li, *The immobilized adult cancellous bone site in a growing rat as an animal model of human osteoporosis.* Journal of Histotechnology, 1997. **20**(3): p. 201-206.
87. Li, X.J. and W.S. Jee, *Adaptation of diaphyseal structure to aging and decreased mechanical loading in the adult rat: a densitometric and histomorphometric study.* Anat Rec, 1991. **229**(3): p. 291-7.
88. Milstead, J.R., S.J. Simske, and T.A. Bateman, *Spaceflight and hindlimb suspension disuse models in mice.* Biomed Sci Instrum, 2004. **40**: p. 105-10.
89. Woodward, A.H. and J. Jowsey, *The effects of glucagon on immobilization osteoporosis in rats.* Endocrinology, 1972. **90**(5): p. 1399-401.
90. Zeng, Q.Q., et al., *S-ketoprofen inhibits tenotomy-induced bone loss and dynamics in weanling rats.* Bone Miner, 1993. **21**(3): p. 203-18.
91. Li, X.J., et al., *Adaptation of cancellous bone to aging and immobilization in the rat: a single photon absorptiometry and histomorphometry study.* Anat Rec, 1990. **227**(1): p. 12-24.
92. Dehority, W., et al., *Bone and hormonal changes induced by skeletal unloading in the mature male rat.* Am J Physiol, 1999. **276**(1 Pt 1): p. E62-9.
93. Jee, W.S.S., X.J. Li, and H.Z. Ke, *The Skeletal Adaptation to Mechanical Usage in the Rat.* Cells and Materials, 1991: p. 131-142.
94. Lepola, V., K. Vaananen, and P. Jalovaara, *The Effect of Immobilization on the Torsional Strength of the Rat Tibia.* Clinical Orthopaedics and Related Research, 1993(297): p. 55-61.
95. Martin, R.K., et al., *Bone loss in the beagle tibia: influence of age, weight, and sex.* Calcif Tissue Int, 1981. **33**(3): p. 233-8.

96. Jee, W.S. and W. Yao, *Overview: animal models of osteopenia and osteoporosis.* J Musculoskelet Neuronal Interact, 2001. **1**(3): p. 193-207.
97. Chow, J.W., C.J. Jagger, and T.J. Chambers, *Reduction in dynamic indices of cancellous bone formation in rat tail vertebrae after caudal neurectomy.* Calcif Tissue Int, 1996. **59**(2): p. 117-20.
98. Bagi, C.M., et al., *Comparative morphometric changes in rat cortical bone following ovariectomy and/or immobilization.* Bone, 1993. **14**(6): p. 877-83.
99. Bagi, C.M. and S.C. Miller, *Comparison of osteopenic changes in cancellous bone induced by ovariectomy and/or immobilization in adult rats.* Anat Rec, 1994. **239**(3): p. 243-54.
100. Turner, R.T., et al., *Animal models for osteoporosis.* Rev Endocr Metab Disord, 2001. **2**(1): p. 117-27.
101. Turner, R.T., B.L. Riggs, and T.C. Spelsberg, *Skeletal effects of estrogen.* Endocr Rev, 1994. **15**(3): p. 275-300.
102. Erben, R.G., *Trabecular and endocortical bone surfaces in the rat: modeling or remodeling?* Anat Rec, 1996. **246**(1): p. 39-46.
103. Tuukkanen, J., et al., *Changes induced in growing rat bone by immobilization and remobilization.* Bone, 1991. **12**(2): p. 113-8.
104. Shaker, J.L., et al., *Wr-2721 Reduces Bone Loss after Hindlimb Tenotomy in Rats.* Journal of Bone and Mineral Research, 1989. **4**(6): p. 885-890.
105. Thompson, D.D. and G.A. Rodan, *Indomethacin Inhibition of Tenotomy-Induced Bone-Resorption in Rats.* Journal of Bone and Mineral Research, 1988. **3**(4): p. 409-414.
106. Weinreb, M., G.A. Rodan, and D.D. Thompson, *Osteopenia in the Immobilized Rat Hind-Limb Is Associated with Increased Bone-Resorption and Decreased Bone-Formation.* Bone, 1989. **10**(3): p. 187-194.
107. Dannucci, G.A., R.B. Martin, and P. Patterson-Buckendahl, *Ovariectomy and trabecular bone remodeling in the dog.* Calcif Tissue Int, 1987. **40**(4): p. 194-9.
108. Young, D.R., W.J. Niklowitz, and C.R. Steele, *Tibial changes in experimental disuse osteoporosis in the monkey.* Calcif Tissue Int, 1983. **35**(3): p. 304-8.
109. Collet, P., et al., *Effects of 1- and 6-month spaceflight on bone mass and biochemistry in two humans.* Bone, 1997. **20**(6): p. 547-51.
110. Foldes, I., et al., *Changes of lumbar vertebrae after Cosmos-1887 space flight.* Physiologist, 1991. **34**(1 Suppl): p. S57-8.
111. Oganov, V.S., et al., *The state of human bone tissue during space flight.* Acta Astronaut, 1991. **23**: p. 129-33.
112. Tilton, F.E., J.J. Degioanni, and V.S. Schneider, *Long-term follow-up of Skylab bone demineralization.* Aviat Space Environ Med, 1980. **51**(11): p. 1209-13.
113. Lang, T.F., et al., *Adaptation of the proximal femur to skeletal reloading after long-duration spaceflight.* J Bone Miner Res, 2006. **21**(8): p. 1224-30.
114. Vico, L., et al., *Effects of long-term microgravity exposure on cancellous and cortical weight-bearing bones of cosmonauts.* Lancet, 2000. **355**(9215): p. 1607-11.
115. Caillot-Augusseau, A., et al., *Bone formation and resorption biological markers in cosmonauts during and after a 180-day space flight (Euromir 95).* Clin Chem, 1998. **44**(3): p. 578-85.

116. Yagodovsky, V.S., L.A. Triftanidi, and G.P. Gorokhova, *Space flight effects on skeletal bones of rats (light and electron microscopic examination).* Aviat Space Environ Med, 1976. **47**(7): p. 734-8.
117. Jee, W.S., et al., *Effects of spaceflight on trabecular bone in rats.* Am J Physiol, 1983. **244**(3): p. R310-4.
118. Vico, L., et al., *Trabecular bone remodeling after seven days of weightlessness exposure (BIOCOSMOS 1667).* Am J Physiol, 1988. **255**(2 Pt 2): p. R243-7.
119. Simmons, D.J., J.E. Russell, and M.D. Grynpas, *Bone maturation and quality of bone material in rats flown on the space shuttle 'Spacelab-3 Mission'.* Bone Miner, 1986. **1**(6): p. 485-93.
120. Zerath, E., et al., *Effects of spaceflight and recovery on rat humeri and vertebrae: histological and cell culture studies.* J Appl Physiol, 1996. **81**(1): p. 164-71.
121. Tamma, R., et al., *Microgravity during spaceflight directly affects in vitro osteoclastogenesis and bone resorption.* FASEB J, 2009. **23**(8): p. 2549-54.
122. Globus, R.K., D.D. Bikle, and E. Morey-Holton, *Effects of simulated weightlessness on bone mineral metabolism.* Endocrinology, 1984. **114**(6): p. 2264-70.
123. Wronski, T.J. and E.R. Morey-Holton, *Skeletal response to simulated weightlessness: a comparison of suspension techniques.* Aviat Space Environ Med, 1987. **58**(1): p. 63-8.
124. Halloran, B.P., et al., *Glucocorticoids and inhibition of bone formation induced by skeletal unloading.* Am J Physiol, 1988. **255**(6 Pt 1): p. E875-9.
125. Shiiba, M., et al., *Regional alterations of type I collagen in rat tibia induced by skeletal unloading.* J Bone Miner Res, 2002. **17**(9): p. 1639-45.
126. Globus, R.K., et al., *Skeletal response to dietary calcium in a rat model simulating weightlessness.* J Bone Miner Res, 1986. **1**(2): p. 191-7.
127. Globus, R.K., D.D. Bikle, and E. Morey-Holton, *The temporal response of bone to unloading.* Endocrinology, 1986. **118**(2): p. 733-42.
128. Sakata, T., et al., *Trabecular bone turnover and bone marrow cell development in tail-suspended mice.* J Bone Miner Res, 1999. **14**(9): p. 1596-604.
129. Bikle, D.D., et al., *The effects of simulated weightlessness on bone maturation.* Endocrinology, 1987. **120**(2): p. 678-84.
130. Kodama, Y., et al., *Inhibition of bone resorption by pamidronate cannot restore normal gain in cortical bone mass and strength in tail-suspended rapidly growing rats.* J Bone Miner Res, 1997. **12**(7): p. 1058-67.
131. Patterson-Buckendahl, P., et al., *Effects of simulated weightlessness on rat osteocalcin and bone calcium.* Am J Physiol, 1989. **257**(5 Pt 2): p. R1103-9.
132. Halloran, B.P., et al., *The role of 1,25-dihydroxyvitamin D in the inhibition of bone formation induced by skeletal unloading.* Endocrinology, 1986. **118**(3): p. 948-54.
133. Machwate, M., et al., *Skeletal unloading in rat decreases proliferation of rat bone and marrow-derived osteoblastic cells.* Am J Physiol, 1993. **264**(5 Pt 1): p. E790-9.
134. Colleran, P.N., et al., *Alterations in skeletal perfusion with simulated microgravity: a possible mechanism for bone remodeling.* J Appl Physiol, 2000. **89**(3): p. 1046-54.
135. Bikle, D.D., T. Sakata, and B.P. Halloran, *The impact of skeletal unloading on bone formation.* Gravit Space Biol Bull, 2003. **16**(2): p. 45-54.
136. Zhang, R.W., et al., *Rat Tail Suspension Reduces Messenger-Rna Level for Growth-Factors and Osteopontin and Decreases the Osteoblastic Differentiation of Bone-Marrow Stromal Cells.* Journal of Bone and Mineral Research, 1995. **10**(3): p. 415-423.

137. Martin, R.B., *Effects of simulated weightlessness on bone properties in rats.* J Biomech, 1990. **23**(10): p. 1021-9.
138. Abram, A.C., T.S. Keller, and D.M. Spengler, *The effects of simulated weightlessness on bone biomechanical and biochemical properties in the maturing rat.* J Biomech, 1988. **21**(9): p. 755-67.
139. Shaw, S.R., et al., *Mechanical, morphological and biochemical adaptations of bone and muscle to hindlimb suspension and exercise.* J Biomech, 1987. **20**(3): p. 225-34.
140. Van Loon, J.J., et al., *Decreased mineralization and increased calcium release in isolated fetal mouse long bones under near weightlessness.* J Bone Miner Res, 1995. **10**(4): p. 550-7.
141. Hughes-Fulford, M., et al., *Effects of microgravity on osteoblast growth.* Gravit Space Biol Bull, 1998. **11**(2): p. 51-60.
142. Hughes-Fulford, M., K. Rodenacker, and U. Jutting, *Reduction of anabolic signals and alteration of osteoblast nuclear morphology in microgravity.* J Cell Biochem, 2006. **99**(2): p. 435-49.
143. Hughes-Fulford, M. and M.L. Lewis, *Effects of microgravity on osteoblast growth activation.* Exp Cell Res, 1996. **224**(1): p. 103-9.
144. Carmeliet, G., G. Nys, and R. Bouillon, *Microgravity reduces the differentiation of human osteoblastic MG-63 cells.* J Bone Miner Res, 1997. **12**(5): p. 786-94.
145. Carmeliet, G., et al., *Gene expression related to the differentiation of osteoblastic cells is altered by microgravity.* Bone, 1998. **22**(5 Suppl): p. 139S-143S.
146. Hughes-Fulford, M., *Function of the cytoskeleton in gravisensing during spaceflight.* Adv Space Res, 2003. **32**(8): p. 1585-93.
147. Hughes-Fulford, M., *Physiological effects of microgravity on osteoblast morphology and cell biology.* Adv Space Biol Med, 2002. **8**: p. 129-57.
148. Akiyama, H., et al., *Expression of PDGF-beta receptor, EGF receptor, and receptor adaptor protein Shc in rat osteoblasts during spaceflight.* Mol Cell Biochem, 1999. **202**(1-2): p. 63-71.
149. Sato, A., et al., *Effects of microgravity on c-fos gene expression in osteoblast-like MC3T3-E1 cells.* Adv Space Res, 1999. **24**(6): p. 807-13.
150. Hoson, T., et al., *Evaluation of the three-dimensional clinostat as a simulator of weightlessness.* Planta, 1997. **203 Suppl**: p. S187-97.
151. Schwarz, R.P., T.J. Goodwin, and D.A. Wolf, *Cell culture for three-dimensional modeling in rotating-wall vessels: an application of simulated microgravity.* J Tissue Cult Methods, 1992. **14**(2): p. 51-7.
152. Huijser, R., *Desktop RPM, New Small Size Microgravity Simulator for the Bioscience Laboratory.* Fokker Space, 2000: p. 1-5.
153. Vico, L., *What do we know about alteration in the osteoblast phenotype with microgravity?* J Musculoskelet Neuronal Interact, 2006. **6**(4): p. 317-8.
154. Basso, N., et al., *The effect of reloading on bone volume, osteoblast number, and osteoprogenitor characteristics: studies in hind limb unloaded rats.* Bone, 2005. **37**(3): p. 370-8.
155. Sheyn, D., et al., *The effect of simulated microgravity on human mesenchymal stem cells cultured in an osteogenic differentiation system: a bioinformatics study.* Tissue Eng Part A, 2010. **16**(11): p. 3403-12.

156. Zheng, Q., et al., *Could the effect of modeled microgravity on osteogenic differentiation of human mesenchymal stem cells be reversed by regulation of signaling pathways?* Biol Chem, 2007. **388**(7): p. 755-63.
157. Bikle, D.D., *IGF-I-deficient mice: Role in skeletal adaptation to load - Reply.* Journal of Bone and Mineral Research, 2003. **18**(5): p. 944-944.
158. Shapiro, J.R., *Microgravity and drug effects on bone.* J Musculoskelet Neuronal Interact, 2006. **6**(4): p. 322-3.
159. Papachroni, K.K., et al., *Mechanotransduction in osteoblast regulation and bone disease.* Trends Mol Med, 2009. **15**(5): p. 208-16.
160. Bikle, D.D., B.P. Halloran, and E. Moreyholton, *Impact of Skeletal Unloading on Bone-Formation - Role of Systemic and Local Factors.* Acta Astronautica, 1994. **33**: p. 119-129.
161. Chen, J.H., et al., *Boning up on Wolff's Law: mechanical regulation of the cells that make and maintain bone.* J Biomech, 2010. **43**(1): p. 108-18.
162. Loesberg, W.A., et al., *Simulated microgravity activates MAPK pathways in fibroblasts cultured on microgrooved surface topography.* Cell Motil Cytoskeleton, 2008. **65**(2): p. 116-29.
163. Boutahar, N., et al., *Mechanical strain on osteoblasts activates autophosphorylation of focal adhesion kinase and proline-rich tyrosine kinase 2 tyrosine sites involved in ERK activation.* J Biol Chem, 2004. **279**(29): p. 30588-99.
164. Buckley, M.J., et al., *Osteoblasts increase their rate of division and align in response to cyclic, mechanical tension in vitro.* Bone Miner, 1988. **4**(3): p. 225-36.
165. Jagodzinski, M., et al., *Effects of cyclic longitudinal mechanical strain and dexamethasone on osteogenic differentiation of human bone marrow stromal cells.* Eur Cell Mater, 2004. **7**: p. 35-41; discussion 41.
166. Jessop, H.L., et al., *Mechanical strain and fluid movement both activate extracellular regulated kinase (ERK) in osteoblast-like cells but via different signaling pathways.* Bone, 2002. **31**(1): p. 186-94.
167. Brouwers, J.E., et al., *Effects of vibration treatment on tibial bone of ovariectomized rats analyzed by in vivo micro-CT.* J Orthop Res, 2010. **28**(1): p. 62-9.
168. Chow, D.H., et al., *Low-magnitude high-frequency vibration (LMHFV) enhances bone remodeling in osteoporotic rat femoral fracture healing.* J Orthop Res, 2010.
169. Rubin, C., S. Judex, and Y.X. Qin, *Low-level mechanical signals and their potential as a non-pharmacological intervention for osteoporosis.* Age Ageing, 2006. **35 Suppl 2**: p. ii32-ii36.
170. Boyd, J.L., J.P. Holcomb, and R.J. Rothenberg, *Physician treatment of osteoporosis in response to heel ultrasound bone mineral density reports.* J Clin Densitom, 2002. **5**(4): p. 375-81.
171. Carvalho, D.C. and A. Cliquet Junior, *The action of low-intensity pulsed ultrasound in bones of osteopenic rats.* Artif Organs, 2004. **28**(1): p. 114-8.
172. Ferreri, S.L., et al., *Mitigation of bone loss with ultrasound induced dynamic mechanical signals in an OVX induced rat model of osteopenia.* Bone, 2011.
173. Agnusdei, D., A. Camporeale, and C. Gennari, *[Ultrasound transmission velocity in the patella of normal subjects and in patients with postmenopausal osteoporosis]*. Minerva Endocrinol, 1991. **16**(2): p. 73-7.

174. Warden, S.J., et al., *Skeletal effects of low-intensity pulsed ultrasound on the ovariectomized rodent.* Ultrasound Med Biol, 2001. **27**(7): p. 989-98.
175. Rubin, J., et al., *Pressure regulates osteoclast formation and MCSF expression in marrow culture.* J Cell Physiol, 1997. **170**(1): p. 81-7.
176. Binderman, I., Z. Shimshoni, and D. Somjen, *Biochemical pathways involved in the translation of physical stimulus into biological message.* Calcif Tissue Int, 1984. **36 Suppl 1**: p. S82-5.
177. Binderman, I., et al., *The transduction of mechanical force into biochemical events in bone cells may involve activation of phospholipase A2.* Calcif Tissue Int, 1988. **42**(4): p. 261-6.
178. Li, J.K., et al., *Cytokine release from osteoblasts in response to ultrasound stimulation.* Biomaterials, 2003. **24**(13): p. 2379-85.
179. Yang, K.H., et al., *Exposure to low-intensity ultrasound increases aggrecan gene expression in a rat femur fracture model.* J Orthop Res, 1996. **14**(5): p. 802-9.
180. Nolte, P.A., et al., *Low-intensity ultrasound stimulates endochondral ossification in vitro.* J Orthop Res, 2001. **19**(2): p. 301-7.
181. Takeuchi, R., et al., *Low-intensity pulsed ultrasound activates the phosphatidylinositol 3 kinase/Akt pathway and stimulates the growth of chondrocytes in three-dimensional cultures: a basic science study.* Arthritis Res Ther, 2008. **10**(4): p. R77.
182. Chapman, I.V., N.A. MacNally, and S. Tucker, *Ultrasound-induced changes in rates of influx and efflux of potassium ions in rat thymocytes in vitro.* Ultrasound Med Biol, 1980. **6**(1): p. 47-58.
183. Kaneko, T., et al., *Power Doppler ultrasonography for the assessment of vascular invasion by pancreatic cancer.* Pancreatology, 2002. **2**(1): p. 61-8.
184. Naruse, K., et al., *Distinct anabolic response of osteoblast to low-intensity pulsed ultrasound.* J Bone Miner Res, 2003. **18**(2): p. 360-9.
185. Baker, K.G., V.J. Robertson, and F.A. Duck, *A review of therapeutic ultrasound: biophysical effects.* Phys Ther, 2001. **81**(7): p. 1351-8.
186. Guignandon, A., et al., *Focal contact clustering in osteoblastic cells under mechanical stresses: microgravity and cyclic deformation.* Cell Commun Adhes, 2003. **10**(2): p. 69-83.
187. Jansen, J.H., et al., *Stretch-induced modulation of matrix metalloproteinases in mineralizing osteoblasts via extracellular signal-regulated kinase-1/2.* J Orthop Res, 2006. **24**(7): p. 1480-8.
188. Plotkin, L.I., et al., *Mechanical stimulation prevents osteocyte apoptosis: requirement of integrins, Src kinases, and ERKs.* Am J Physiol Cell Physiol, 2005. **289**(3): p. C633-43.
189. Tang, L., Z. Lin, and Y.M. Li, *Effects of different magnitudes of mechanical strain on Osteoblasts in vitro.* Biochem Biophys Res Commun, 2006. **344**(1): p. 122-8.
190. Hsu, H.C., et al., *Ultrasound induces cyclooxygenase-2 expression through integrin, integrin-linked kinase, Akt, NF-kappaB and p300 pathway in human chondrocytes.* Cell Signal, 2007. **19**(11): p. 2317-28.
191. Tang, C.H., et al., *Ultrasound induces hypoxia-inducible factor-1 activation and inducible nitric-oxide synthase expression through the integrin/integrin-linked kinase/Akt/mammalian target of rapamycin pathway in osteoblasts.* J Biol Chem, 2007. **282**(35): p. 25406-15.

192. Tang, C.H., et al., *Ultrasound stimulates cyclooxygenase-2 expression and increases bone formation through integrin, focal adhesion kinase, phosphatidylinositol 3-kinase, and Akt pathway in osteoblasts.* Mol Pharmacol, 2006. **69**(6): p. 2047-57.
193. Yang, R.S., et al., *Regulation by ultrasound treatment on the integrin expression and differentiation of osteoblasts.* Bone, 2005. **36**(2): p. 276-83.
194. Olkku, A., et al., *Ultrasound-induced activation of Wnt signaling in human MG-63 osteoblastic cells.* Bone, 2010. **47**(2): p. 320-30.
195. Hundt, W., et al., *Comparison of continuous vs. pulsed focused ultrasound in treated muscle tissue as evaluated by magnetic resonance imaging, histological analysis, and microarray analysis.* Eur Radiol, 2008. **18**(5): p. 993-1004.
196. Kobayashi, Y., et al., *Low-intensity pulsed ultrasound stimulates cell proliferation, proteoglycan synthesis and expression of growth factor-related genes in human nucleus pulposus cell line.* Eur Cell Mater, 2009. **17**: p. 15-22.
197. Lu, H., et al., *Identification of genes responsive to low-intensity pulsed ultrasound stimulations.* Biochem Biophys Res Commun, 2009. **378**(3): p. 569-73.
198. Tabuchi, Y., et al., *DNA microarray analyses of genes elicited by ultrasound in human U937 cells.* Biochem Biophys Res Commun, 2002. **290**(1): p. 498-503.
199. Kiratli, B.J., et al., *Bone mineral and geometric changes through the femur with immobilization due to spinal cord injury.* J Rehabil Res Dev, 2000. **37**(2): p. 225-33.
200. Little, D.G., et al., *Effect of pamidronate on distraction osteogenesis and fixator-related osteoporosis.* Injury, 2001. **32 Suppl 4**: p. SD14-20.
201. Gerstenfeld, L.C., et al., *Comparison of effects of the bisphosphonate alendronate versus the RANKL inhibitor denosumab on murine fracture healing.* J Bone Miner Res, 2009. **24**(2): p. 196-208.
202. Bain, S.D., et al., *Strontium ranelate improves bone strength in ovariectomized rat by positively influencing bone resistance determinants.* Osteoporos Int, 2009. **20**(8): p. 1417-28.
203. Ma, B., et al., *Strontium fructose 1,6-diphosphate prevents bone loss in a rat model of postmenopausal osteoporosis via the OPG/RANKL/RANK pathway.* Acta Pharmacol Sin. **33**(4): p. 479-89.
204. Hock, J.M., et al., *Human parathyroid hormone-(1-34) increases bone mass in ovariectomized and orchidectomized rats.* Endocrinology, 1988. **122**(6): p. 2899-904.
205. Li, X., et al., *Sclerostin antibody treatment increases bone formation, bone mass, and bone strength in a rat model of postmenopausal osteoporosis.* J Bone Miner Res, 2009. **24**(4): p. 578-88.
206. Pohl, P., E. Rosenfeld, and R. Millner, *Effects of ultrasound on the steady-state transmembrane pH gradient and the permeability of acetic acid through bilayer lipid membranes.* Biochim Biophys Acta, 1993. **1145**(2): p. 279-83.
207. Heckman, J.D., et al., *Acceleration of tibial fracture-healing by non-invasive, low-intensity pulsed ultrasound.* J Bone Joint Surg Am, 1994. **76**(1): p. 26-34.
208. Azuma, Y., et al., *Low-intensity pulsed ultrasound accelerates rat femoral fracture healing by acting on the various cellular reactions in the fracture callus.* J Bone Miner Res, 2001. **16**(4): p. 671-80.
209. Jingushi, S., *[Bone fracture and the healing mechanisms. Fracture treatment by low-intensity pulsed ultrasound]*. Clin Calcium, 2009. **19**(5): p. 704-8.

210. Jingushi, S., et al., *Low-intensity pulsed ultrasound treatment for postoperative delayed union or nonunion of long bone fractures.* J Orthop Sci, 2007. **12**(1): p. 35-41.
211. Cook, S.D., et al., *Acceleration of tibia and distal radius fracture healing in patients who smoke.* Clin Orthop Relat Res, 1997(337): p. 198-207.
212. Cook, S.D., et al., *Low-intensity pulsed ultrasound improves spinal fusion.* Spine J, 2001. **1**(4): p. 246-54.
213. Saito, M., et al., *Effect of low- and high-intensity pulsed ultrasound on collagen post-translational modifications in MC3T3-E1 osteoblasts.* Calcif Tissue Int, 2004. **75**(5): p. 384-95.
214. Fuller, K., et al., *TNFalpha potently activates osteoclasts, through a direct action independent of and strongly synergistic with RANKL.* Endocrinology, 2002. **143**(3): p. 1108-18.
215. Yoshitake, F., et al., *Interleukin-6 directly inhibits osteoclast differentiation by suppressing receptor activator of NF-kappaB signaling pathways.* J Biol Chem, 2008. **283**(17): p. 11535-40.
216. Bhang, S.H., et al., *Cyclic mechanical strain promotes transforming-growth-factor-beta1-mediated cardiomyogenic marker expression in bone-marrow-derived mesenchymal stem cells in vitro.* Biotechnol Appl Biochem, 2010. **55**(4): p. 191-7.
217. Khayat, G., D.H. Rosenzweig, and T.M. Quinn, *Low frequency mechanical stimulation inhibits adipogenic differentiation of C3H10T1/2 mesenchymal stem cells.* Differentiation. **83**(4): p. 179-84.
218. Pelaez, D., C.Y. Huang, and H.S. Cheung, *Cyclic compression maintains viability and induces chondrogenesis of human mesenchymal stem cells in fibrin gel scaffolds.* Stem Cells Dev, 2009. **18**(1): p. 93-102.
219. Qi, M.C., et al., *Mechanical strain induces osteogenic differentiation: Cbfa1 and Ets-1 expression in stretched rat mesenchymal stem cells.* Int J Oral Maxillofac Surg, 2008. **37**(5): p. 453-8.
220. Luu, Y.K., et al., *Development of diet-induced fatty liver disease in the aging mouse is suppressed by brief daily exposure to low-magnitude mechanical signals.* Int J Obes (Lond). **34**(2): p. 401-5.
221. Ozcivici, E., et al., *Mechanical signals as anabolic agents in bone.* Nat Rev Rheumatol, 2010. **6**(1): p. 50-9.
222. Yang, X., et al., *Cyclic tensile stretch modulates osteogenic differentiation of adipose-derived stem cells via the BMP-2 pathway.* Arch Med Sci. **6**(2): p. 152-9.
223. Yamazaki, S., et al., *Regulation of osteogenetic differentiation of mesenchymal stem cells by two axial rotational culture.* J Artif Organs. **14**(4): p. 310-7.
224. Vico, L., et al., *Osteobiology, strain, and microgravity. Part II: studies at the tissue level.* Calcif Tissue Int, 2001. **68**(1): p. 1-10.
225. Lai, C.H., et al., *Effects of low-intensity pulsed ultrasound, dexamethasone/TGF-beta1 and/or BMP-2 on the transcriptional expression of genes in human mesenchymal stem cells: chondrogenic vs. osteogenic differentiation.* Ultrasound Med Biol. **36**(6): p. 1022-33.
226. Meyers, V.E., et al., *Modeled microgravity disrupts collagen I/integrin signaling during osteoblastic differentiation of human mesenchymal stem cells.* J Cell Biochem, 2004. **93**(4): p. 697-707.

227. Sheyn, D., et al., *The effect of simulated microgravity on human mesenchymal stem cells cultured in an osteogenic differentiation system: a bioinformatics study.* Tissue Eng Part A. **16**(11): p. 3403-12.
228. Liu, J., et al., *Pressure-loaded MSCs during early osteodifferentiation promote osteoclastogenesis by increase of RANKL/OPG ratio.* Ann Biomed Eng, 2009. **37**(4): p. 794-802.
229. Rubin, J., et al., *Mechanical strain inhibits expression of osteoclast differentiation factor by murine stromal cells.* Am J Physiol Cell Physiol, 2000. **278**(6): p. C1126-32.
230. Marie, P.J., et al., *Osteobiology, strain, and microgravity: part I. Studies at the cellular level.* Calcif Tissue Int, 2000. **67**(1): p. 2-9.
231. Qin, Y.-X., *Challenges to the musculoskeleton during a journey to Mars: Assessment and Counter Measures.* Journal of Cosmology, 2010. **12**: p. 3778 - 3780.
232. Nabavi, N., et al., *Effects of microgravity on osteoclast bone resorption and osteoblast cytoskeletal organization and adhesion.* Bone. **49**(5): p. 965-74.
233. Uddin, S.M.Z., et al., *Low-Intensity Amplitude Modulated Ultrasound Increases Osteoblastic Mineralization.* Cellular and Molecular Bioengineering, 2011. **4**(1): p. 81-90.
234. Raucci, A., et al., *Osteoblast proliferation or differentiation is regulated by relative strengths of opposing signaling pathways.* J Cell Physiol, 2008. **215**(2): p. 442-51.
235. Pre, D., et al., *Effects of low-amplitude, high-frequency vibrations on proliferation and differentiation of SAOS-2 human osteogenic cell line.* Tissue Eng Part C Methods, 2009. **15**(4): p. 669-79.
236. Chen, S.H., et al., *Effect of low intensity ultrasounds on the growth of osteoblasts.* Conf Proc IEEE Eng Med Biol Soc, 2007. **2007**: p. 5834-7.
237. Alvarenga, E.C., et al., *Low-intensity pulsed ultrasound-dependent osteoblast proliferation occurs by via activation of the P2Y receptor: role of the P2Y1 receptor.* Bone, 2010. **46**(2): p. 355-62.
238. de Gusmao, C.V.B., et al., *Low-intensity Ultrasound Increases FAK, ERK-1/2, and IRS-1 Expression of Intact Rat Bones in a Noncumulative Manner.* Clinical Orthopaedics and Related Research, 2010. **468**(4): p. 1149-1156.
239. Hou, C.H., et al., *Ultrasound Stimulates NF-kappa B Activation and iNOS Expression Via the Ras/Raf/MEK/ERK Signaling Pathway in Cultured Preosteoblasts.* Journal of Cellular Physiology, 2009. **220**(1): p. 196-203.
240. Takeuchi, R., et al., *Low-intensity pulsed ultrasound activates the phosphatidylinositol 3 kinase/Akt pathway and stimulates the growth of chondrocytes in three-dimensional cultures: a basic science study.* Arthritis Research & Therapy, 2008. **10**(4): p. -.
241. Tang, C., et al., *Ultrasound induces hypoxia-inducible factor-1 activation and iNOS expression through integrin/ILK/Akt pathway in cultured osteoblasts.* Journal of Bone and Mineral Research, 2007. **22**: p. S360-S360.
242. Lynch, M.P., et al., *The influence of type I collagen on the development and maintenance of the osteoblast phenotype in primary and passaged rat calvarial osteoblasts: modification of expression of genes supporting cell growth, adhesion, and extracellular matrix mineralization.* Exp Cell Res, 1995. **216**(1): p. 35-45.
243. Cheung, W.H., et al., *Low intensity pulsed ultrasound enhances fracture healing in both ovariectomy-induced osteoporotic and age-matched normal bones.* J Orthop Res, 2011.

244. Cheung, W.H., et al., *Low-intensity pulsed ultrasound accelerated callus formation, angiogenesis and callus remodeling in osteoporotic fracture healing.* Ultrasound Med Biol, 2011. **37**(2): p. 231-8.
245. Huang, C. and R. Ogawa, *Mechanotransduction in bone repair and regeneration.* FASEB J, 2010. **24**(10): p. 3625-32.
246. Geiger, B. and A. Bershadsky, *Exploring the neighborhood: adhesion-coupled cell mechanosensors.* Cell, 2002. **110**(2): p. 139-42.
247. Ingber, D.E., *Cellular mechanotransduction: putting all the pieces together again.* FASEB J, 2006. **20**(7): p. 811-27.
248. Pavalko, F.M., et al., *A model for mechanotransduction in bone cells: the load-bearing mechanosomes.* J Cell Biochem, 2003. **88**(1): p. 104-12.
249. Li, J., et al., *The role of extracellular matrix, integrins, and cytoskeleton in mechanotransduction of centrifugal loading.* Mol Cell Biochem, 2008. **309**(1-2): p. 41-8.
250. Kook, S.H., et al., *Mechanical force induces type I collagen expression in human periodontal ligament fibroblasts through activation of ERK/JNK and AP-1.* J Cell Biochem, 2009. **106**(6): p. 1060-7.
251. Landis, W.J., *Mineral characterization in calcifying tissues: atomic, molecular and macromolecular perspectives.* Connect Tissue Res, 1996. **34**(4): p. 239-46.
252. Landis, W.J., et al., *Structural relations between collagen and mineral in bone as determined by high voltage electron microscopic tomography.* Microsc Res Tech, 1996. **33**(2): p. 192-202.
253. Landis, W.J., et al., *Mineralization of collagen may occur on fibril surfaces: evidence from conventional and high-voltage electron microscopy and three-dimensional imaging.* J Struct Biol, 1996. **117**(1): p. 24-35.
254. Saxena, R., G. Pan, and J.M. McDonald, *Osteoblast and osteoclast differentiation in modeled microgravity.* Ann N Y Acad Sci, 2007. **1116**: p. 494-8.